NEW FAMILIES OF EMBEDDED TRIPLY PERIODIC MINIMAL SURFACES OF GENUS THREE IN EUCLIDEAN SPACE

Adam G. Weyhaupt

Accepted by the Graduate Faculty, Indiana University, in partial fulfillment of the requirements for the degree of Doctor of Philosophy.

_____

Matthias Weber, Ph.D.

_____

Jiri Dadok, Ph.D.

_____

Bruce Solomon, Ph.D.

_____

Peter Sternberg, Ph.D.

4 August 2006

To Julia
— my source of strength, my constant companion, my love forever

and

to Brandon and Ryan
— whose exuberance and smiles lift my spirits daily
and have changed my life in so many wonderful ways.

Acknowledgements

I can not imagine having completed graduate school with a different advisor: thank you, Matthias Weber, for your encouragement, your guidance, your constant availability, and for making me feel like a colleague. The following email exchange is typical of my interaction with him:

> Me: ...I need an infusion of optimism and a fresh pair of eyes.
> Him: It's ok. Can't promise fresh ice, but as infusion there will be tea.

Especially, thank you for introducing me to the beautiful study of minimal surfaces. Thank you to the other members of my committee for their improvement of this work; I have particularly been helped by conversations throughout the years with Jiri Dadok.

My time at Indiana has been enjoyable and fruitful because of innumerable people, most of whom I will undoubtedly forget to mention. Particularly, I thank Misty Cummings for ensuring that I (and all the graduate students) haven't run administratively amuck; Kent Orr for enjoyable discussions about math and family; and Jennifer Franko, Noah Salvaterra, and Eric Wilson for being my colleagues and friends through these changing years (and without whose companionship while studying I might not have passed my Tier 1 exams). Prior to Indiana, my teachers at Marquette Catholic High School and Eastern Illinois University helped to form me into an academic, especially Peter Andrews, Charles Delman, Greg Galperin, Lou Hencken, Suzer Phelps, Ira Rosenholz, Rosemary Schmalz, Margaret Weaver, and Keith Wolcott. Thinking back about you all reminds me that, as a teacher, nearly everything we do can impact our students.

Education has always been a focus in my life, thanks to my mother and father who have always encouraged me to "study hard, get a good job", and do something I enjoy. They have given me many opportunities and much encouragement through these years, and I am forever grateful. The memory of my grandfather, Joseph Weyhaupt, encourages me to work

harder and supports me when I'm feeling low, and the rest of my family is always there for me. My own family, Julia, Brandon, and Ryan, have put up with *so* much through these years and have always encouraged me and stood with me. You have never been a hindrance, but rather, have given me three wonderful reasons to continue.

Abstract

Until 1970, all known examples of embedded triply periodic minimal surfaces (ETPMS) contained either straight lines or curves of planar symmetry. In 1970, Alan Schoen discovered the gyroid, an ETPMS that contains neither straight lines nor planar symmetry curves. Meeks discovered in 1975 a 5-parameter family of genus 3 ETPMS that contained all known examples of genus 3 ETPMS except the gyroid. A second example lying outside the Meeks family was proposed by Lidin in 1990. Große-Brauckmann and Wohlgemuth showed in 1996 the existence and embeddedness of the gyroid and "Lidinoid". In a series of investigations the scientists, Lidin, et. al., numerically indicate the existence of two 1-parameter families of ETPMS that contain the gyroid and one family that contains the Lidinoid. In this thesis, we prove the existence of these families. To prove the existence of these families, we describe the Riemann surface structure using branched covers of non-rectangular tori. The holomorphic 1-forms Gdh, $\frac{1}{G}dh$, and dh each place a cone metric on the torus; we develop the torus with this metric into the plane and describe the periods in terms of these flat structures. Using this description of the periods, we define moduli spaces for the horizontal and vertical period problems so that Weierstraß data (X, G, dh) solves the period problem if the flat structures of X induced by these 1-forms are in the moduli spaces. To show that there is a curve of suitable data, we use an intermediate value type argument.

Contents

CHAPTER 1

Introduction

As early as 1762, Lagrange's newly developed calculus of variations broached the problem of finding the surface of smallest area with a prescribed space curve as its boundary. (The general problem of determining the existence and properties of minimizing surfaces with prescribed space curve boundary is called the Plateau problem.) He derived the partial differential equation which must be satisfied by all such surfaces. Explicit examples of such surfaces were provided by Euler (the catenoid, shortly before 1762) and Meunsier (the helicoid, around 1765) [**Nit75**]. All such area minimizing surfaces have vanishing mean curvature H. In modern language, the study of "minimal surfaces" is the study of all real 2-dimensional surfaces in $\mathbb{R}^3$ with $H \equiv 0$. Locally, these surfaces minimize area with respect to the boundary (of the local surface patch). All complete minimal surfaces without boundary are necessarily non-compact.

In this thesis, we are concerned with the study of *triply periodic minimal surfaces*. A triply periodic minimal surface is a minimal surface M that is invariant under the action of a rank 3 lattice Λ. M is, of course, non-compact; we often work with the much more tractable quotient M/Λ which is compact.

The ultimate goal of the study of triply periodic minimal surfaces is to classify all embedded triply periodic minimal surface of a fixed genus. Many examples are known. The first examples of a triply periodic minimal surface were given by Schwarz [**Sch90**] in 1865 when he exhibited the P, D, and H surfaces (see Figure 1.2). Early examples were constructed by solving the Plateau problem for non-planar polygons in space, such as on some of the edges of a cube (see Figure 1.1). After considerable attention in the late nineteenth and early twentieth centuries, triply periodic minimal surfaces experienced a slow-down of activity until the late 1960's, when physical scientists began to investigate them for possible

applications to materials science, biology, and chemistry. Chemists and materials scientists are now finding triply periodic minimal surfaces in images (on the nanometer scale) of the interface between two compounds in block co-polymers. They believe that the geometry of these interfacial surfaces significantly influence the physical properties of the compound [**TAHH88, FH99**]. Biologists have identified triply periodic minimal surfaces as membranes in certain cellular structures [**DM98**].
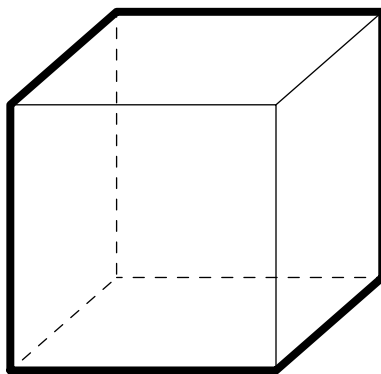

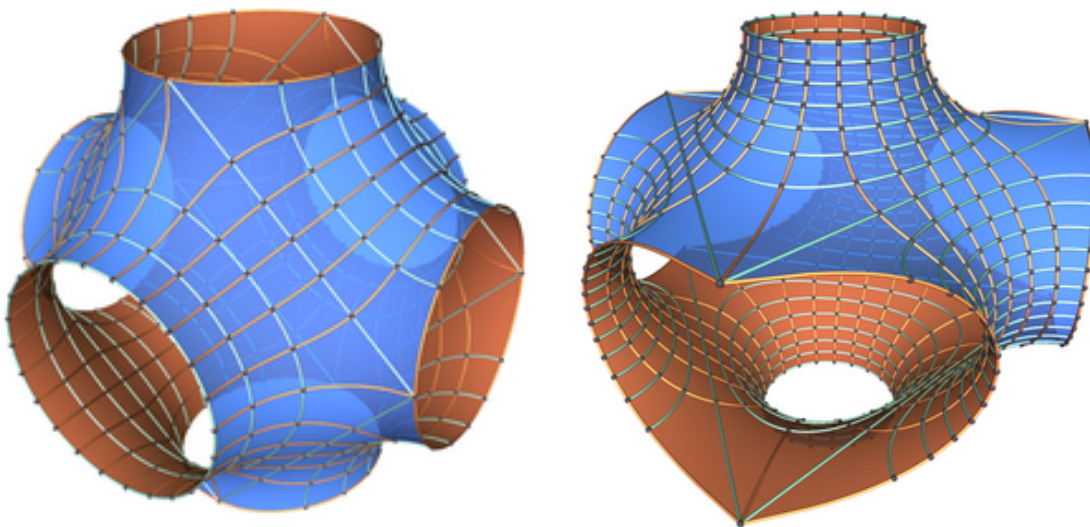FIGURE 1.1. The D surface solves the Plateau problem for the highlighted contour.

FIGURE 1.2. (left) A translational fundamental domain of the Schwarz P surface. (right) A fundamental domain of the Schwarz H surface.

In 1970, Alan Schoen [**Sch70**], a NASA crystallographer interested in strong but light materials, showed the existence of 12 previously undiscovered triply periodic minimal surfaces. Among these was the gyroid, an embedded surface containing no straight lines or planar symmetry curves (unlike other known examples at the time) [**Kar89, GBW96**]. In his 1975 Ph.D. thesis, Bill Meeks [**Mee75**] discovered a 5-parameter family of embedded genus 3 triply periodic minimal surfaces. Specifically,

THEOREM 1.1 (Meeks, 1975). *There is a real five-dimensional family V of periodic hyperelliptic Riemann surfaces of genus three. These are the surfaces which can be represented as two-sheeted covers of S^2 branched over four pairs of antipodal points. There exists two distinct isometric minimal embeddings for each $M_3 \in V$.*

The Meeks' family contained *all* triply periodic minimal surfaces of genus 3 known at that time — except for the gyroid. (In fact, most of the members of the Meeks' family were previously undiscovered surfaces. Many surfaces in his family have no straight lines and no planar symmetries.) In 1990, Sven Lidin discovered a related surface, christened by Lidin the HG surface but commonly called the "Lidinoid" [**LL90**]. (Minimal surface nomenclature leaves much to be desired. One of Schoen's surfaces is typically called "Schoen's Unnamed Surface Number 12". We do not help this any by adopting in this work the notation of Fogden, Haeberlein, and Lidin in [**FHL93**].) Although Schoen's surfaces were studied by crystallographers and physical scientists early on, it was not until the early 1990's that these surfaces entered the mathematical mainstream. In 1995, Große-Brauckmann and Wohlgemuth [**GBW96**] proved that the gyroid and Lidinoid are embedded.

The Meeks' family ensures that every currently known triply periodic minimal surface except for the gyroid and Lidinoid is deformable, i.e., for each triply periodic minimal surface M (M not the gyroid or Lidinoid) there is a continuous family of embedded triply periodic minimal surfaces M_η, $\eta \in (-\epsilon, \epsilon)$ such that $M = M_0$. Note that, in general, the lattices *may vary with η*, so that generically $\Lambda_{\eta_1} \neq \Lambda_{\eta_2}$ (we conjecture that it is never the case that the lattice is constant in a deformation, see Conjecture 6.1). We are primarily concerned with the following question:

MAIN QUESTION. *Do there exist continuous deformations of the gyroid and the Lidinoid?*

In a series of papers, the crystallographers and physical chemists Fogden, Haeberlein, Hyde, Lidin, and Larsson numerically indicate the existence of two 1-parameter families of embedded triply periodic minimal surfaces that contain the gyroid and two additional families that contain the Lidinoid [**FHL93, FH99, LL90**]. While even accompanied by very convincing computer-generated images, their work does not provide an existence proof, and the mathematical landscape is fraught with examples where pictures mislead (see, for example, [**Web98**]). Our main result of this thesis, then, is:

THEOREM 1.2. *There is a one parameter family of minimal embeddings $tG_\eta \subset \mathbb{R}^3/\Lambda_\eta$, $\eta \in \mathbb{R}^+$, such that tG_η is an embedded minimal surface of genus 3.The gyroid is a member of this family. Furthermore, each tG_η admits a rotational symmetry of order 2.*

(Note that the t is *not a parameter*. The "t" stands for "tetragonal"; [**FHL93**] call this a tetragonal deformation because crystallographers typically call a deformation of a cubical lattice tetragonal if the lattice admits an order 2 rotational symmetry throughout the deformation.) This shows that the gyroid is deformable. Our other two main theorems prove the existence of a Lidinoid family and an additional gyroid family:

THEOREM 1.3. *There is a one parameter family of minimal embeddings $rL_\eta \subset \mathbb{R}^3/\Lambda_\eta$, $\eta \in \mathbb{R}^+$, such that rL_η is an embedded minimal surface of genus 3.The Lidinoid is a member of this family. Furthermore, each rL_η admits a rotational symmetry of order 3.*

THEOREM 1.4. *There is a one parameter family of minimal embeddings $rG_\eta \subset \mathbb{R}^3/\Lambda_\eta$, $\eta \in \mathbb{R}^+$, such that rG_η is an embedded minimal surface of genus 3.The gyroid is a member of this family. Furthermore, each rG_η admits a rotational symmetry of order 3.*

Since the Lidinoid also admits an order 2 symmetry similar to the gyroid, we would expect to obtain a family of Lidinoids that preserves an order 2 symmetry. A survey of the literature seems to turn up no such family; a preliminary analysis shows that this family would be distinctly different conformally, and we defer its investigation to a future paper. As a consequence of these results, we have shown:

All currently known examples of genus 3 triply periodic minimal surfaces admit deformations.

As far as we know, none of these new examples are members of the Meeks' family.

1.1. Applications of the flat structure technique to the classification of triply periodic minimal surfaces

Perhaps the most ambitious problem in the theory of triply periodic minimal surfaces is to obtain a classification. In addition to constructing families of gyroids and Lidinoids, we also outline a method for approaching a classification of triply periodic minimal surfaces using techniques similar to those in the construction of the families. While we do not obtain any new families with this approach, we are able to classify surfaces that have sufficiently many symmetries.

Since the surface M/Λ is compact in the flat 3-torus $\mathbb{R}^3/\Lambda$, it is most natural to first consider a classification by genus.

THEOREM 1.5 (Meeks, 1975). *If $M/\Lambda \subset \mathbb{R}^3/\Lambda$ is a connected triply periodic minimal surface of genus g, then $g \geq 3$.*

In early 2006, Martin Traizet [**Tra06**] showed that

THEOREM 1.6. *For any flat 3-torus $\mathbb{R}^3/\Lambda$ and for any integer $g \geq 3$, there exists a sequence of orientable, compact, embedded minimal surfaces $M_n \in \mathbb{R}^3/\Lambda$ which have genus g. Moreover, the area of M_n goes to infinity as $n \to \infty$.*

(In the case of genus 3 surfaces, Traizet explicitly computes only one example; this is a known example in the Meeks family. However, Traizet mentions that "we find numerically that there are other balanced configurations which are not as symmetric as the one we discussed ... [t]his confirms the already suspected fact that the space of genus 3 minimal surfaces in a 3-torus is quite intricate." It is quite possible that these additional surfaces are previously undiscovered. Nonetheless, Traizet's construction method ensures that these surface come in a family, so our statement about all currently known surfaces admitting deformations remains true.)

In this thesis, we concentrate on the topologically most simple case; all surfaces M we consider have genus 3. There are two types of classification questions we consider. The first can be loosely described as follows: given a fixed set of symmetries, what genus 3 embedded triply periodic minimal surfaces admit these symmetries? The flat structure approach is well-suited to this type of investigation, because the presence of symmetries allows one to narrow the moduli spaces to consider, creating problems that, in principle, are easier to solve. In Chapter 3, we obtain a classification for certain fixed symmetries. The motivation here is the P surface, which provides a model surface with a large number of symmetries. For example, one of the results we obtain in Chapter 3 is

THEOREM 3.14. *Let M be an embedded triply periodic minimal surface of genus 3 that admits a rotational symmetry ρ of order 3 about an axis L in $\mathbb{R}^3$. Assume that M/Λ admits a reflection in a plane containing L so that the fixed point set in $M/\Lambda/\rho$ consists of two components. Then M is a member of the rPD or rH families.*

On the other hand, any complete classification would have to consider surfaces with essentially no symmetries. Here, the gyroid and Lidinoid families that we have constructed could be useful examples in the study of such surfaces. In particular, Traizet's method of "opening nodes" around a set of "balanced points" [**Tra02, Tra06**] may be a useful approach. A full understanding of the families indicated here may provide examples of new "balanced configuration" that can be exploited using Traizet's technique. At the very least, one could hope for a larger family of gyroids than a 1-parameter family.

1.2. Survey of techniques used

Here we briefly indicate some of the techniques employed by others to construct triply periodic minimal surfaces. Each is useful in certain contexts, but are a modification of several methods is necessary for constructing gyroid families.

1.2.1. Survey of techniques used by other authors. One method for constructing triply periodic surfaces is the conjugate Plateau method, a general tool useful in many settings (even in non-Euclidean space forms). It was employed by Karcher [**Kar89, Kar05**]

to construct many surfaces and their deformations; surfaces that have fundamental domains bounded by straight lines or planar symmetry curves are well-suited for this method. Karcher's method transforms the problem into one of finding a minimal disk with boundary a polygon in $\mathbb{R}^3$. Since the gyroid contains neither straight lines nor planar symmetry curves [**Kar89**], we cannot make use of this construction.

Meeks obtains his 5-parameter family by exploiting a hidden symmetry that many surfaces share. Every genus 3 surface can be represented conformally as a two-sheeted branched cover of S^2 with eight branch points (Proposition 2.10). Meeks considers only those surfaces which are branched over four *pairs of antipodal* points on the sphere. In homogeneous coordinates on $\mathbb{C}P^1 \cong S^2$, the antipodal map is represented by $z \mapsto -\frac{1}{\bar{z}}$. He then obtains a map f from the 2-fold branch cover of the sphere to $\mathbb{C}^3/L$, where L is a (complex) lattice in $\mathbb{C}^3$. That this construction is invariant under complex conjugation implies the existence of two rank 3 invariant sublattices, namely, representing the real and imaginary sublattices. Then the maps Re f and Im f provide the two distinct embeddings of the branched sphere. The period problem is automatically solved because of the invariance of this sublattice. The 5-parameter family comes from 8 parameters possible from picking four of the branch points, less 3 parameters since scaling and rotation is not considered a "deformation" in any reasonable sense. Meek's method fails to produce gyroid or Lidinoid examples, however, since neither is in a real or imaginary subspace of their embedding, as we shall see in the construction of the gyroid in Section 4.2.

A third method involves the modification of certain holomorphic data that describe a minimal surface. Minimal surfaces are described by three data (called the Weierstraß data): a meromorphic function G and a holomorphic 1-form dh defined on a Riemann surface X. G, the Gauß map or stereographic projection of the normal map, is a meromorphic function on a minimal surface. After choosing a base point $p \in X$, the 1-forms $\omega_1 = \frac{1}{2}(\frac{1}{G} - G)dh$, $\omega_2 = \frac{i}{2}(\frac{1}{G} + G)dh$, and $w_3 = dh$ parameterize the minimal surface as the image of $F : X \to \mathbb{R}^3$ defined by

$$(1.1) \qquad F(z) = \text{Re}\left(\int^z \omega_1, \int^z \omega_2, \int^z \omega_3 \right)$$

Furthermore, given a Riemann surface, any meromorphic G and holomorphic 1-form dh that satisfy $\omega_1^2 + \omega_2^2 + \omega_3^2 \equiv 0$ (and $|\omega_1|^2 + |\omega_2|^2 + |\omega_3|^2 \neq 0$) yield a minimal surface (in general, this surface is not even immersed). One method of constructing surfaces is to find compatible G and dh (along with a Riemann surface) that give an immersed minimal surface. Immersion is accomplished by solving the *period problem*: closed curves on the Riemann surface must map under Equation 1.1 to closed curves in space (or, in the case of triply periodic minimal surfaces, closed curves in the 3-torus). (We make these notions precise in Section 2.1.) Except in the most simple cases, however, (and certainly for the gyroid) this period problem is difficult to solve: the required dh alone is determined by an unwieldy elliptic integral. Constructing a family in this way would require the simultaneous control of three elliptic integrals, a task best suited for numerical computation.

Finally, a new technique employed by Traizet shows great promise in constructing minimal surfaces. For technical details, we refer the reader to [**Tra02, Tra06**]. Compare Figures 4.5, 4.14, and 4.20. In each case, as $\tau \to 0$, the surfaces limit to a lamination of $\mathbb{R}^3$ by planes with tiny (singular) catenoidal necks placed periodically throughout. Traizet derives a set of "balancing equations" that, if satisfied by a set of points on k-distinct planes (the balancing equations have interaction between adjacent planes) can construct a minimal surface family. To construct the family, Traizet "opens nodes" at the singularities to obtain a Riemann surface. These tiny catenoidal necks are opened using a modification of the implicit function theorem. The period problem is solved because of the balancing equations. The difficulty, then, is finding solutions to the balancing equations that yield interesting surfaces. We find it quite appealing that these "balanced points" can be considered as electrostatic forces in a stable configuration. Since we have no suggestions of what a "limit of gyroids" might look like, we have no guidance for finding an appropriate set of points that might yield a gyroid family. We hope that Traizet's method could be employed to study the gyroid after we more fully understand the families we have constructed here.

1.2.2. Overview of proof. We instead construct our family using the flat structure method introduced in [**WW98**]. To construct a family of surfaces M_t, we first start with

an embedded surface M_0. This surface will have many symmetries, and we fix a symmetry that we want the entire family to have; for instance, all M_t will be invariant under rotation by π about a vertical axis. This gives as an appropriate conformal model for our family of surfaces a two fold (since the rotation has order 2) branched cover of a torus. In order for the surfaces to be immersed, we need to solve the period problem, that is, we need closed cycles on the branched cover of a torus to map to closed cycles on $M_t/\Lambda_t \subset \mathbb{R}^3/\Lambda_t$ for some lattice Λ_t. We introduce the holomorphic 1-forms $G\,dh$, $\frac{1}{G}dh$, and dh; these induce cone metrics on the torus which allow us to understand the periods of these forms in terms of Euclidean polygons (these polygons are the development of the cone metric induced on the torus by the 1-form into the Euclidean plane). We describe two moduli spaces of polygons – one for the horizontal period problem and one for the vertical period problem; these spaces have the property that when the developed flat structures are contained in the moduli spaces, the period problem is solved. The problem of finding a family of surfaces is therefore reduced to showing that there exists a curve of Weierstraß data (a torus which gives a conformal model, and a Gauß map and height differential) so that the developed flat structures are in these moduli spaces. We obtain this curve nonconstructively as the zero set of a certain map. Embeddedness is a consequence of the continuity of the construction and the maximum principle for minimal surfaces.

1.3. Outline of dissertation

We begin in Chapter 2 with a discussion of the major tools used to construct the new families of surfaces: the Weierstraß data, theta functions, and cone structures on tori. We also include a selection of facts about triply periodic minimal surface that provide a window into the current status of a classification.

In Chapter 3, we provide a framework for classifying triply periodic minimal surface of genus 3 using the flat structure technique. After assuming the presence of sufficiently many symmetries, we are able to classify all embedded, genus 3 triply periodic minimal surfaces admitting these symmetries.

In Chapter 4, we begin the heart of the thesis by reviewing several known examples of triply periodic minimal surfaces. In each case considered here, we obtain a continuous family of minimal surfaces. This chapter also will construct the gyroid and Lidinoid using the perspective in Chapter 3 and the tools in Chapter 2. (We relegate some technical details from the construction of the P surface to Appendix A.) Again, we explore each surface using flat structures.

In Chapter 5, we set up the moduli spaces used to solve the period problem for each of the two gyroid families tG and rG and for the Lidinoid family rL. We prove in Chapter 5 the existence of the tG family in detail. The existence of the other two families are proved similarly, and we indicate any significant differences when describing the moduli spaces.

Finally, Chapter 6 contains a collection of questions and conjectures for future investigation. In particular, we indicate a number of questions that could be used to expand the classification framework to a more general classification. Also, we indicate here a number of questions about the gyroid and Lidinoid families.

CHAPTER 2

Preliminaries

Minimal surfaces have been profitably studied both from a geometric viewpoint and from the perspective of partial differential equations. We take the geometric viewpoint, where the foundational tool is the ability to describe minimal surfaces using the *Weierstraß data*.

2.1. Weierstraß data and the period problem

For this section, we refer the reader to [**DHKW92, Oss69, Nit75**] for further details and history. Let $\Omega \subset \mathbb{C}$ denote a simply connected open domain and let $h = (h_1, h_2, h_3) : \Omega \to \mathbb{C}^3$ be a non-constant holomorphic map so that $h_1^2 + h_2^2 + h_3^2 \equiv 0$ and $|h_1(z)|^2 + |h_2(z)|^2 + |h_3(z)|^2 \neq 0 \ \forall z \in \Omega$. A direct computation shows that $F : \Omega \to \mathbb{R}^3$ defined by

$$(2.1) \qquad p \mapsto \operatorname{Re} \int_{\cdot}^{p} (h_1 dz, h_2 dz, h_3 dz)$$

is a minimal surface $M \subset \mathbb{R}^3$. The *normal map*, $N : M \to S^2$ assigns to each point $p \in M$ the normal at p. The Gauß map, $G : M \to \mathbb{C} \cup \infty$ is the stereographic projection of the normal map. (Of course, all of this discussion of the normal map and stereographic projection depends upon the choice of orientation and of projection. The results are, of course, independent of choice.)

To relate Equation 2.1 to the geometry of the surface, note that we can rewrite Equation 2.1 as

$$(2.2) \qquad p \mapsto \operatorname{Re} \int_{\cdot}^{p} \frac{1}{2} \left(\frac{1}{G} - G, \frac{i}{G} + iG, 1 \right) dh.$$

The meromorphic function G in Equation 2.2 is the Gauß map:

$$(2.3) \qquad G = -\frac{h_1 + ih_2}{h_3}.$$

11

(dh is a holomorphic differential, often called the height differential.) Furthermore, given any minimal surface M, there exists a height differential dh so that it, along with the Gauß map, provide the above parameterization of a surface patch. Therefore, simply connected surface patches are fully parameterized.

The following result of Osserman gives us a way to parameterize non-simply connected surfaces.

THEOREM 2.1 (Osserman, [**Oss69**]). *A complete regular minimal surface M having finite total curvature, i.e. $\int_M |K| dA < \infty$, is conformally equivalent to a compact Riemann surface X that has finitely many punctures.*

Notice that since our triply periodic minimal surfaces M are compact in the quotient M/Λ, they necessarily have finite total curvature and therefore can be parameterized on a Riemann surface. Instead of using a simply connected domain Ω and meromorphic functions h_1, h_2, h_3, we instead consider three holomorphic 1-forms $\omega_1, \omega_2, \omega_3$ defined on a Riemann surface X, again with $\sum \omega_i^2 \equiv 0$ and $\sum |\omega_i|^2 \neq 0$ (making sense of this first quantity pointwise and locally). We can then write

$$(2.4) \qquad F : X \to \mathbb{R}^3 \qquad \text{by} \qquad p \mapsto \text{Re} \int_{\cdot}^{p} (\omega_1, \omega_2, \omega_3)$$

with

$$(2.5) \qquad \omega_1 = \frac{1}{2}(\frac{1}{G} - G)dh \quad \omega_2 = \frac{i}{2}(\frac{1}{G} + G)dh \quad w_3 = dh.$$

Since the domain is no longer simply-connected, integration of the Weierstraß data over a homotopically non-trivial loop γ on X is generically no longer zero. This integration leads to a translational symmetry of the surface.[1] We define the *period of γ* by

$$(2.6) \qquad P(\gamma) := \text{Re} \int_{\gamma} (\omega_1, \omega_2, \omega_3).$$

---

[1]The surface need not, at this point, be embedded or even immersed, so the term "symmetry" is perhaps misleading here. More precisely, if $F(p) = (q_1, q_2, q_3) \in \mathbb{R}^3$ for some choice of path of integration from the base point to p, then for any other choice of path of integration, $F(p) = (q_1, q_2, q_3) + \int_{\gamma} (\omega_1, \omega_2, \omega_3)$ for some $\gamma \in H_1(X, \mathbb{Z})$.

In order for a surface to be non-periodic, we must have $P(\gamma) = 0$ for all $\gamma \in H_1(X, \mathbb{Z})$. For a surface to be triply periodic with lattice $\Lambda \subset \mathbb{R}^3$, we must have

$$(2.7) \qquad P(\gamma) \in \Lambda \qquad \forall \gamma \in H_1(X, \mathbb{Z}).$$

Notice that we can write

$$(2.8) \qquad F_1(z) + iF_2(z) = -\int_{\cdot}^{z} G \, dh + \overline{\int_{\cdot}^{z} \frac{1}{G} dh},$$

so we can instead write the periods as

$$(2.9) \qquad P(\gamma) = \begin{pmatrix} \mathrm{Re} \left(-\int_\gamma G \, dh + \overline{\int_\gamma \frac{1}{G} dh} \right) \\ \mathrm{Im} \left(-\int_\gamma G \, dh + \overline{\int_\gamma \frac{1}{G} dh} \right) \\ \mathrm{Re} \int_\gamma dh \end{pmatrix}.$$

LEMMA 2.2. *Let X be a Riemann surface of genus g. Let $G : X \to \mathbb{C} \cup \infty$ be meromorphic, and let dh be a holomorphic 1-form defined on X. Furthermore, assume that*

(1) *if G has a zero or pole of order k at p, then dh also has a zero at p. Conversely, if dh has a zero of order k at p, then G must have a zero or pole of order k at p.*

(2) *there exists a lattice $\Lambda \subset \mathbb{R}^3$ such that for all $\gamma \in H_1(X, \mathbb{Z})$, $P(\gamma) \in \Lambda$.*

Then the Weierstraß data (X, G, dh) define an immersed triply periodic minimal surface of genus g.

PROOF. Define ω_i as described in Equation 2.5. One trivially checks that $\sum_i \omega_i^2 \equiv 0$. We need only to see that $\sum_i |\omega_i|^2$ never vanishes. Since

$$(2.10) \qquad \sum_i |\omega_i|^2 = \frac{1}{2} \left(|G| + \frac{1}{|G|} \right) |dh|,$$

Condition 1 is precisely what is needed so that the right hand side of Equation 2.10 is non vanishing. Incidentally, the quantity in Equation 2.10 is the square of the conformal stretch factor $|ds|$ (hence the reason why it must not vanish). The problem of finding data so that Condition 2 is satisfied is often called the *period problem* (or, more violently, *killing periods*). $\qquad \square$

The Weierstraß representation immediately indicates the following well-known construction of a minimal surface. Let M_0 be a minimal surface defined by Weierstraß data (X, G, dh).[2] We construct a new minimal surface M_θ using Weierstraß data $(X, G, e^{i\theta} dh)$. Note that the data still satisfies the requirements of Lemma 2.2, especially that $\sum_j e^{2i\theta} \omega_j^2 \equiv 0$. The family of surfaces M_θ $(0 \leq \theta \leq \frac{\pi}{2})$ is called the *associate family* of M_0. (Sometimes these surfaces M_θ are also called the *Bonnet transformation* of M_0.[**Nit75, Bon53**]) Notice that if the period problem is solved for M_0, it will in general not be solved for M_θ, since $P_{M_\theta}(\gamma)$ is a linear combination of $P_{M_0}(\gamma)$ and $P_{M_{\frac{\pi}{2}}}(\gamma)$, which need not be either zero or in a lattice. The associate family plays an crucial role in the construction of the gyroid and Lidinoid.

2.2. Theta functions

One task we undertake is to explicitly write down a meromorphic function on a torus $\mathbb{C}/\Gamma$ for the Gauß map G. This permits us to do some computations and to generate the pictures in Chapter 4. We accomplish this with the use of the *theta function* $\theta(z, \tau)$. We refer the reader to Mumford [**Mum83**] and Weber [**Web05**] for further details (and caution the reader to see Equation 2.20 for notation).

The meromorphic functions on $\mathbb{C}$ are precisely the (possibly infinitely many) products and quotients of linear functions. When we seek a similar building block for meromorphic functions on tori, Liouville's theorem says we must not expect doubly-periodic holomorphic functions to build such functions since all doubly periodic holomorphic functions are constant. Instead we seek a formula for a function that is as close to periodic as possible, that is, periodic in the real direction and periodic in the imaginary direction up to multiplication by a factor. More precisely, we construct a function $f : \mathbb{C} \to \mathbb{C} \cup \infty$ that satisfies

$$(2.11) \qquad\qquad f(z + 1) = f(z)$$

$$(2.12) \qquad\qquad f(z + \tau) = e^{az+b} f(z).$$

---

[2]For the purpose of this paragraph, X could be either an open domain or a Riemann surface.

By applying both Equations 2.11 and 2.12, we see that on the one hand

$$(2.13) \qquad\qquad f(z + \tau + 1) = f(z + \tau) = e^{az+b} f(z)$$

while on the other hand

$$(2.14) \qquad\qquad f(z + 1 + \tau) = e^{a(z+1)+b} f(z+1) = e^a e^{az+b} f(z).$$

Together, Equations 2.13 and 2.14 show that $a = 2\pi i n$ for some $n \in \mathbb{Z}$.

Equation 2.11 permits us to write down a complex Fourier series for f:

$$(2.15) \qquad\qquad f(z) = \sum_{j \in \mathbb{Z}} c_j e^{2\pi i j z}$$

We compute both sides of Equation 2.12 using the Fourier series to obtain on the left side

$$(2.16) \qquad\qquad f(z + \tau) = \sum_{j \in \mathbb{Z}} c_j e^{2\pi i j z} e^{2\pi i j \tau}$$

and on the right side

$$
\begin{aligned}
e^{az+b} f(z) &= e^{2\pi i n z} e^b f(z) \\
&= e^{2\pi i n z} e^b \sum_{j \in \mathbb{Z}} c_j e^{2\pi i j z} \\
&= e^b \sum_{j \in \mathbb{Z}} c_j e^{2\pi i (j+n)z} \\
(2.17) \qquad &= e^b \sum_{j \in \mathbb{Z}} c_{j-n} e^{2\pi i j z}
\end{aligned}
$$

after relabeling the indices. Combining Equations 2.16 and 2.17, we obtain

$$(2.18) \qquad\qquad c_j e^{2\pi i j \tau} = e^b c_{j-n}$$

If $n = 0$, then $f(z) = e^{2\pi i z}$, which while satisfying all of our relations is not a very interesting function. If $n > 0$, the coefficients c_j grow rapidly and the series (2.15) will not converge. For $n < 0$, we will get many different quasi-periodic functions satisfying our requirements. We will focus on the simplest case $n = -1$. Then, after setting $c_0 = 1$, we

can solve for the remaining c_j and obtain

$$(2.19) \qquad f(z) = \sum_{j \in \mathbb{Z}} e^{-jb - \pi i j \tau} e^{\pi i j^2 \tau + 2\pi i j z}$$

Seeking the simplest such function, we set $b = -\pi i \tau$ to obtain

$$(2.20) \qquad \theta_{0,0}(z, \tau) := f(z) = \sum_{j \in \mathbb{Z}} e^{\pi i j^2 \tau + 2\pi i j z}$$

This is commonly referred to as "the" theta function. We will make further normalizations, though, and set:

$$(2.21) \qquad \theta(z, \tau) := e^{\pi i \frac{\tau}{4} + \pi i (z + \frac{1}{2})} \theta_{0,0}(z + \frac{1}{2} + \frac{\tau}{2}, \tau)$$

The motivation for this normalization is the following lemma which outlines some useful properties of $\theta(z, \tau)$:

LEMMA 2.3. *The function $\theta(z, \tau)$ has the following useful properties*

a) $\theta(z + 1, \tau) = -\theta(z, \tau)$

b) $\theta(z + \tau, \tau) = -e^{-2\pi i (z + \frac{\tau}{2})} \theta(z, \tau)$

c) $\theta(0, \tau) = 0$ (furthermore, this is a simple zero)

d) $\theta(z, \tau)$ has no further zeros in $[0, 1) \times [0, \tau) \subset \mathbb{R}^2$

PROOF. Parts (a) and (b) are a direct computation. Furthermore, one checks directly that

$$(2.22) \qquad \theta(-z, \tau) = -\theta(z, \tau)$$

showing immediately that $\theta(0, \tau) = 0$. We show parts c and d by using contour integration on the contour $\sigma = \sigma_1 + \sigma_2 + \sigma_3 + \sigma_4$ defined in Figure 2.1.
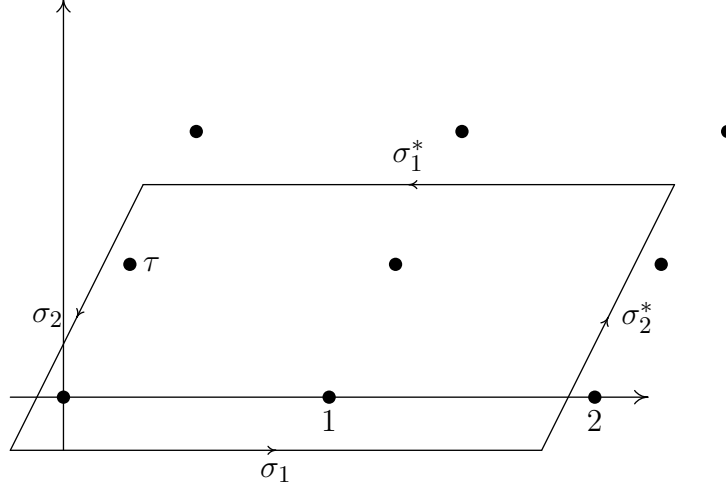
FIGURE 2.1. The contour of integration for Lemma 2.3. Zeros of $\theta(z, \tau)$ are shown as black dots. The lemma follows once we show that exactly four zeros are inside the contour.

Next, note that

$$\theta(z + 2\tau) = -e^{-2\pi i(z + \tau \frac{\tau}{2})}\theta(z + \tau) \tag{2.23}$$

$$= e^{-2\pi i(z + \tau \frac{\tau}{2})}e^{-2\pi i(z + \frac{\tau}{2})}\theta(z + \tau) \tag{2.24}$$

$$= e^{-4\pi i\tau} \cdot e^{-4\pi iz} \cdot \theta(z, \tau). \tag{2.25}$$

To count zeros, we need to compute

$$\# \text{ of zeros of } \theta(z, \tau) = \frac{1}{2\pi i}\int_\sigma (\log \theta)'. \tag{2.26}$$

(In the equations that follow, we drop the variable τ from $\theta(z, \tau)$ when there is no confusion.)

For $\sigma_2 + \sigma_2^*$, we have

$$\int_{\sigma_2} (\log \theta(z))' + \int_{\sigma_2^*} (\log \theta(z))' = \int_{\sigma_2} (\log \theta(z))' - \int_{\sigma_2} (\log \theta(z + 2))' \tag{2.27}$$

$$= \int_{\sigma_2} (\log \theta(z))' - \int_{\sigma_2} (\log \theta(z))'$$

Since $\theta(z)$ is periodic with period 2 in the real direction. For the other two contours:

$$(2.28) \quad \int_{\sigma_1} (\log \theta(z))' + \int_{\sigma_1^*} (\log \theta(z))' = \int_{\sigma_1} (\log \theta(z))' - \int_{\sigma_1} (\log \theta(z+\tau))'$$

$$(2.29) \qquad\qquad\qquad\qquad = \int_{\sigma_1} (\log \theta(z))' - \int_{\sigma_1} (\log(e^{-4\pi i \tau} \cdot e^{-4\pi i z} \cdot \theta(z,\tau)))'$$

$$(2.30) \qquad\qquad\qquad\qquad = \int_{\sigma_1} (\log \theta(z))' - \int_{\sigma_1} (-4\pi i \tau + -4\pi i z + \log(\theta(z)))'$$

$$(2.31) \qquad\qquad\qquad\qquad = -\int_{\sigma_1} -4\pi i$$

$$(2.32) \qquad\qquad\qquad\qquad = 4 \cdot 2\pi i.$$

Thus, there are precisely four zeros (counted with multiplicity) inside σ. Since we already know of four zeros in the region, each must be simple, and there cannot be any more zeros. $\qquad\square$

These properties allow us to construct meromorphic functions with prescribed zeros and poles on the torus $\mathbb{C}/\{1,\tau\}$.

PROPOSITION 2.4. *Consider points* $\{p_i\}_{i=1}^n, \{q_i\}_{i=1}^n \in [0,1] \times [0,\tau]$ *(with the* $\{p_i\}$ *(and also the* $\{q_i\}$*) not necessarily distinct). Then the function*

$$(2.33) \qquad\qquad\qquad g(z) = \prod_{i=1}^n \frac{\theta(z - p_i, \tau)}{\theta(z - q_i, \tau)}$$

has the following properties:

    (1) $g(z)$ *has a simple zero at* p_i
    (2) $g(z)$ *has a simple pole at* q_i
    (3) $g(z+1) = g(z)$
    (4) $g(z+\tau) = e^{2\pi i \sum_i (p_i - q_i)} g(z)$

Note that if we choose these points and exponents so that $\sum_i (p_i - q_i) \in \mathbb{Z}$, then g is *doubly periodic* with periods 1 and τ, and therefore is well-defined on the torus $\mathbb{C}/\langle 1, \tau \rangle$.

We will use functions like $g(z)$ later for the Gauß map of our surfaces.

2.3. Some facts about triply periodic minimal surfaces

We collect here some basic facts about triply periodic minimal surfaces; unless otherwise stated we refer the reader to Meeks' groundbreaking work [**Mee75, Mee90**].

PROPOSITION 2.5 ([**Mee75**]). *If $f : M_g \to \mathbb{R}^3/\Lambda$ is a triply periodic minimal surface of genus $g \geq 1$, then the normal map $N : M_g \to S^2$ represents M as a $(g-1)$-sheeted conformal branched cover of S^2.*

PROOF. By virtue of being a minimal surface, the Gauß map is holomorphic (see Section 2.1). Thus, as a map between Riemann surfaces, $N : M_g \to S^2$ is holomorphic, N is a conformal branched covering map (this is a local property, so it suffices to consider the local behavior of a holomorphic map). It only remains to determine the degree of N. Since M_g has mean curvature $H \equiv 0$, we have $K \leq 0$, where K is the Gaußian curvature (product of the principal curvatures). The Gauß-Bonnet theorem provides the remaining needed step:

$$
\begin{aligned}
-4\pi \deg(N) &= -\int_M |K| dA && \text{for all surfaces} \\
&= \int_M K dA && \text{since } K \leq 0 \text{ for minimal surfaces} \\
&= 2\pi \chi(M) && \text{by Gauß-Bonnet} \\
&= 4\pi(1-g),
\end{aligned}
$$

which shows that $\deg(N) = (g-1)$. □

PROPOSITION 2.6 ([**Mee75**]). *Let M be a connected, complete, embedded, non-flat triply periodic minimal surface in $\mathbb{R}^3$ invariant under the action of a lattice Λ. Then the genus of M/Λ is at least 3.*

PROOF. By Proposition 2.5, M is a $(g-1)$ degree cover of S^2. If $g = 2$, then M is a degree one cover of a sphere, and so must have genus 0. If $g = 1$, then by Gauß-Bonnet, $\int_M K dA = 0$. Since on a minimal surface $K \leq 0$, we must have $K = 0$, so M is a flat torus. The genus $g \neq 0$, since by the Gauß-Bonnet theorem any metric on the sphere must have Gaußian curvature somewhere positive. □

By abuse of language, we frequently refer to the genus of M/Λ as the "genus of M". Traizet [**Tra06**] shows that every genus occurs:

THEOREM 2.7 (Traizet, 2006). *For every lattice Λ and every $g \geq 3$, there exists a complete, embedded, orientable triply periodic minimal surface M with* genus$(M/\Lambda) = g$.

We study in this paper only surfaces of genus 3. These are, topologically, the most simple case. We will soon state some facts specific to genus three surfaces. First, we need the following definition.

DEFINITION 2.8. *A Riemann surface X is called hyperelliptic if it can be represented as a 2-sheeted, branched cover $H : X \to S^2$.*

Hyperelliptic surfaces have many special properties:

LEMMA 2.9. *Let X be a hyperelliptic Riemann surface of genus g covered by $H : X \to S^2$. Then:*

(1) *H has exactly $2g + 2$ branch points $\mathcal{B} = \{p_1, p_2, \ldots, p_{2g+2}\}$ (called the Weierstraß points)*

(2) *There exists an automorphism $\iota : X \to X$ such that $\iota(p_i) = p_i$ and that interchanges the two sheets. ι is called the* hyperelliptic involution. *Furthermore, ι is the unique involution that fixes the Weierstraß points.*

(3) *For every $T \in \mathrm{Aut}(X)$, $T(\mathcal{B}) = \mathcal{B}$*

(4) *If $T \in \mathrm{Aut}(X)$ is not ι, then T fixes at most four points.*

This is relevant to our discussion of genus 3 surfaces, because:

PROPOSITION 2.10 ([**Mee75**]). *An embedded triply periodic minimal surface $f : X \to \mathbb{R}^3/\Lambda$ is hyperelliptic if and only if X has genus 3. Furthermore, if X is hyperelliptic, the hyperelliptic points can be identified under the embedding f with the order 2 elements of Λ (inside the additive group $\mathbb{R}^3/\Lambda$).*

Lastly, we state a fact about a general (not necessarily triply periodic) minimal surface:

PROPOSITION 2.11. *Let M be a minimal surface patch with boundary. Suppose that ∂M contains a straight line l, and let $R_l M$ denote rotation of M by π about l. Then $M \cup R_l M$ defines a smooth minimal surface. Similarly, if ∂M contains a geodesic in a plane, then extension of the surface by reflecting in the plane also generates a minimal surface.*

2.4. Cone metrics and Schwarz-Christoffel maps on tori

The period problem is, in general, a difficult analytic problem to solve. The method introduced in [**WW98**] and described in detail in [**WW02**] by Weber and Wolf takes this difficult analytic problem and transfers it to one involving Euclidean polygons. To do this, they relate the analytic Weierstraß data of a surface (or a purported surface whose existence is being proven) to cone metrics on the underlying Riemann surface. We introduce in this section the notion of cone metrics and of a special class of maps that we will use to create cone metrics.

2.4.1. Cone metrics. Let X be a Riemann surface with charts (U_α, g_α), $g_\alpha : U \to \mathbb{C}$. We say that (U_α, g_α) endows X with a *flat structure* if the transition maps $g_{\alpha\beta} : \mathbb{C} \to \mathbb{C}$ are *Euclidean isometries*. When the isometries $g_{\alpha\beta}$ are just translations, we call the flat structure a *translation structure.*

In general, a Riemann surface will not admit complete flat structures (the Gauß-Bonnet theorem requires non-zero curvature for all surfaces that are not tori). However, once we admit certain mild singularities, called cone points, every Riemann surface has (many) flat structures.

Any Riemann surface with a flat structure can be *developed* into the plane using the *developing map*. The developing map is a well-defined map on the universal cover $\widetilde{X}$.

DEFINITION 2.12. *Fix a point $p \in X$ and a coordinate (U_0, g_0) containing p. We consider the universal cover to be the space of all homotopy paths based at p. Define the* developing *map*

$$\mathrm{dev} : \widetilde{X} \to \mathbb{C}$$

as follows: Take any path $\gamma \in X$. We cover γ with coordinates $U_0, U_1, \ldots U_k$. In each coordinate patch U_i, map $\gamma \cap U_i$ to $\mathbb{C}$ using g_i. Since the change of coordinates $g_{i,i+1}$ are Euclidean isometries, these developed segments $g(\gamma \cap U_i)$ fit together to form a curve in $\mathbb{C}$. This new curve is $\mathrm{dev}(\gamma)$. We will also sometimes denote this as $\mathrm{dev}_\gamma(p)$, or, when the choice of path is clear, the developed image of p.

We are now ready to discuss the singularities our flat structures will be permitted to have. We remind the reader that the *pre-Schwarzian derivative* of a function f is f''/f', when it exists.

DEFINITION 2.13. *A (Euclidean) cone C_θ with angle $\theta \in \mathbb{R}$ is the punctured disk D^*, together with a flat structure, so that the pre-Schwarzian derivative of the developing map extends meromorphically to 0 with a simple pole at 0 and residue given by*

$$(2.34) \qquad \theta = 2\pi(\mathrm{res}_0 \frac{\mathrm{dev}''(z)}{\mathrm{dev}'(z)} + 1).$$

This rather dense abstract definition is motivated by the following example:

EXAMPLE 2.14 (Positive cone angle). *We will construct a Euclidean cone with positive cone angle $\theta > 0$. Consider the punctured disk D^* with a flat structure defined by*

$$g(z) = z^{\frac{\theta}{2\pi}}$$

(with the U_α being any covering of D^* by simply connected subsets). Certainly this is a flat structure, as the change of coordinates are simply rotations. Notice that continuation of a point $z \in D^*$ is simply $ag(z) + b$ for $a, b \in \mathbb{C}$, so that

$$(2.35) \qquad \mathrm{dev}(z) = ag(z) + b.$$

The pre-Schwarzian becomes

$$(2.36) \qquad \frac{\mathrm{dev}''(z)}{\mathrm{dev}'(z)} = \frac{ag''(z)}{ag'(z)} = \frac{g''(z)}{g'(z)} = \left(\frac{\theta}{2\pi} - 1\right)\frac{1}{z}$$

with residue $\left(\frac{\theta}{2\pi} - 1\right)$. This defines a cone of angle θ — which agrees with our geometric intuition of the defined flat structure.

We call a flat structure with cone singularities a *cone metric*. When it is apparent from context that we are dealing with cone metrics, we will often refer to simply a flat structure. Cone metrics are abundant for Riemann surfaces – every holomorphic 1-form gives rise to a cone metric structure (recall that a Riemann surface of genus g has g linearly independent holomorphic 1-forms, see, for example, [**GH78**]).

PROPOSITION 2.15. *Let X be a Riemann surface with meromorphic 1-form ω. Let U_α be an open covering of X by simply connected sets, with distinguished points $p_\alpha \in U_\alpha$. Define $g_\alpha : U_\alpha \to \mathbb{C}$ by*

$$(2.37) \qquad g_\alpha(z) = \int_{p_\alpha}^{z} \omega.$$

Then (U_α, g_α) endows X with a flat structure (in fact, a translation structure).

PROOF. First, note that since U_α is simply connected, the integral $\int_{p_\alpha}^{z} \omega$ does not depend on the choice of p_α – changing p_α simply adds a constant.

Away from the zeros of ω, g_α is invertible so we have

$$(2.38) \qquad g_{\alpha\beta}(z) = z + \int_{p_\beta}^{p_\alpha} \omega = z + \text{const},$$

giving X a translation structure.

Notice that the developing map of the flat structure is given by

$$(2.39) \qquad \text{dev}(\gamma) = \int_{\gamma} \omega.$$

If ω has a zero or pole at a point p (without loss of generality, we take $p = 0$), this developing map extends meromorphically with pre-Schwarzian derivative

$$(2.40) \qquad \frac{\text{dev}''}{\text{dev}'}(z) = \frac{d\omega}{\omega}.$$

In the neighborhood of a zero or pole, we can locally write

$$\omega = z^k h$$

for a meromorphic function h with $h(0) \neq 0$. The residue of the pre-Schwarzian becomes

$$(2.41) \qquad \text{res}_0 \frac{\text{dev}''}{\text{dev}'}(z) = \text{res}_0 \frac{k}{z}$$

giving a cone of angle $2\pi(k+1)$.   □

2.4.2. Meromorphic Forms on Tori / Schwarz-Christoffel Maps on Tori. Recall that the classical Schwarz-Christoffel map provides a recipe for constructing a function mapping the upper half plane to any given planar polygon. Specifically, the Schwarz-Christoffel map

(2.42)
$$f(z) = C_1 \int^z \prod_j (w - t_j)^{a_j} dz + C_2$$

maps the points t_j on the real axis to the vertices of a Euclidean polygon with angles $\pi(a_j + 1)$, with the upper half plane mapped to interior of the polygon. By adjusting the location of the $t_j \in \mathbb{R}$, we can adjust all of the edge lengths in the polygon.

The quotients of triply periodic surfaces that we consider in this paper are parameterized on tori (note that we are only considering surfaces of genus 3). Since the development of a cone metric on a torus into the plane is a polygon that is periodic (in a sense we will make precise soon), we will find it helpful to have a version of Schwarz-Christoffel for tori. Here, theta functions take the role of the linear functions $w - t_j$.

DEFINITION 2.16. *A periodic polygon is a simply connected domain $\mathcal{P} \subset \mathbb{C}$ such that*

  (1) $\partial\mathcal{P}$ has two connected components
  (2) each component of $\partial\mathcal{P}$ is a piecewise linear curve with discrete vertices
  (3) $\mathcal{P}$ is invariant under translation by $\tau \in \mathbb{C}$

An immediate consequence of Conditions (1-3) is that $\mathcal{P}$ is conformally equivalent to an infinite strip $\mathbb{R} \times [0, a]$ by the Riemann Mapping Theorem, i.e., there exists

$$\widetilde{f} : \mathcal{P} \to \mathbb{R} \times [0, a]$$

that is conformal on the interior, extends continuously to the boundary, and is equivariant, i.e., $\widetilde{f}(p+1) = \widetilde{f}(p) + \tau$ (that this map is periodic by 1 in the domain is achieved by scaling the strip, which amounts to choosing the appropriate value of the conformal parameter $a \in \mathbb{R}$).

We denote the vertices of the boundary arcs of $\mathcal{P}$ by $\{q_i\}_{i \in \mathbb{Z}}$, with the notational convention that

$$p_i := \widetilde{f}^{-1}(q_i) \in \mathbb{R} \times \{0\} \text{ (resp. } \mathbb{R} \times \{a\}) \quad \text{if} \quad i \geq 0 \text{ (resp. } i \leq 0).$$

By the Schwarz Reflection Principal, reflection of the domain in the segment $\overline{p_i, p_{i+1}}, i \geq 0$ induces a continuous map from $\mathbb{R} \times [-a, a]$ that fails to be conformal only at the points p_i (and their conjugates in the extended domain). Extending in this way repeatedly gives a multi-valued map $f : \mathbb{C} \to \mathbb{C}$ that is conformal on simply connected domains that exclude the reflected images of the p_i.

LEMMA 2.17. *The pre-Schwarzian $\alpha := \frac{f''}{f'}$ is a well-defined, singled valued holomorphic 1-form on $\mathbb{C} - \{p_i\}$ that extends meromorphically to $\mathbb{C}$ and is doubly periodic, i.e., $\alpha(z+1) = \alpha(z)$ and $\alpha(z + 2ai) = \alpha(z)$.*

PROOF. The proof consists of three parts: 1) showing that α is single valued, 2) showing that α extends meromorphically into the punctures, and 3) showing that α is doubly periodic.

To show that α is single valued (1), consider the set of images of a point p under f. These correspond to a choice of analytic continuation along a closed curve γ based at p. When we analytically continue along γ, each time γ leaves a strip $\mathbb{R} \times [0 + n, a + n]$ ($n \in \mathbb{Z}$), the image of f (the periodic polygon) is reflected. Since we must enter a strip the same number of times as we leave it (since γ is closed), we complete an even number of reflections. Therefore, continuation along γ changes the periodic polygon $\mathcal{P}$ to a *congruent* polygon $\widetilde{f}(\mathbb{R} \times [0, a])$, so

(2.43)
$$\widetilde{f}(p) = af(p) + b$$

for $a, b \in \mathbb{C}$ (in fact, $|a| = 1$). Since each of the images of p is related to the others by a linear map, the pre-Schwarzian α is a well-defined single-valued function.

Secondly (2), we need to show that α extends meromorphically into the punctures. We direct the reader to [**Web04**] for details of this computation for the case of non-periodic polygons. The computation is identical, but we repeat it here for completeness. Without

loss of generality, we work at a puncture $p_j = 0$. After a rotation, we may assume that the $f(\overline{p_j p_{j+1}}) \subset \mathbb{R}$ (rotations do change change the pre-Schwarzian). We introduce the function

$$(2.44) \qquad\qquad\qquad\qquad h(z) = f(z)^{\frac{\alpha_j}{\pi}}.$$

Geometrically, the function h maps the semi-neighborhood $B_r(0) \cap \mathbb{R} \times [0, a]$ to a topological disk D in $\mathbb{C}$ with $D \cap \mathbb{R} \subset \partial D$. By the Schwarz reflection principal, we may extend to a well-defined, bounded holomorphic function. Therefore, h extends holomorphically into 0 with a simple zero. Since we are only working locally, we may write $h(z) = z h_0(z)$ where $h_0(0) \neq 0$. Then, writing $f(z) = h(z)^{\frac{\pi}{\alpha}}$. We may then (locally) write

$$(2.45) \qquad\qquad\qquad \frac{f''}{f'}(z) = \frac{(\alpha_j/\pi) - 1}{z} + \text{const.} + \dots$$

Thus, α extends meromorphically into the punctures.

Finally (3), we need to show that α is doubly periodic. Since $f(z) = f(z+1)$, it is clear that $\alpha(z) = \alpha(z+1)$. Note that $f(z + 2ai)$ is obtained by $f(z)$ by reflecting the polygon *twice*. Therefore, by the same argument as in part (1), $\alpha(z + 2ai) = \alpha(z)$. (We need to reflect an even number of times for part (1) to work, hence the reason why α is not periodic with period ai.) $\qquad\qquad\qquad\qquad\qquad\qquad\qquad\qquad\qquad\qquad\qquad\qquad\quad \square$

We will use the following lemma of Mumford to give an explicit expression for the map f:

LEMMA 2.18 (Chapter I, Section 6 of [**Mum83**]). *Let* $\Gamma = \langle 1, \tau \rangle$ *be a (real) lattice in* $\mathbb{C}$. *Let* $p_1, \dots, p_k \in \mathbb{C}$ *and* $\lambda_1, \dots, \lambda_k \in \mathbb{C}$ *such that* $\sum \lambda_i = 0$. *Then*

$$(2.46) \qquad\qquad\qquad \text{const.} + \sum_i \lambda_i \frac{\mathrm{d}}{\mathrm{d}z} \log \theta(z - p_k, \tau)$$

is a doubly periodic meromorphic function on $\mathbb{C}$ *with simple poles at* p_i *of residue* λ_i.

For the proof, we refer the reader to the excellent introduction to theta functions in [**Mum83**]. Finally we are able to prove a version of Schwarz Christoffel on rectangular tori:

PROPOSITION 2.19. *Let $\mathcal{P}$ be a periodic polygon with vertices q_i, $-n \leq i \leq n-1$ and interior angles α_i at q_i in a bounded fundamental domain. Then there exists points p_i, $-n \leq i \leq n-1$ and a $\tau \in \mathbb{C} \cap i\mathbb{R}$ such that the multivalued map $h : \mathbb{C} \to \mathbb{C}$ defined by*

$$(2.47) \qquad h(z) := \int_{\cdot}^{z} \prod_{i=-n}^{n-1} \theta(w - p_i, \tau)^{\frac{\alpha_i}{\pi} - 1}$$

maps the strip $\mathbb{R} \times [0, \mathrm{Im}\, \tau]$ to $\mathcal{P}$, is conformal on the interior, and is continuous up to the boundary.

PROOF. By the discussion preceding Lemma 2.17, there exists a multivalued map $f : \mathbb{C} \to \mathbb{C}$ mapping a horizontal strip to $\mathcal{P}$. As in Lemma 2.17, the pre-Schwarzian of f is denoted by α; α is well-defined on the flat rectangular torus $\mathbb{C}/\langle 1, 2ai \rangle$. We seek an explicit formula for f. Since α is doubly periodic, Lemma 2.18 gives a formula for α in terms of the residues of α.

To compute the residues of α, we may assume without loss of generality that we are computing the residues at $p_i = 0$ (since the residues of meromorphic function are invariant under translation). Consider a small, positively oriented circle γ containing 0 and no other p_j. Recall that the interior angle of $\mathcal{P}$ at $\widehat{f}(p_i)$ is α_i.

As noted in the proof of Lemma 2.17, in a neighborhood of p_i, analytic continuation along γ produces a map $\widetilde{f}$ with the property $\widetilde{f} = e^{2\pi i \left(\frac{\alpha}{\pi} - 1\right)} f + b$, so that $\widetilde{f}'(z) = e^{2\pi i \left(\frac{\alpha}{\pi} - 1\right)} f'(z)$. Then

$$\begin{aligned} \lambda_i &= \frac{1}{2\pi i} \oint_{\gamma} \alpha \\ &= \frac{1}{2\pi i} (\log f')\Big|_{\gamma} \\ &= \frac{1}{2\pi i} (2\pi i) \left(\frac{\alpha_i}{\pi} - 1\right) \\ &= \frac{\alpha_i}{\pi} - 1 \end{aligned}$$

Since α is doubly periodic, we write

$$(2.48) \qquad \alpha = \mathrm{const.} + \sum_{i} \left(\frac{\alpha_i}{\pi} - 1\right) \frac{\mathrm{d}}{\mathrm{d}z} \log \theta(z - a_k, 2ai)$$

using Lemma 2.18.

To determine the constant, let λ denote the (straight line) curve between $0 + \frac{a}{2}i$ and $1 + \frac{a}{2}i$. Then

$$(2.49) \qquad\qquad \int_\lambda \alpha = 0$$

since

$$(2.50) \qquad\qquad \int \alpha = \int \left(\log f' \right)' = \log f'$$

and f is equivariant. Since our $\theta(z+1, \tau) = -\theta(z, \tau)$ and we are taking the quotient of the same number of theta functions, the requirement that $\int_\lambda \alpha = 0$ forces the constant to be 0.

Integrating both sides of Equation 2.48, we obtain

$$f' = \exp\left(\log f' \right)$$

$$= \exp\left(\int \alpha \right)$$

$$= \exp\left(\sum_i \left(\frac{\alpha_i}{\pi} - 1 \right) \log \theta(z - a_k, \tau) \right)$$

$$= \prod_{i=-n}^{n-1} \theta(z - p_i, \tau)^{\frac{\alpha_i}{\pi} - 1}.$$

Integrating again yields the multivalued map f with the claimed properties. $\qquad\square$

Notice that the Schwarz-Christoffel integrand df is a meromorphic 1-form and, therefore, places a cone metric on the torus. The developing map is exactly f, and the cone-angles are measured in terms of the pre-Schwarzian α (compare Section 2.4.1).

EXAMPLE 2.20. *Consider the torus defined by $\mathbb{C}/\langle 1, \tau \rangle$ for some $\tau \in i\mathbb{R}$. The periodic polygon shown in Figure 2.2 has alternating interior angles $\frac{\pi}{2}$ and $\frac{3\pi}{2}$.*

Define

$$\omega = \left(\frac{\theta(z, \tau)\theta(z - \frac{\tau}{2}, \tau)}{\theta(z - \frac{1}{2}, \tau)\theta(z - \frac{\tau}{2} - \frac{1}{2}, \tau)} \right)^{\frac{1}{2}} dz.$$

ω defines a meromorphic 1-form on the torus. We can use this 1-form to put a flat structure with cone points on the torus, as in Section 2.4.1. The cone metric has cone angles π at the points $\frac{1}{2}$ and $\frac{\tau}{2} + \frac{1}{2}$ and cone angles of 3π at the points 0 and $\frac{\tau}{2}$. Developing the domain
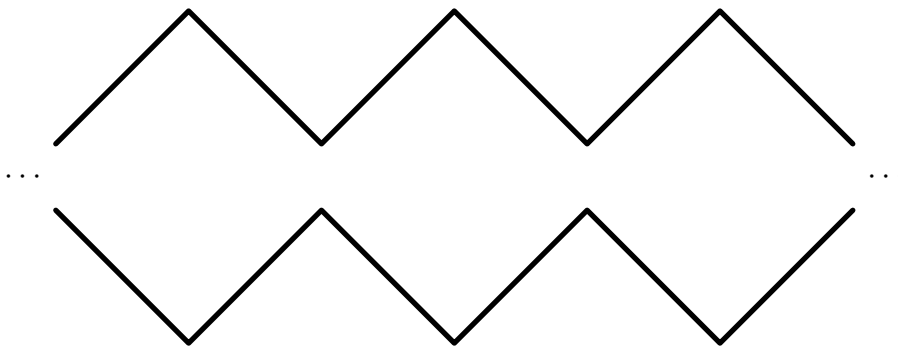
FIGURE 2.2. The developed image of the lower half of the torus with the cone metric induced by ω.

$\mathbb{R} \times \left[0, \frac{\text{Im}(\tau)}{2}\right]$ *into the Euclidean plane, we obtain the periodic polygon shown in Figure 2.2. The developed image is in fact this polygon (and not another with the same angles) because the domain is symmetric about a reflection in the line containing 0 and $\frac{\tau}{2}$, so the developed image must also share this symmetry. (Notice that because we are only taking "half" of the cone angle in the region R, the developed images have angles $\frac{\pi}{2}$ and $\frac{3\pi}{2}$. The fact that we get truly "half" of the cone angle is because the fundamental domain is bounded by a reflective symmetry of the torus.)*

CHAPTER 3

Symmetries and Quotients (Outline of a Classification)

One overarching goal in the study of minimal surfaces is achieving some sort of a classi-
fication. What embedded surfaces exist? What properties do they share? Can we explicitly
write down all the surfaces?

Traizet shows that in every lattice Λ, there exist embedded triply periodic minimal
surface of every genus $g \geq 3$. There are no connected triply periodic minimal surface of
genus $g \leq 2$. We restrict our attention for the remainder of this thesis to surfaces of genus
3. The most recognized genus 3 triply periodic minimal surface is the Schwarz P surface.
(The P surface actually comes in a family, as we shall see in Section 4.1. We are referring
here to *the* most symmetric P surface.) We describe the P surface and its symmetries, and
use the P surface as a model surface for the development of a classification outline.

Let $\mathcal{C}$ be the piecewise linear space curve obtained by removing two opposite edges from
the 1-skeleton of a regular tetrahedron. Schwarz described his P (for "primitive" lattice)
as the solution to the Plateau problem with contour $\mathcal{C}$. The complete surface is obtained
by rotating this surface patch across straight line segments in the boundary. The lattice Λ
is the cubical lattice $\langle e_1, e_2, e_3 \rangle$. In Chapter 4 we study the P surface in detail. Figure 3.1
shows two views of the P surface.

The P surface admits the following symmetries:

- An order 2 rotational symmetry about each of the x_1, x_2, and x_3 axes.
- An order 2 rotational symmetry about an axis in the x_1, x_2 plane containing the
  point $(1, 1, 0)$.
- An order 3 rotational symmetry about the line containing the origin and the point
  $(1, 1, 1)$ (there are three such similar symmetries).
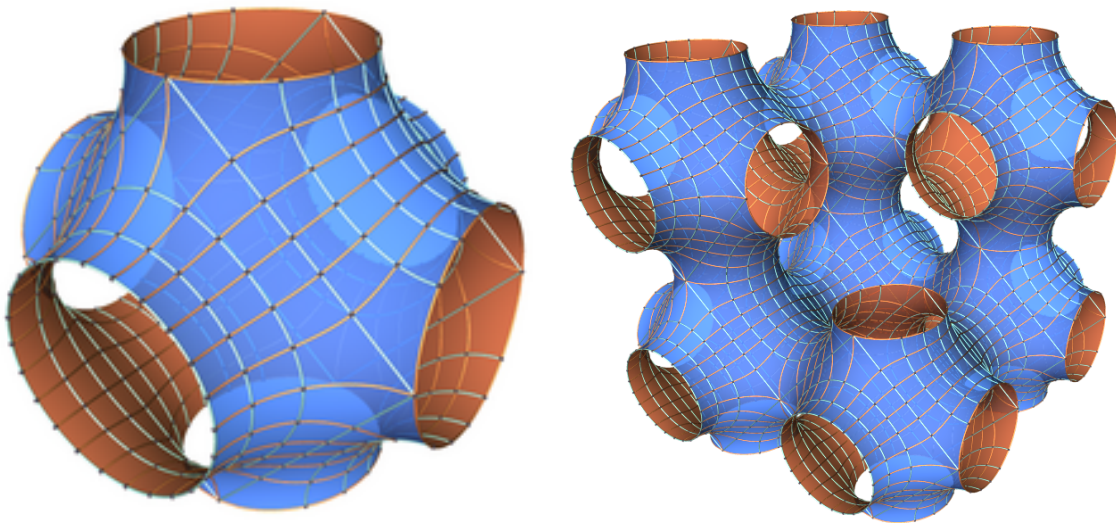- An order 4 rotational symmetry about each of the coordinate axes.

FIGURE 3.1. The Schwarz P surface. In this figure, the x_i axes do not intersect the surface (they go "through the handles").

- Three reflectional symmetries – one in each plane containing e_i and e_j.
- An additional three reflectional symmetries – one in each plane containing the x_i axis and a fixed Weierstraß point.
- Reflection about any of the lines it contains

In fact, the P surface is, in some sense, the "most symmetric" triply periodic minimal surface. We let $I(M)$ denote the isometry group of a triply periodic surface $M/\Lambda \subset \mathbb{R}^3/\Lambda$.

PROPOSITION 3.1 ([**Mee75**]). *If $g : M \to \mathbb{R}^3/\Lambda$ is a minimal surface, then $|I(M)| \leq |I(P)| = 96$, with equality if and only if M is the Schwarz P or D surface. Furthermore, each isometry of P or D is induced by a symmetry of the surface in space.*

Using the P surface as motivation, we outline a classification of surfaces by symmetries.

3.1. Classification by symmetries

We now outline a classification of triply periodic minimal surfaces by isometries of the surface that are induced by symmetries of $\mathbb{R}^3$. For reference, we recall the Riemann-Hurwitz formula and some of its corollaries (a good reference for this theorem and its corollaries is [**FK92**]).

THEOREM 3.2 (Riemann-Hurwitz formula). *Let $f : N' \to N$ be a (non-constant) holo-morphic map between a compact Riemann surface N' of genus g and a compact Riemann surface N of genus γ. Let the degree of f be n. Define the total branching number of the mapping to be $B = \sum_{P \in N'} b_f(P)$. Then*

$$g = n(\gamma - 1) + 1 + \frac{B}{2}.$$

COROLLARY 3.3 ([**FK92**], V.1.5). *For $1 \neq T \in \mathrm{Aut}(M)$,*

$$|\mathrm{fix}(T)| \leq 2 + \frac{2g}{\mathrm{order}(T) - 1} + \frac{2\gamma \, \mathrm{order}(T)}{\mathrm{order}(T) - 1}$$

with equality if $\mathrm{order}(T)$ *is prime.*

COROLLARY 3.4 ([**FK92**], proof of V.1.5).

$$(2g - 2) = \mathrm{order}(T)(2\gamma - 2) + \sum_{j=1}^{\mathrm{order}(T)-1} \left| \mathrm{fix}(T^j) \right|$$

With these tools, we are able to begin our outline. Our first task is to consider which Riemann surfaces arise as quotients of a triply periodic minimal surface M by a rotational symmetry ρ.

PROPOSITION 3.5. *Let M be an embedded triply periodic minimal surface admitting a rotational symmetry ρ with axis of symmetry x_3. Then the quotient surface $M/\Lambda/\rho$ has genus one.*

PROOF. We utilize the Riemann-Hurwitz formula. Notationally, N' is M/Λ, N is $M/\Lambda/\rho$, and f is the quotient map $f : M/\Lambda \to M/\Lambda/\rho$. Note that $\gamma \neq 3$, since f is not degree 1. Similarly, if $\gamma = 2$, then by Riemann-Hurwitz

(3.1) $$2 = n + \frac{B}{2},$$

so either $n = 2$ *and the map is unbranched* or $n = 1$ (impossible since rotational symmetries have order at least 2). If $n = 2$, then by Corollary 3.3 the map ρ must have 4 fixed points on M/Λ, implying that f is branched, a contradiction.

Furthermore, the quotient cannot have genus $\gamma = 0$, since the height differential dh is *invariant* under ρ — therefore it descends holomorphically to the quotient $M/\Lambda/\rho$. Of

course, a surface of genus 0 has no holomorphic differentials, so $\gamma \neq 0$. The only remaining possibility is $\gamma = 1$. □

Since we know, a priori, that M is hyperelliptic, the following proposition severely restricts the order of a symmetry ρ which has $M/\Lambda/\rho$ a torus. This shows that the P surface model exhibits all possible rotational symmetries induced by a symmetry of $\mathbb{R}^3$.

PROPOSITION 3.6 (Theorem 4, [**KK79**]). *Let X be a hyperelliptic Riemann surface of genus 3, and let $T \in Aut(X)$. If $X/\langle T \rangle$ has genus 1, then T has order 2, 3, or 4.*

We know, therefore, that any genus 3 surface admitting a rotational symmetry has, as a conformal model, a branched cover of a torus, and that the order of the symmetry is 2, 3, or 4. This fact is a central theme of this thesis, as we always work with the underlying torus to deform the conformal structure. By scaling, we can always normalize so that the torus is $\mathbb{C}/\langle 1, \tau \rangle$, $\tau \in \mathbb{C}$. When $\tau \in i\mathbb{R}$, the torus is rectangular, and this case is much easier to work with than any others. (The case when the torus is rhombic will be studied in a future paper, see Conjecture 6.0.5.) We will always assume the presence of sufficiently many reflectional symmetries so that the quotient torus is rectangular. More specifically:

LEMMA 3.7. *Let M/Λ be an embedded triply periodic minimal surface with rotational symmetry ρ. Without loss of generality, the axis of rotation of ρ is assumed to be the x_3 axis. Assume that M/Λ admits a reflection in a plane containing the x_3 so that the fixed point set in $M/\Lambda/\rho$ consists of two components. Then the quotient torus $M/\Lambda/\rho$ is rectangular. Furthermore, dh descends to the quotient torus as either dz or $e^{i\pi/2}dz$.*

PROOF. The vertical plane of reflection is compatible with the rotation ρ because the plane contains the x_3 axis; therefore, the action of the reflection descends to the quotient. Thus $M/\Lambda/\rho$ must admit an orientation reversing symmetry whose fixed point set has two components — the only such tori are rectangular.

On the developed image of the torus using the cone metric induced by dh, the curves of planar symmetry lying in the vertical plane will develop to horizontal curves. (To see this fact, consider the conjugate surface. Here, the vertical symmetry curve is transformed to

a horizontal straight line. On this line, Re dh is constant, so the developed image must be vertical. Taking the conjugate surface again to return to our original surface places this line horizontally.) This line of symmetry of the dh flat structure is horizontal only if $dh = e^{i\theta}dz$, where $\theta = 0, \frac{\pi}{2}$. $\qquad\square$

We also need a tool to help locate the branch points of the branched covering map on the torus. To do this, we use Abel's Theorem to restrict their location:

THEOREM 3.8 (Abel's Theorem). *Let Γ be a $\mathbb{Z}-$ lattice in $\mathbb{C}$. There is an elliptic function f on the torus $\mathbb{C}/\Gamma$ with divisor $\sum_j n_j P_j$ if and only if*

(1) $\sum_j n_j = 0$
(2) $\sum_j n_j P_j \in \Gamma$

We are now ready to being our outline of a classification.

3.1.1. Classification of surfaces admitting an order 2 rotation with rectangular quotient torus. Intuitively, we would expect that surfaces admitting only an order 2 symmetry would be "flabbier" than those admitting an order 3 or 4 symmetry. As we shall see, this is the case, and a classification of surfaces admitting an order 2 symmetry is somewhat more difficult to control. The assumptions that we make to obtain our results are a bit stronger than for the other two cases.

Let M/Λ be an embedded genus 3 triply periodic minimal surface and $\rho \in \text{Aut}(M)$ with order$(\rho) = 2$. Using a rigid motion, we orient M so that the axis of rotational symmetry is the x_3 - axis. By Proposition 3.16, M/ρ is a torus, and so by Corollary 3.3 ρ has exactly 4 fixed points (none are Weierstraß points). The fixed points are precisely those points with vertical normal, and we scale M so that the torus generators are $1, \tau$ with $\tau \in \mathbb{C} \cap \{\text{Im } \tau > 0\}$.

The squared Gauß map G^2 descends to the quotient torus. The orders of the zeros and poles are determined by:

LEMMA 3.9. *G^2 has two single order poles and two single order zeros at 0.*

PROOF. Abel's Theorem (Part 1) tells us that there must be an equal number of zeros and poles. Suppose, by way of contradiction, that G^2 had a double order zero at 0. Thus

G has at least a double order zero on the genus 3 surface P. Since dh is the lift of dz and since dz has no zeros, dh has at most single order zeros on the genus 3 surface in space (locally, the pullback map looks like z^2 at a branch point). However, in order for the metric on the minimal surface to be non-degenerate and to have no ends, dh must have at least an order 2 zero, a contradiction. Therefore, G^2 can have at most a single order zero. The same reasoning holds for the single order poles. □

Without loss of generality, one of the branch points can be placed at 0 in the torus $\mathbb{C}/\langle 1, \tau \rangle$. Also, we lose no generality by demanding that the branch point at 0 is a zero of the Gauß map. Unfortunately, Abel's Theorem does not rigidly restrict the location of the remaining three branch points. Let 0, $a_1 + b_1 i$ be the location of the branch points corresponding to zeros of the Gauß map, and let $a_2 + b_2 i$ and $a_3 + b_3 i$ be the location of the branch points corresponding to poles of the Gauß map. Abel's Theorem simply requires that

$$(3.2) \qquad \sum_{j=1}^{3} a_j + i b_j \in \langle 1, \tau \rangle.$$

This is a somewhat unsavory conclusion (for classification purposes) in that it allows for much flexibility in the branch points. In fact, Abel's theorem does not even force a discrete set of possibilities for the branch points. It is likely possible to obtain additional minimal surface families by modifying the location of the branch points. We will use the following lemma to help restrict the location of the branch points:

LEMMA 3.10. *Let M/Λ be a triply periodic minimal surface with an order 2 symmetry so that the quotient is a (branched) torus. If the quotient is fixed under the involution $-id$ centered at $\frac{1}{2} + \frac{\tau}{2}$, then the four branch points are at $0, \frac{1}{2}, \frac{\tau}{2}$, and $\frac{1}{2} + \frac{\tau}{2}$.*

PROOF. Without loss of generality, we translate so that one of the branch points corresponding to a zero of G is at $0 \in \mathbb{C}/\langle 1, \tau \rangle$. Let $\frac{1}{2} + \frac{\tau}{2} + a + bi$ denote the location of a branch point corresponding to a pole of G; suppose that $a + bi$ is not a fixed point of $-id$. Then the point $\frac{1}{2} + \frac{\tau}{2} - a - bi$ is also a branch point corresponding to a pole of G. Denote

by $c + di$ the remaining branch point. Abel's Theorem gives

$$(3.3) \qquad 0 + c + di - \left(\frac{1}{2} + \frac{\tau}{2} + a + bi\right) - \left(\frac{1}{2} + \frac{\tau}{2} - a - bi\right) = c + di - 1 - \tau$$

which is an element of the lattice $\langle 1, \tau \rangle$ only if $c + di$ is in the lattice, a contradiction (since then $c + di$ would be equivalent to 0, which is already a branch point). Thus, $a + bi$ must be one of the four fixed points: 0, $\frac{1}{2}$, $\frac{\tau}{2}$, or $\frac{1}{2} + \frac{\tau}{2}$. Continuing in this way, all the branch points must be at fixed points of $-id$. $\qquad \square$

We now have enough tools to prove our first of three classification theorems:

THEOREM 3.11. *Let M/Λ be an embedded triply periodic minimal surface of genus 3 that admits a rotational symmetry ρ of order 2 about an axis L in $\mathbb{R}^3$. Assume that M/Λ admits a reflection in a plane containing L axis so that the fixed point set in $M/\Lambda/\rho$ consists of two components. Assume further that the branch points of f are at the fixed points of the involution $-id$. Then M is a member of the tP, tD, or $tCLP$ families.*

PROOF. By Lemma 3.10, the locations of the branch points must be at 0, $\frac{1}{2}$, $\frac{\tau}{2}$, and $\frac{1}{2} + \frac{\tau}{2}$. Without loss of generality, we place a branch point corresponding to a zero of the Gauss map at at 0. We refer to the location of the other zero as z_1, and the poles as p_1, p_2.

(1) $z = \frac{\tau}{2}, p_1 = \frac{1}{2}, p_2 = \frac{1}{2} + \frac{\tau}{2}$. In Section 4.1, we show that every surface generated by this Weierstraß data is, in fact, embedded. This data generates the tP family.

(2) $z = \frac{1}{2}, p_1 = \frac{\tau}{2} p_2 = \frac{1}{2} + \frac{\tau}{2}$. In Section 4.1.3, we show that every surface generated by this Weierstraß data is also embedded — this family is called the tD family.

(3) $z = \frac{1}{2} + \frac{\tau}{2}, p_1 = \frac{1}{2}, p_2 = \frac{\tau}{2}$. In Section 4.6, we show prove that this, the $tCLP$ family, is embedded.

Certainly this data determines the conformal structure of the Riemann surface X as a double cover of a rectangular torus branched over these points. We can use theta functions as in Section 4.1 to construct a Gauß map G. We have already shown (Lemma 3.7) that dh is defined as either dz or idz (on the quotient torus). But notice that rotation of the branch points by i only yields another case (the conjugate of the tP is the tD family, while the

$tCLP$ family is self-adjoint). Therefore, a surface is determined uniquely by its quotient torus and location of the branch points (and choice of dh).

$\square$

3.1.2. Classification of surfaces admitting an order 3 rotation with rectangular quotient torus. Let M/Λ be a genus 3 triply periodic minimal surface and $\rho \in \operatorname{Aut}(M)$ be a rotation of order 3. Using a rigid motion, we orient M so that the axis of rotational symmetry is the x_3 - axis. By Proposition 3.16, $M/\Lambda/\rho$ is a torus, and so by Corollary 3.3 ρ has exactly 2 fixed points.

PROPOSITION 3.12. *Let M be a hyperelliptic Riemann surface with $\rho \in \operatorname{Aut}(M)$ of order 3. Then every fixed point of ρ is a hyperelliptic point.*

PROOF. By Lemma 2.9, $\rho(\mathcal{B}) = \mathcal{B}$ (recall that $\mathcal{B}$ is the set of Weierstraß points). We can view this action as an order 3 action on the eight point set $\mathcal{B}$, so we think of ρ as an order 3 element of the permutation group S_8. Since ρ has order three, it must be represented in S_8 as $\sigma_1 \cdot \sigma_2$, where the σ_i are disjoint 3-cycles (one is possibly the trivial cycle). In any case, at least two elements of $\mathcal{B}$ are fixed by this action, and ρ fixes only 2 points, so all fixed points are hyperelliptic. $\square$

Therefore, both fixed points of ρ are Weierstraß points. Notice that the fixed points are precisely those points with vertical normal, i.e., zeros and poles of the Gauß map G. By scaling the surface M, we can normalize the torus so that the generators are $1, \tau$, $\tau \in \mathbb{C} \cap \{\operatorname{Im} \tau > 0\}$ (note that the torus is given a flat structure by dh, which descends trivially to the quotient).

The Gauß map G is not well defined on the quotient torus, but G^3 *does* descend to the quotient torus. G^3 has exactly 1 pole and exactly 1 zero. Without loss of generality, one of the branch points can be placed at 0 in the torus $\mathbb{C}/\langle 1, \tau \rangle$. We denote the location of the pole by p. Abel's Theorem says that the order of the pole cannot be 1 (since then $p \in \{1, \tau\}$ which each are the location of zeros of the Gauß map). But also, the order cannot be larger than 2:

LEMMA 3.13. G^3 *has a double order pole at* p *and a double order zero at* 0. *Furthermore,* $p = \frac{1}{2}, \frac{\tau}{2}$, *or* $\frac{1}{2} + \frac{\tau}{2}$.

PROOF. Suppose, by way of contradiction, that G^3 had a triple order zero at 0. Thus G has at least a triple order zero on the genus 3 surface P. Since dh is the lift of dz and since dz has no zeros, dh has at most double order zeros on the genus 3 surface in space (locally, the pullback map looks like z^3 at a branch point). However, in order for the metric on the minimal surface to be non-degenerate and to have no ends, dh must have at least an order 3 zero. Therefore, G^2 can have at most a double order zero. The same reasoning holds for the double order pole. The location of p follows directly from Abel's Theorem. □

By analyzing the possible locations of branch points and restricting the conformal type of the torus, we are able to prove an order 3 classification theorem:

THEOREM 3.14. *Let* M *be an embedded triply periodic minimal surface of genus 3 that admits a rotational symmetry* ρ *of order 3 about an axis* L *in* $\mathbb{R}^3$. *Assume that* M/Λ *admits a reflection in a plane containing* L *so that the fixed point set in* $M/\Lambda/\rho$ *consists of two components. Then* M *is a member of the* rPD *or* rH *families.*

PROOF. We know that f has exactly two branch points. Without loss of generality, we place the branch point that corresponds to a zero of the Gauß map at 0. The location of the other branch point p must be one of:

(1) $p = \frac{1}{2}$. In Section 4.3, we show that every surface generated by this Weierstraß data is, in fact, embedded. This data generates the rH family.

(2) $p = \frac{\tau}{2} + \frac{1}{2}$. In Section 4.5, we show that this data also generates an embedded triply periodic minimal surface for every torus. This is the rPD family. This family has the curious property that it is *self-adjoint*; it is possible to continuously deform a surface into its conjugate *without* changing the angle of association.

(3) $p = \frac{\tau}{2}$. Even though the periods close for surfaces with this Weierstraß data, the surfaces are not embedded. Repeated rotation of the any surface in this family about its (large number of) straight lines generates surfaces shown in Figure 3.2.
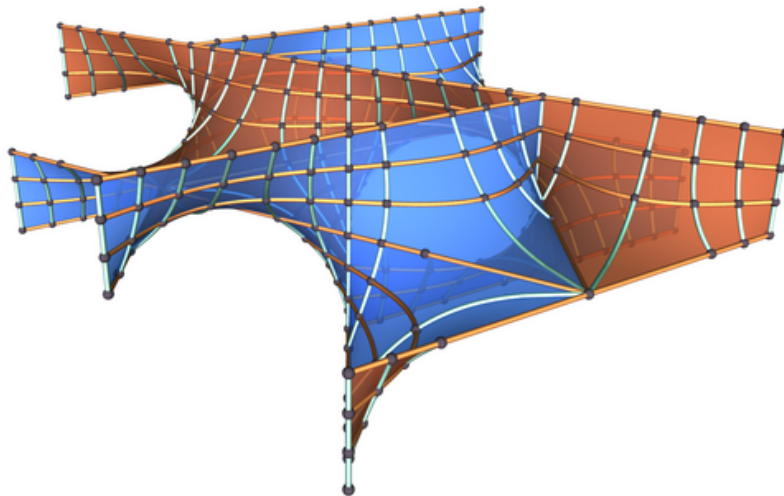
FIGURE 3.2. Adjoint surfaces to the rH family are clearly not embedded.

Since these are the only possibilities for the location of branch points, the theorem is proven. □

3.1.3. Classification of surfaces admitting an order 4 rotation with rectangular quotient torus. Intuitively, we expect the least flexibility from this case. In fact, we will show that every family admissible here is in fact already classified. (While it is tempting to conclude immediately that every family here is also invariant under order 2 and has thus already been considered, but this is not quite true. While every surface invariant under an order 4 rotation is also invariant under an order 2 rotation, the theorem we proved for order 2 surfaces is more restrictive than the theorem below.)

Let M/Λ be a genus 3 triply periodic minimal surface and $\rho \in \text{Aut}(M)$ with order 4. Using a rigid motion, we orient M so that the axis of rotational symmetry is the x_3 - axis. By Proposition 3.16, $M/\Lambda/\rho$ is a torus. Notice that since ρ is order 4, ρ^2 is order 2, and the surface is also invariant by ρ^2.

THEOREM 3.15. *Let M/Λ be an embedded triply periodic minimal surface of genus 3 that admits a rotational symmetry ρ of order 4 about an axis L in $\mathbb{R}^3$. Assume that M/Λ*

admits a reflection in a plane containing L so that the fixed point set in $M/\Lambda/\rho$ consists of two components. Then M is a member of the tP or tD families.

PROOF. Since ρ^2 is a symmetry of M/Λ of order 2, $g : M/\Lambda \to M/\Lambda/\rho^2$ has exactly four branch points, and the quotient torus $M/\Lambda/\rho^2$ is rectangular because of the presence of an orientation-reversing symmetry with disjoint fixed point sets (if the sets are disjoint under identification by $\langle\rho\rangle$, then then are disjoint under $\langle\rho^2\rangle$). The automorphism ρ (obviously) commutes with ρ^2 and so descends to the quotient as an order 2 automorphism of the torus. Furthermore, this automorphism preserves height (since in space it is a rotation), so it must leave Re dh invariant. The only order 2 automorphism of the square torus $\mathbb{C}/\langle 1, \tau\rangle$ that leaves height invariant is the translation by $\frac{\tau}{2}$ if $dh = dz$, or by $\frac{1}{2}$ if $dh = idz$. Therefore, if we place a branch point corresponding to a zero of the Gauß map at 0 and denote the location of the other zero by z, then:

(1) $z = \frac{1}{2}$. This is precisely the situation studied in Theorem 3.11, where we determined that this torus generates the tD family.

(2) $z = \frac{\tau}{2}$. This configuration is also subsumed by Theorem 3.11and is shown to yield the tP family.

$\square$

3.2. Classification by conformal automorphisms

As a final classification remark, we note that there is, in general, no reason to assume that a surface admits any symmetries at all. There is another type of automorphism of surfaces that may be useful in a classification — an isometry of the surface that is not induced by a symmetry in space. Here, the following may be useful.

PROPOSITION 3.16 (Theorem 1, [**KK79**]). *Let X be a hyperelliptic Riemann surface of genus 3, and let $T \in Aut(X)$. If $X/\langle T\rangle$ has genus 0, then T has order 2, 4, 6, 8, 12, or 14. If $\operatorname{order}(T) = 2$, then T is the hyperelliptic involution.*

There is some hope that one could deal with these cases using flat structures, even when there is no symmetry in space that induces the automorphism. We mention other generalizations of this method in Chapter 6.

CHAPTER 4

Review of Known Examples

We formulate some known examples of triply periodic minimal surfaces and obtain deformations (1-parameter families) of these surfaces using the flat structure viewpoint. This serves to introduce the idea and terminology behind our proof of the existence of a family of gyroids and Lidinoids. For the P surface, we obtain two 1-parameter families, the tP family that admits an order 2 rotational symmetry, and the rPD family that admits an order 3 rotational symmetry. For the H surface, we here obtain a single 1-parameter family of triply periodic minimal surfaces, the rH family, that is invariant under an order 3 symmetry (see Chapter 6 for comments on the probable existence of a second H surface family). A third family, the $tCLP$ family, preserves the order 2 symmetry inherent in the CLP surface. During the discussion of the P and H surfaces, we discuss the gyroid and Lidinoid surfaces; we construct these surfaces from a flat structure perspective, calculate the periods, and compute many pictures of these somewhat mystifying surfaces. We begin with the canonical example of a triply periodic minimal surface: the P surface.

4.1. The P Surface and tP deformation

The Schwarz P surface (Figure 1.2) can be constructed in a number of different ways.[1] We have described the geometric properties of the P surface in Chapter 3. We now construct this surface using a flat structure approach from which it will be easy to see that the P surface admits a deformation. While there are more efficient routes to this deformation, we take this viewpoint to illustrate the technique used for the gyroid deformation.

---

[1]It is not a trivial matter to even see that different methods are generating the same surface. Compare Figures 1.2 and 4.20 (the second for $\tau \approx 1.5$). Even though these are the *same* surface, the difference in viewpoints makes it difficult to see the similarities.

The P surface admits an order 2 rotational symmetry $\rho_2 : \mathbb{R}^3 \to \mathbb{R}^3$ with axis the x_3 coordinate axis. Since the rotation is compatible with the action of Λ on $\mathbb{R}^3$, ρ_2 descends to an order 2 symmetry of the quotient surface P/Λ (abusing notation, we also call the induced symmetry on the quotient ρ_2). ρ_2 has four fixed points on P/Λ as illustrated in Figure 4.3. (The fixed points of a rotation about a vertical axis are exactly those points with vertical normal. For any genus 3 triply periodic minimal surface, there are at most four points with vertical normal since the degree of the Gauß map is 2). The quotient $P/\Lambda/\rho_2$ is a (conformal) torus $\mathbb{C}/\Gamma$ (compare Proposition 3.16 and Corollary 3.3, noticing that ρ_2 is *not* the hyperelliptic involution since it fixes only four points).

The lattice Λ is the cubical lattice generated by the unit length standard basis vectors $\{e_1, e_2, e_3\}$. We restrict the conformal structure of the torus C/Γ by considering reflectional symmetries. The P surface admits a reflectional symmetry that also commutes with ρ_2 – the reflection in the plane containing x_1 and x_3. Its fixed point set consists of two *disjoint* totally geodesic curves. Since this reflection commutes with ρ_2, it descends to the torus $\mathbb{C}/\Gamma$ as a symmetry which yields two disjoint fixed point sets. The only conformal tori that admit two disjoint fixed point sets of a single (orientation reversing) isometry are the rectangular tori (rhombic tori admit orientation reversing isometries with a connected fixed point set). Therefore, Γ is generated by $b \in \mathbb{R}$ and $\tau \in i \cdot \mathbb{R}$. Since the conformal structure is unchanged by a dilation in space, we may dilate so that we can take $\Gamma = \langle 1, \tau \rangle$ with $\tau = ai$, $a \in \mathbb{R}$. (Note that the dilation required to achieve this normalization of the torus may change the lattice Λ so that the generators no longer have unit length.) We do not currently need to compute the value of a that yields the standard, most symmetric P surface described in Chapter 3. It can be computed using Schwarz-Christoffel maps, see Appendix A. The map $P/\Lambda \to (P/\Lambda)/\rho^2 = \mathbb{C}/\Gamma$ is a branched covering map. We can identify (using the aforementioned symmetries) the location (on the torus) of the branch points of of this map: branch points corresponding to zeros of G are located at 0 and $\frac{\tau}{2}$, while branch points corresponding to poles of G are located at $\frac{1}{2}$ and $\frac{1}{2} + \frac{\tau}{2}$.

Since the x_3 coordinate is invariant under ρ_2, the height differential dh descends holomorphically to the quotient torus as $re^{i\theta}dz$ for some $r \in \mathbb{R}, 0 \leq \theta \leq \frac{\pi}{2}$ (since dz is, up to a

constant multiple, the only holomorphic 1-form on $\mathbb{C}/\Gamma$). Varying r only scales the surface in space, so r is determined by our requirement that one of the generators of the torus is 1 (we will drop the r for the remainder of this work, since scaling is inconsequential to us). θ is the important Bonnet transformation parameter (see Section 2.1). For the P surface, $\theta = 0$. As noted in Section 3.1.1, the squared Gauß map G^2 has simple poles and zeros at the branch points.

We can explicitly write the[2] formula for G^2 using theta functions (Section 2.2):

$$(4.1) \qquad\qquad G^2(z) := \rho \frac{\theta(z, ai)\ \theta(z - \frac{a}{2}i, ai)}{\theta(z - \frac{1}{2}, ai)\ \theta(z - \frac{1+ai}{2}, ai)}.$$

The multi-valued function G on $\mathbb{C}/\Gamma$ is obtained by $G(z) = \sqrt{G^2(z)}$. (That the square root is justifiable here is the content of Section 2.4.2.) The factor ρ is called the Lopez-Ros factor[3] and gives rise to many interesting deformations of minimal surfaces, most of which are not embedded [**LR91**]. If $\rho = r_1 e^{i\phi}$, varying ϕ simply produces a rotation of the minimal surface in space. We will typically be non-committal about the value of ϕ and will use it indirectly to normalize certain quantities. We will also determine the real part r of ρ by a normalization, although varying r is highly destructive – in general, if a surface is embedded for $\rho = \rho_0$, modifying ρ will instantly yield a non-immersed surface (*à la* the Bonnet transformation). We will determine an appropriate value of ρ in Section 4.1.1.3.

Notice that the torus and the branch points are invariant under the symmetry $-id$, with quotient $S = (\mathbb{C}/\Gamma)/(-id)$ a sphere with 4 branch points.

4.1.1. Flat structures. The 1-forms Gdh, $\frac{1}{G}dh$, and dh each place a flat structure on the torus which, after taking the quotient with $-id$, descends to the sphere. We study here the developed image of each flat structure, which we will then use to compute periods. We study each flat structure independently.

4.1.1.1. *dh flat structure for the P surface.* Since the *dh* flat structure descends as $e^{i\theta}dz$, the developed image of the flat structure for the torus is simply the rectangle. Consider

---

[2]On a given torus, the locations and orders of the zeros and poles uniquely determine a meromorphic function up to constant multiple (if you have two such maps, divide them and use Liouville's Theorem).
[3]The notation is historical and is unrelated to our symmetry ρ_2.

the "lower half" of the rectangle as a fundamental domain for the action $-id$, and note the additional identification induced. One can then see directly the sphere S. The dh flat structure is, in fact, a rectangle with $\frac{\tau}{2}$ directly above 0. This is because there is a horizontal plane of reflection that interchanges the zeros and poles of the Gauß map. This horizontal symmetry curve descends to the quotient torus as a vertical straight line. This only interchanges the branch points if the torus is oriented so that the points corresponding to 0 and $\frac{\tau}{2}$ in the developed flat structure have the same imaginary part.

4.1.1.2. *Gdh flat structure for the P surface.* As noted in Section 2.4.2, the order of the zeros and poles of the 1-form Gdh produce cone angles on the torus of 3π at each of 0 and $\frac{\tau}{2}$ and of π at each of 0 and $\frac{1}{2} + \frac{\tau}{2}$. The involution $-id$ halves the cone angles in the quotient, so that on the sphere the cone angles are:

- A cone point of angle $\frac{3\pi}{2}$ at each of 0 and $\frac{\tau}{2}$.
- A cone point of angle $\frac{\pi}{2}$ at each of 0 and $\frac{1}{2} + \frac{\tau}{2}$.
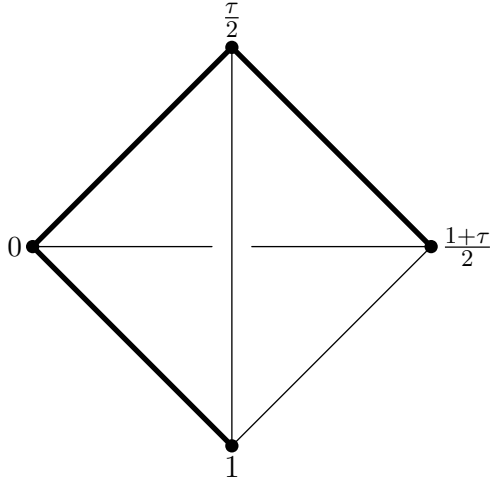

FIGURE 4.1. A three-dimensional topological picture of the sphere S with flat structure induced by Gdh (note that the angles are *not* drawn correctly). Cone points are visible at the marked vertices. Thick black lines indicate cuts made to develop the sphere (tetrahedron) into the plane. Although this is conformally not the Gdh cone metric, this tetrahedron is *conformally* the development of the dh cone metric (since all points are regular for dh).

Developing the sphere with cone metric induced by Gdh gives a hexagon:

LEMMA 4.1. *By cutting along the shortest geodesics on the sphere from $\frac{\tau}{2}$ to 0, 0 to $\frac{1}{2}$, and from $\frac{1}{2}$ to $\frac{1}{2} + \frac{\tau}{2}$ and developing into the plane, we obtain a hexagon shown in Figure 4.2. The hexagon has the following properties:*

 i) *the length of l_i is equal to the length of l_i^* for $i = 1, 2, 3$*

 ii) *the angle between l_1 and l_2 and the angle between l_1^* and l_2^* are both $\frac{3\pi}{4}$.*

 iii) *the angle between l_1 and l_1^* and the angle between l_3 and l_3^* are both $\frac{\pi}{2}$.*

PROOF. Since $T/-id$ is a sphere and since ι fixes the branch points of T, the flat structure induced by Gdh makes T/ι a tetrahedron with cone angle $\frac{3\pi}{2}$ at 0 and $\frac{w_2}{2}$ and with cone angle $\frac{\pi}{2}$ at $\frac{w_1}{2}$ and $\frac{w_1+w_2}{2}$. By making the indicated cuts, we obtain a hexagon with sides $l_1, l_2, l_3, l_1^*, l_2^*$, and l_3^*. We call the points in the developed image corresponding to $\frac{1}{2}, 0, \frac{\tau}{2}$, and $\frac{1}{2} + \frac{\tau}{2} \in T$ the points p_1, p_2, p_3, and p_4 respectively. By making a translation, we arrange so that $p_2 = 0 \in \mathbb{C}$. Each l_i was identified with l_i^* before the cutting, therefore, the length of l_i is equal to l_I^*. Also, since there is a $\frac{\pi}{2}$ cone angle at $\frac{w_1}{2}$, the angle between lines l_1 and l_1^* must be $\frac{\pi}{2}$ (similarly for l_3).

Let α denote the angle between l_1 and l_2 and let α^* denote the angle between l_1^* and l_2^*. The cone angle at 0 is $\frac{3\pi}{2}$, therefore, since both p_2 and p_2^* correspond to $0 \in T$, the sum $\alpha + \beta = \frac{3\pi}{2}$.

The torus T is invariant under reflection in the line L through $\frac{\tau}{2}$ and $\frac{1}{2} + \frac{\tau}{2}$. L is totally geodesic (as the fixed point set of an isometry), and $-id(L) = L$, therefore, L maps to a geodesic on the quotient $T/-id$. Since the quotient has flat structure, L maps to an edge connecting p_3 and p_4, and the isometry extends to the quotient tetrahedron by rotating about the edge. Since this reflection halves the cone angle, the angle between l_1 and l_2 must be $\frac{3\pi}{4}$. □

At this point, we have not yet determined the value of a for the torus. What is clear is that once a is chosen, the entire Gdh flat structure will be fixed. For the moment, we describe the flat structures and study the period problem with this determinacy still unresolved.

4.1.1.3. $\frac{1}{G}dh$ *flat structure for the P surface.* Notice that $G^2(z + \frac{1}{2})$ and $\left(\frac{1}{G}\right)^2(z)$ have precisely the same zeros and poles to the same order. By Liouville's theorem, the quotient is constant (since it is holomorphic *(no poles)* and doubly periodic):

$$(4.2) \qquad\qquad G^2\left(z + \frac{1}{2}\right) \bigg/ \left(\frac{1}{G}\right)^2(z) = r_1 e^{i\phi_1}$$

By adjusting the Lopez-Ros parameter, we can ensure that this factor is 1, and we do that for the P surface. *Therefore, the $\frac{1}{G}dh$ flat structure is simply a translation of the (infinite, periodic) Gdh flat structure.* (We can, in fact, calculate the value of ρ that achieves this normalization. The value is $\rho = 1$, and we calculate it in Appendix A.) This is reflected in the blue outline of the $\frac{1}{G}dh$ flat structure in Figure 4.2.
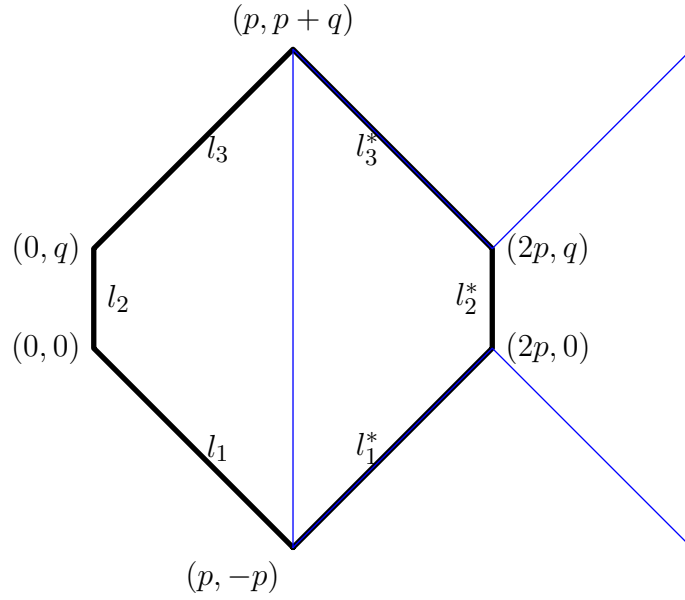

FIGURE 4.2. The Gdh (in black) and $\frac{1}{G}dh$ (in blue) flat structures for the P surface. Labeled vertices are for the Gdh flat structure (the corresponding points on $\frac{1}{G}dh$ are obtained by translation by $(-p, p)$.

4.1.1.4. *Compatibility of Gdh, $\frac{1}{G}dh$, and dh.* We have drawn Gdh and dh both oriented a specific way, namely, that the dh flat structure is horizontal and that the Gdh flat structure has the line segment l_2 vertical. We have not yet justified the latter of these two assertions. More generally, any time one prescribes all three data – Gdh, $\frac{1}{G}dh$, and dh, one has to ensure that $Gdh \cdot \frac{1}{G}dh = dh^2$. This compatibility is a serious problem when showing the

existence of surfaces in general, but the approach taken in Chapter 5 avoids this problem completely.

For the P surface, one can see that this orientation is correct as follows. There exists a vertical symmetry plane that interchanges the two zeros of the Gauß map. This reflection descends to the torus, and the symmetry curve is exactly the horizontal line at $y = \frac{\text{Im } \tau}{4}$ (recall we have fixed a fundamental domain of the torus). After a translation, dh is *real* on this symmetry curve. Under the flat structure Gdh, this symmetry curve develops to the line segment from $(0, \frac{q}{2})$ to $(2p, \frac{q}{2})$. Again, after a vertical translation, $\int Gdh$ is *real* on this segment. This is also true for $\frac{1}{G}dh$ (the developed flat structure is only a translation of that for Gdh). Thus we see that both Gdh and $\frac{1}{G}dh$ are real on thus segment, and this is compatible with dh. (The only possible inconsistency is the rotational orientation of Gdh, so it suffices to check one curve.)
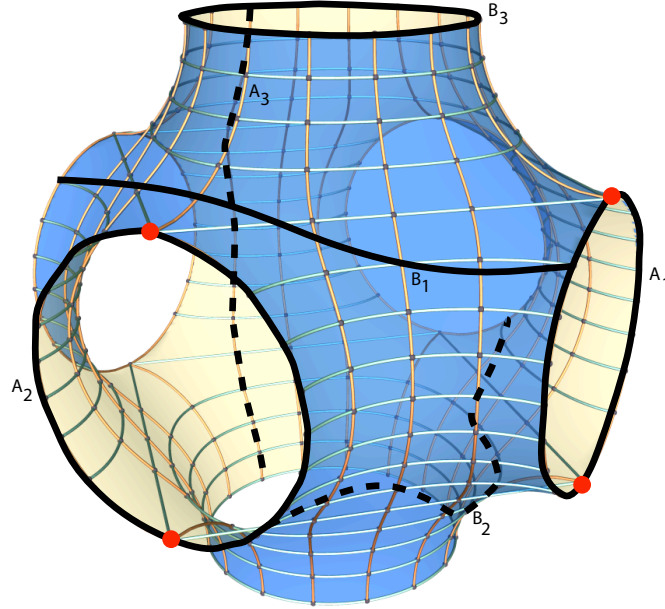

FIGURE 4.3. P surface with generators for the homology. Fixed points of ρ_2 are shown in red.

4.1.2. The period problem for the P surface. The six cycles shown if Figure 4.3 generate the homology $H_1(P/\Lambda, \mathbb{Z})$. Figure 4.4 shows these cycles on the 2-sheeted branched

torus, along with cuts to identify this structure with the surface in space. To compute the periods, we need to compute compute $\int_\gamma Gdh$ for each generator γ of the homology (and the same for $\frac{1}{G}dh$). Since $\int Gdh$ is simply the developing map of the Gdh flat structure on the torus, we can compute in terms of the cycles' image on the developed flat structure. To calculate the periods, we first obtain the horizontal contribution from the Gdh and $\frac{1}{G}dh$ flat structures:

$$(4.3) \qquad \int_{A_1} Gdh = (1+i)(p+pi) = 2p \cdot i$$

$$(4.4) \qquad \int_{A_1} \frac{1}{G}dh = (1-i)(p-pi) = -2p \cdot i$$

$$(4.5) \qquad \int_{B_1} Gdh = (1+i)(2p+q)i = (i-1)(2p+q)$$

$$(4.6) \qquad \int_{B_1} \frac{1}{G}dh = (1-i)qi = q+qi$$

$$(4.7) \qquad \int_{A_2} Gdh = (i-1)(p-pi) = 2p \cdot i$$

$$(4.8) \qquad \int_{A_2} \frac{1}{G}dh = (1-i)(p-pi) = -2p \cdot i$$

$$(4.9) \qquad \int_{B_2} Gdh = q+qi$$

$$(4.10) \qquad \int_{B_2} \frac{1}{G}dh = (1+i)(2p+q)i = (i-1)(2p+q)$$

$$(4.11) \qquad \int_{A_3} Gdh = (-1-i)(p-pi) = -2p$$

$$(4.12) \qquad \int_{A_3} \frac{1}{G}dh = (-1-i)(p-pi) = -2p$$

$$(4.13) \qquad \int_{B_3} Gdh = 0$$
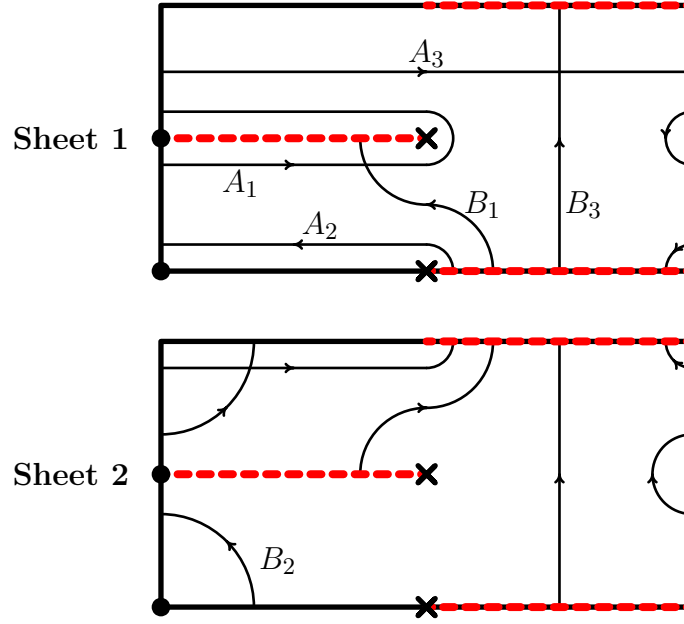
$$(4.14) \qquad \int_{B_3} \frac{1}{G}dh = 0$$

FIGURE 4.4. The conformal model of the P surface showing the homology generators. Cuts to reconstruct the surface by gluing are shown in red.

The vertical periods are easily read off of the torus as simply the difference in the endpoints of the curves drawn on the torus in Figure 4.3. Recalling that

$$(4.15) \qquad P(\gamma) = \begin{pmatrix} \mathrm{Re}\left(-\int_\gamma G\,dh + \overline{\int_\gamma \frac{1}{G}dh}\right) \\ \mathrm{Im}\left(-\int_\gamma G\,dh + \overline{\int_\gamma \frac{1}{G}dh}\right) \\ \mathrm{Re}\ \int_\gamma dh \end{pmatrix}$$

we write (transposing for compactness of notation)

$$(4.16) \qquad P(A_1) = (0,0,0)$$

$$(4.17) \qquad P(A_2) = (0,0,0)$$

$$(4.18) \qquad P(A_3) = (0,0,1)$$

$$(4.19) \qquad P(B_1) = (2(p+q), -2(p+q), 0)$$

$$(4.20) \qquad P(B_2) = (-2(p+q), -2(p+q), 0)$$

$$(4.21) \qquad P(B_3) = (0,0,0)$$

(This last horizontal period is zero due to the 2-fold symmetry of this curve. Since the cycle continues onto both sheets, we develop from p_1 to p_4, then rotate $180°$ (to get on the other sheet), then develop the same length again. This causes the horizontal period for B_3 to vanish.) It is immediately clear that these periods generate a 3-dimensional lattice Λ *for all values of p and q.* In other words, the period problem is solved no matter what the actual lengths of the segments in the developed flat structure are. Thus *any value of a (and therefore, any quotient torus) solves the period problem.*

While we have phrased this section as if we were describing the P surface, what we have actually seen is that there is a family of immersed triply periodic minimal surfaces that contains the P surface.

THEOREM 4.2. *There exists a continuous family of embedded triply periodic minimal surfaces of genus 3 that contains the P surface (the tP family). Each member of the family admits an order 2 rotational symmetry and has a horizontal reflective symmetry plane.*

PROOF. Let X_τ be the genus 3 Riemann surface which is a branched, double cover of a (conformal) flat rectangular torus $\mathbb{C}/\langle 1, \tau \rangle$ with cuts as shown in Figure 4.3. Define dh to be the lift of dz. Define G as in the discussion above, so that branch points occur at the half lattice points of $\mathbb{C}/\langle 1, \tau \rangle$. G and dh determine Weierstraß data which solves the period problem (because of the above calculations). The Weierstraß data and X define an immersed minimal surface M_τ. Embeddedness follows from Proposition 5.6 (which is a consequence of the embeddedness of the P surface and the continuity of the family). Since we have placed the branch points at half-lattice points of the 2-torus, reflection about the vertical line in the plane containing the point $\frac{1}{4}$ is a symmetry of the torus which interchanges zeros and poles. This is compatible with the rotation ρ_2 and lifts to a reflective symmetry (which is a horizontal plane since the line is vertical). □

We will call this family of minimal surfaces the tP family (Figure 4.5) because the lattice remains "tetragonal" throughout the deformation (see, e.g., [**FH99**]). Notice that the limit $\tau \to 0$ looks like a pair of parallel planes joined with small catenoidal necks. The

limit $\tau \to \infty$ looks like a pair of perpendicular planes that are desingularized along the intersection by adding handles (like the singly periodic Scherk surface).

4.1.3. The tD family. We remark briefly that one can also obtain an embedded family of surfaces by considering the conjugate surface to each member of the tP family. To compute the periods, multiply Gdh and $\frac{1}{G}dh$ by i; a simple computation shows that the periods do, in fact, close. We show this well known family in Figure 4.6.

4.2. The gyroid

We are finally ready to describe the gyroid minimal surface. In his 1970 paper [**Sch70**], Schoen describes a surface that is associate to the P and D surfaces and is embedded. Prior to Schoen's paper, it was known that only countably many surfaces associate to the P surface are immersed. Schoen reproves this fact, and finds a unique embedded surface – the gyroid.

Let (X, G, dh) be the Weierstraß data describing the P surface (see Section 4.1). Recall that a surface is called *associate* to (X, G, dh) if its Weierstraß data is $(X, G, e^{i\theta}dh)$. For a single value of θ, this associate surface is an embedded minimal surface, which Schoen called the gyroid.[4] In his description of the gyroid, Schoen provided the following estimate for θ:

$$\theta \approx 38.0147740°.$$

That this value of θ, and only this value[5], produces an embedded minimal surface is something of a curiosity. In [**GBW96**], the gyroid is described geometrically as follows:

> The P-surface can be tessellated by square catenoids with vertical axes. These catenoids have boundary on a rectangular box of height 1 with a square bottom of edge length $\sqrt{2}$. Their waist is almost a circle of diameter 1.[6]

---

[4]The name likely came from the gyrating ribbons seen in Figure 4.9. These "square ribbons" come from opening up the square catenoids of the P surface in the associate family.

[5]Except, of course, when $\theta = 0$ (P surface) and $\theta = \frac{\pi}{2}$ (D surface).

[6]That the waist is not a true circle is easily seen by Björling's formula [**DHKW92**]. If it were a circle, the normals along the curve would be the radius. The catenoid contains the same curve with the same normal, and Björling's formula asserts there is a unique minimal surface containing a given curve and normal field along the curve.
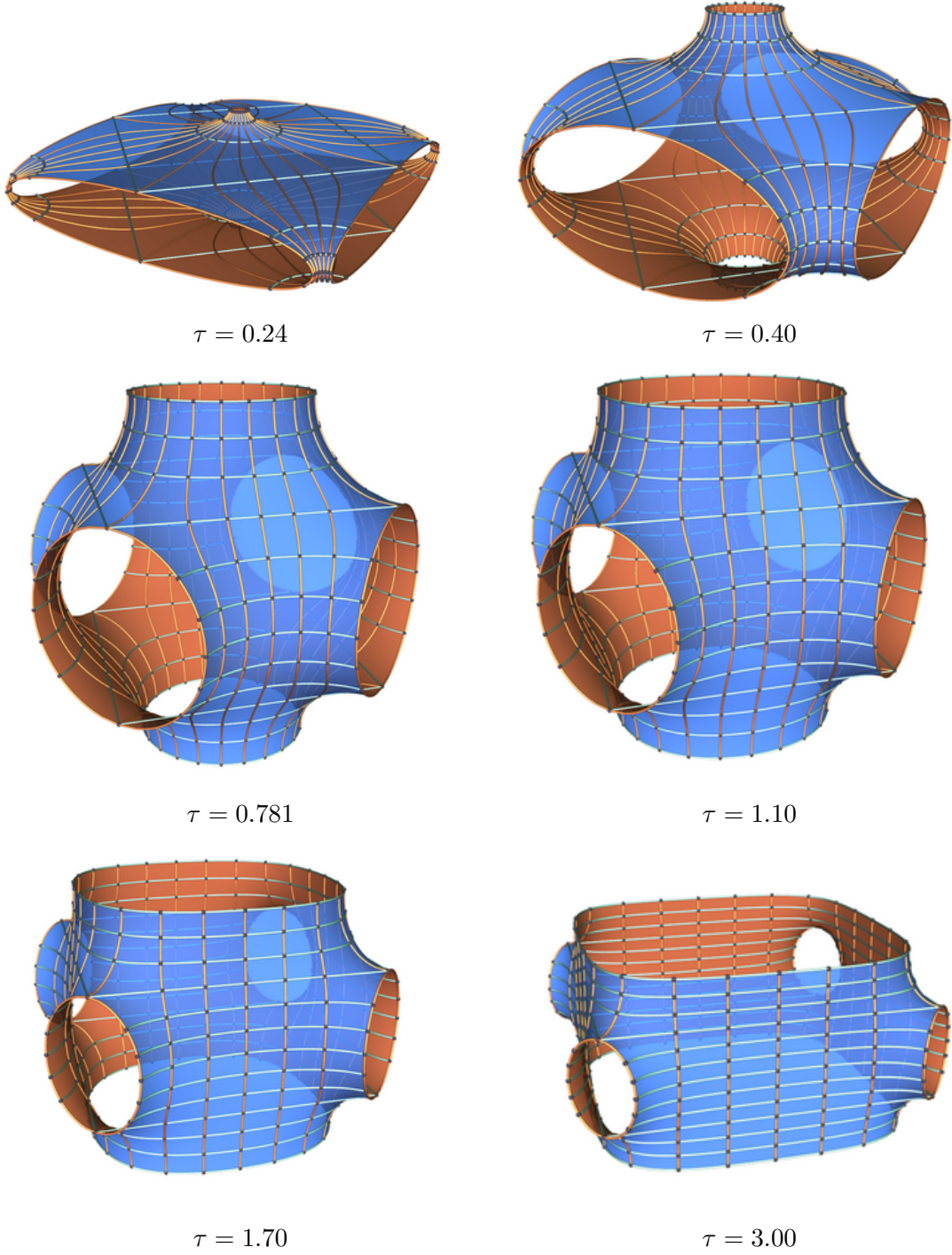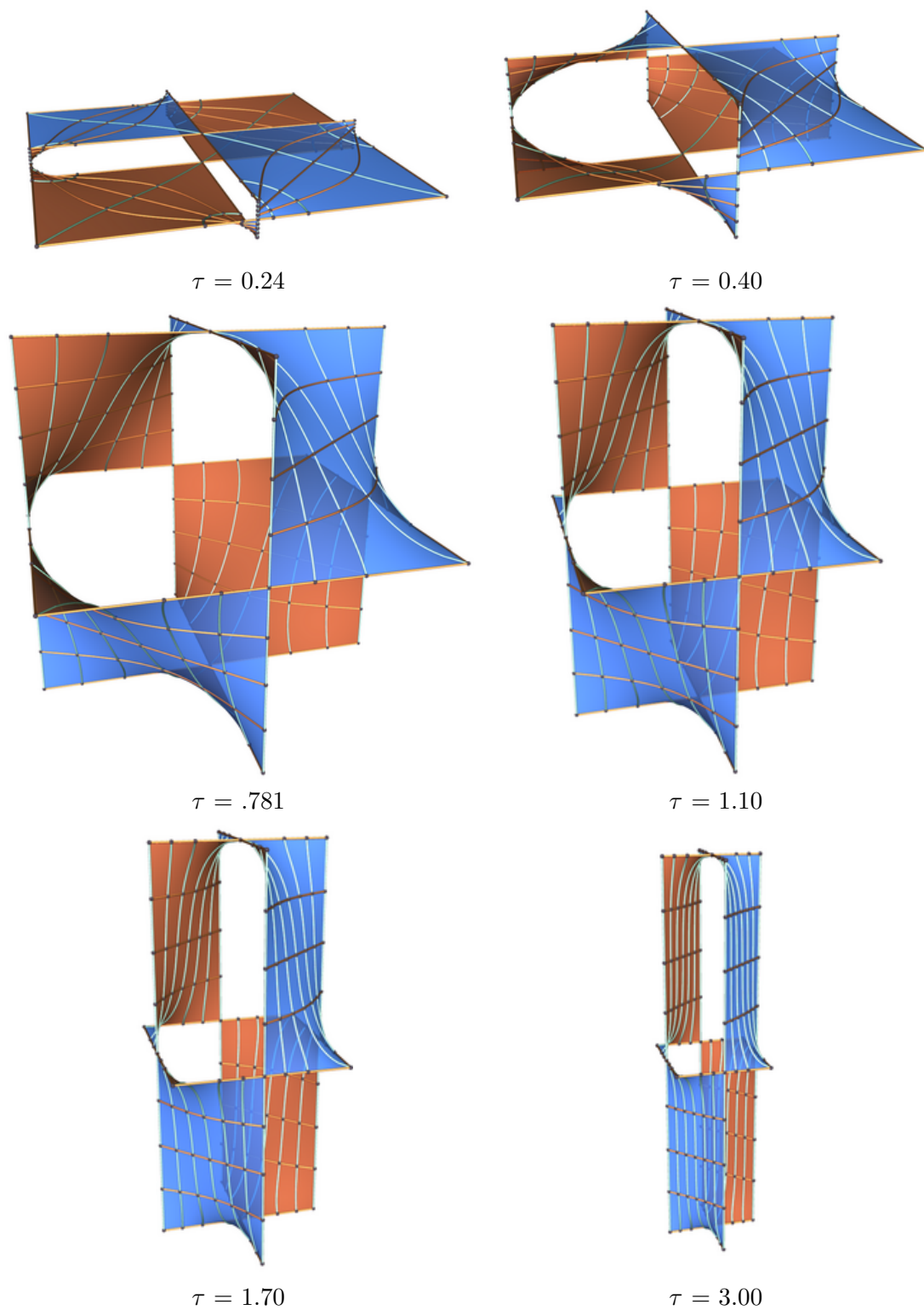
FIGURE 4.5. The tP deformation of the P surface, for different values of τ.

$\tau = 0.24$ $\tau = 0.40$

$\tau = 0.781$ $\tau = 1.10$

$\tau = 1.70$ $\tau = 3.00$

FIGURE 4.6. The tD family for various τ.

$\tau = 0.24$

$\tau = 0.40$

$\tau = .781$

$\tau = 1.10$

$\tau = 1.70$

$\tau = 3.00$
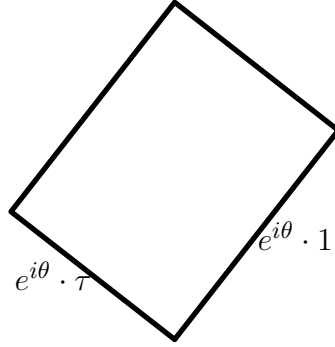
FIGURE 4.7. The alignment of the *dh* flat structure for the gyroid, showing the location of the branch points.

Notice that the "square bottom" refers to a curve which is homologous to the curve B_3 on our description of the P surface. The "height" of the "rectangular box" refers to twice the vertical period of the curve A_3.

Later from the same paper, Große-Brauckmann and Wohlgemuth write:

> When we run through the associated family from P to D these catenoids open up and a vertical period arises. ... The square curves of our catenoids become square helices in vertical distance 1. ... The vertical translation t of a square helix increase with the angle of association from 0 for P to about [the circumference of the waist] for D ... Only for $t > 1$ the ribbon does not self-intersect and then it leaves an 'empty ribbon' of height $t - 1$ in between. For $t = 2$ the later height is also 1, and the four adjacent vertical square cylinders fill exactly in.

This "opening up" of the P surface can be seen in Figure 4.8. Translating Große-Brauckmann and Wohlgemuth's terminology into ours, the angle of associate for the gyroid is such that the waist opens up to have period twice that of the period giving the height of the box. In other words, the vertical period of B_3 must be twice that of A_3. Since the B_3 curve continues on both sheets of the torus, we need the images of the curves on *a single* sheet of the developed image of the *dh* flat structure of the torus to have *equal real part*. This is equivalent to choosing θ so that the rotated flat structure places the point $1 + \tau$ directly above 0 in the developed image (see Figure 4.7). Therefore,

$$(4.22) \qquad\qquad\qquad \theta = \operatorname{arccot} \operatorname{Im} \tau.$$

Unfortunately, even this simple definition is not as simple as it seems. The value of τ that gives the standard, most symmetric P surface still must be determined by an elliptic integral. In other words, if (X, G, dh) is any member of the tP family, then $(X, G, e^{i\theta}dh)$ is an embedded surface only if $\theta = 0$, $\theta = \frac{\pi}{2}$, or (X, G, dh) describe the most symmetric (what we call the "standard") P surface. As an unfortunate consequence of this fact, we see that varying $\tau \in i \cdot \mathbb{R}$ is not enough to yield a family of gyroids – we must consider $\tau \in \mathbb{C}$.

We can calculate the periods of the gyroid by using the P surface flat structures. For instance, since for the P surface,

$$(4.23) \qquad \int_{A_1} Gdh = (1 + i)(p + pi) = 2p \cdot i$$

$$(4.24) \qquad \int_{A_1} \frac{1}{G}dh = (1 - i)(p - pi) = -2p \cdot i$$

for a member of the associate family, the corresponding developed cycle is

$$(4.25) \qquad \int_{A_1} Gdh = e^{i\theta}2p \cdot i$$

$$(4.26) \qquad \int_{A_1} \frac{1}{G}dh = -2e^{i\theta}p \cdot i$$

so that the period becomes

$$(4.27) \qquad P(A_1) = (4p\sin(\theta), 0, --)$$

Applying a similar computation to the B_1 period, we obtain

$$(4.28) \quad P(B_1) = (2p\cos(\theta) + 2q\cos(\theta) + 2p\sin(\theta), -2p\cos(\theta) - 2q\cos(\theta) + 2p\sin(\theta), --)$$

Since $P(A_2) = (0, 4p\sin(\theta), --)$, $P(A_1)$ and $P(A_2)$ will generate at least the horizontal part of the lattice. This forces either

$$(4.29) \qquad 2p\cos(\theta) + 2q\cos(\theta) + 2p\sin(\theta) = 4p\sin(\theta)$$

or

$$(4.30) \qquad -2p\cos(\theta) - 2q\cos(\theta) + 2p\sin(\theta) = 4p\sin(\theta)$$

FIGURE 4.8. Six members of the associate family of the P surface.

$\theta = 0$ $\theta = 5\pi/180$

$\theta = 30\pi/180$ $\theta = 0.6634$

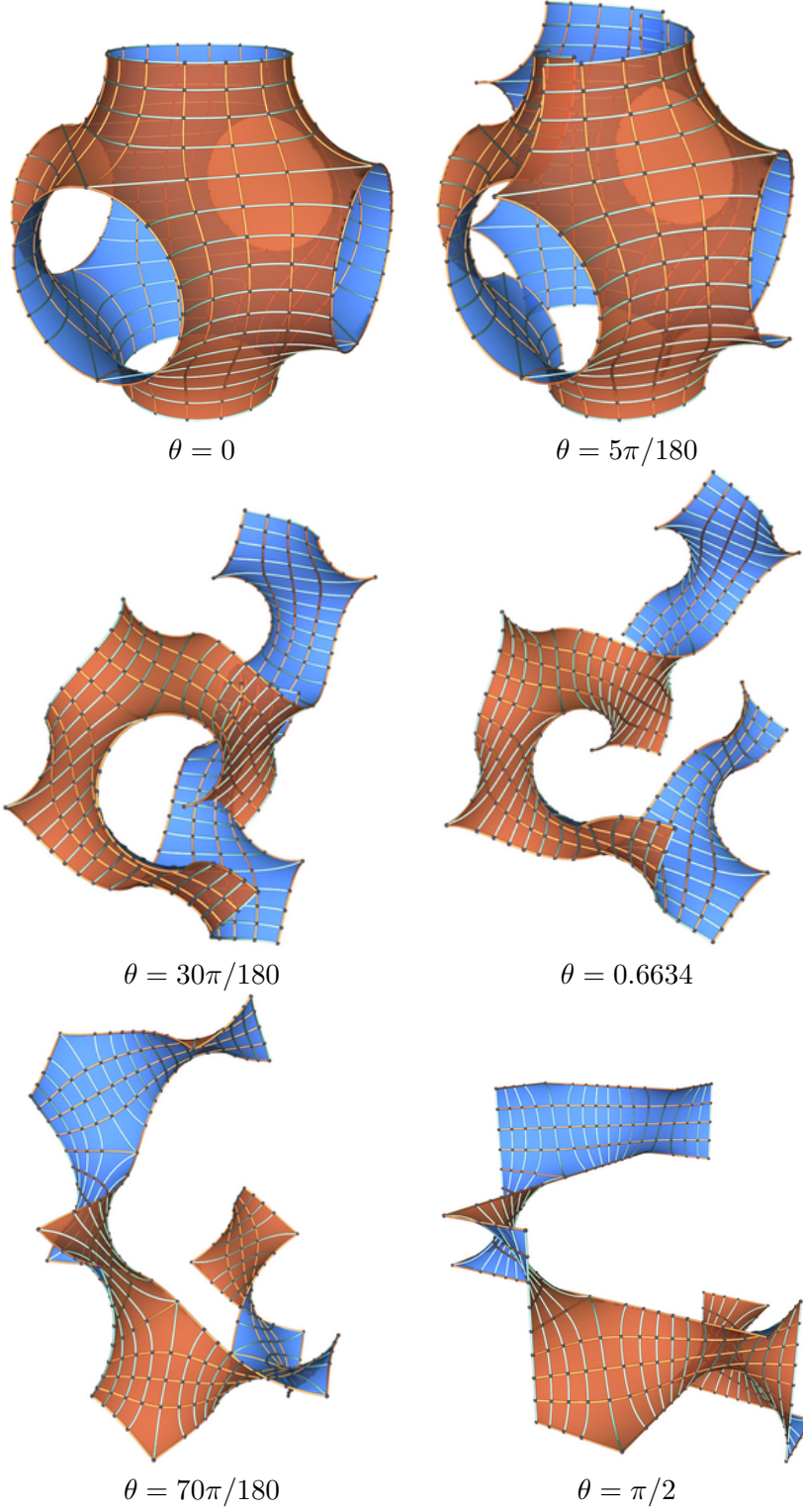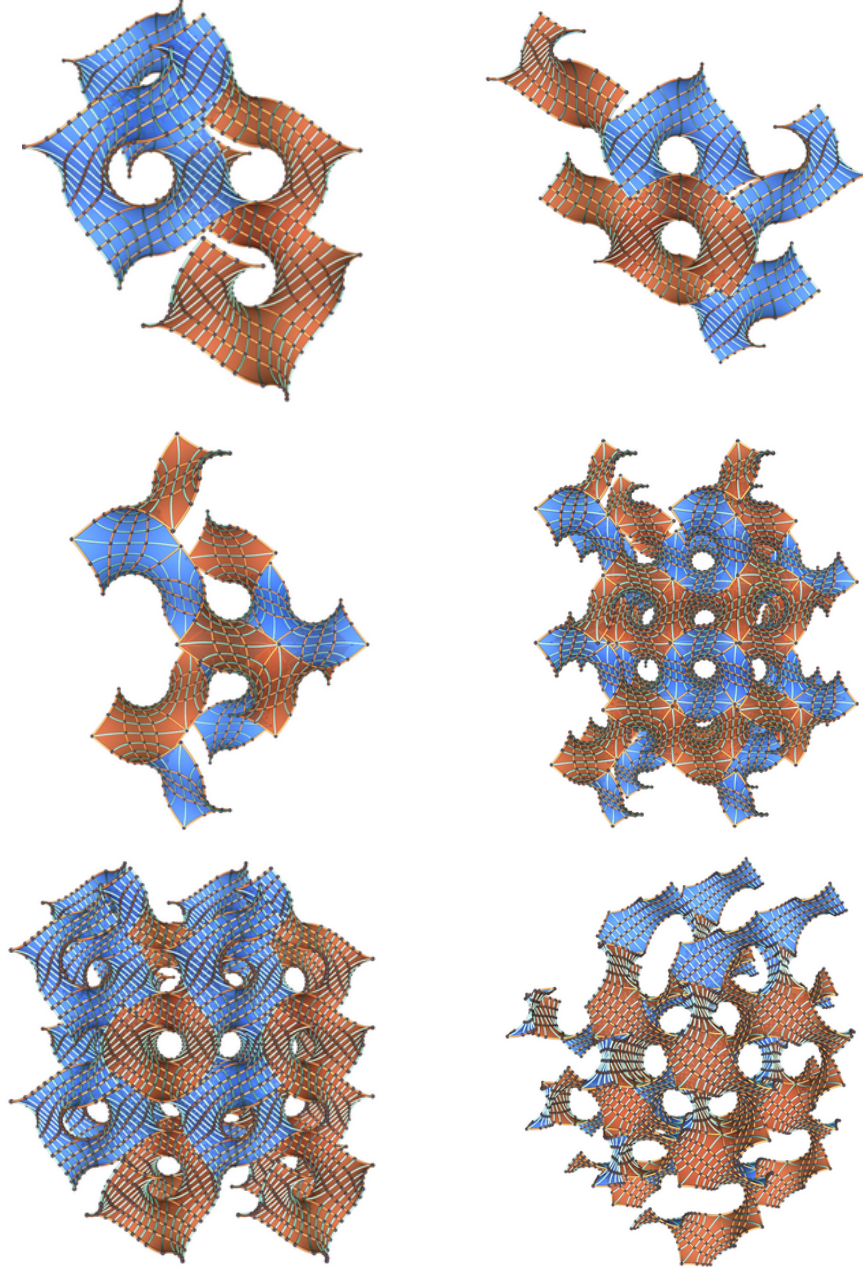$\theta = 70\pi/180$ $\theta = \pi/2$

FIGURE 4.9. Shown here are various views of a translational fundamental domain of the gyroid, including several assembled fundamental domains. Notice the "gyrating" ribbons. To obtain a translational fundamental domain, one takes the surface patch shown in Figure 4.8 and connects a copy after a glide reflection.
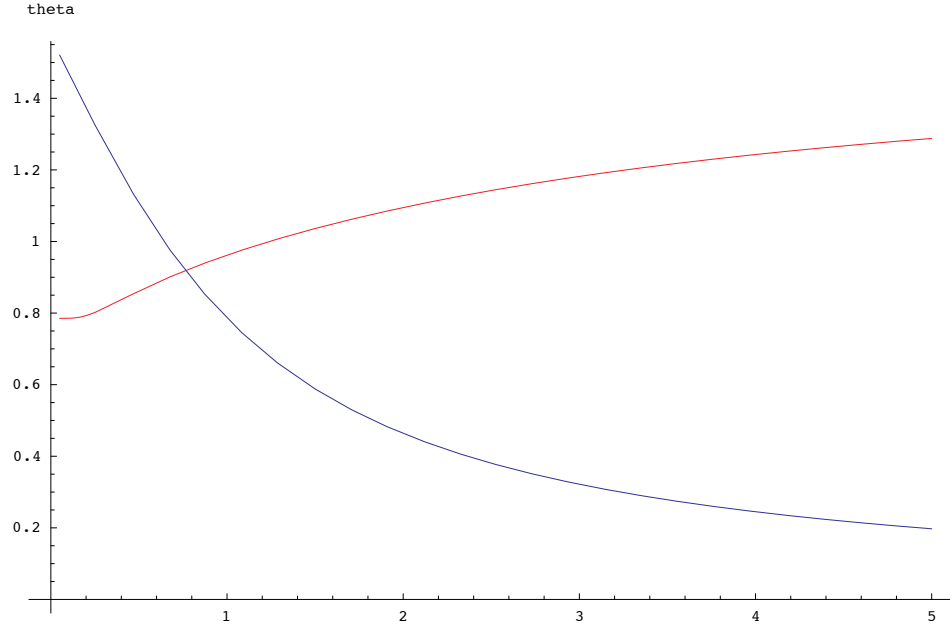
FIGURE 4.10. Plots of the value of θ required to solve the horizontal (in red) and vertical (in blue) period problems vs. a. The intersection point is the gyroid.

Since $\cos(\theta) \geq 0$ for $0 \leq \theta \leq \frac{\pi}{2}$, Equation 4.29 must hold. Thus, given p and q, θ is *uniquely determined* by the horizontal period problem.[7] However, the values of p and q are determined by the generators of the torus, namely, by $\tau = a \cdot i$. But Equation 4.22 also defines a unique θ that solves the *vertical* period problem. These two conditions are compatible for only one torus: that which defines the standard P surface. Figure 4.10 shows the behavior of these two curves.

The periods of the gyroid are calculated as:

$$(4.31) \qquad\qquad P(A_1) = (1, 0, 0)$$

$$(4.32) \qquad\qquad P(A_2) = (1, 0, 0)$$

$$(4.33) \qquad\qquad P(A_3) = (0, 1, 1)$$

$$(4.34) \qquad\qquad P(B_1) = (1, 0, -1)$$

$$(4.35) \qquad\qquad P(B_2) = (-1, 0, -1)$$

---

[7]We've only shown that this is a necessary condition, which is all we need at the moment.

$$(4.36) \qquad\qquad P(B_3) = (0, 0, 2)$$

We remark that we have gone through a fairly complicated set of gymnastics to show that the gyroid is even immersed. We have used this method to show that the gyroid is immersed because it sets up the period problem nicely for Chapter 5 where we prove the existence of two families of gyroids. There is, however, a much easier way to see that the gyroid is immersed. Instead of considering the flat structures induced by Gdh, $\frac{1}{G}dh$, and dh, consider instead the Weierstraß 1-forms ω_1, ω_2, and $\omega_3 = dh$. The standard P surface admits an order 3 rotational symmetry that interchanges each of the coordinate axis; the action of this rotation on the space of holomorphic forms permutes the 1-forms ω_i. The flat structures, therefore, are all congruent; furthermore, all of the periods can be expressed in terms of these 1-forms. Since the associate family parameter θ solves the vertical period problem and since the flat structures of these forms are all congruent, the period problem is completely solved. Even this (almost) one line proof easily shows that the gyroid is immersed, this technique seems to fail miserably to achieve a family of gyroids. As soon as we lose the symmetry of the standard P surface, we do not find this technique terribly useful.

4.3. The H surface

The H surface (Figure 1.2) is a genus 3 triply periodic minimal surface that admits an order 3 rotational symmetry. The H surface can be thought of as a "triangular catenoid" in the same way that the P surface contains "square catenoids". The H surface lattice is spanned by a planar hexagonal lattice (along with a vertical component), in contrast to the square planar lattice for the P surface. We proceed precisely analogously to the P surface, and omit most of the narrative of the construction.

The order 3 rotation $\rho_3 : \mathbb{R}^3 \to \mathbb{R}^3$ again is compatible with the action of Λ and so descends on H/Λ to a well-defined isometry with 2 fixed points (note that by Corollary 3.12 these are both hyperelliptic points). As noted in Chapter 3, there are only two possible locations for the pole of the Gauß map on the torus, $\frac{1}{2}$ or $\frac{1}{2} + \frac{\tau}{2}$. Since there is a reflective

symmetry of H whose fixed point set contains both fixed points of the map, the same must be true on the torus. This forces the pole to be located at $\frac{1}{2}$. Again, symmetry considerations force the torus to be rectangular, and we normalize so that it is generated by $\langle 1, \tau \rangle, \tau \in i\mathbb{R}$. By Lemma 3.13, the zero and poles are double order.

We write

$$(4.37) \qquad\qquad G^3(z) := \rho \frac{\theta_{11}(z, \tau)}{\theta_{11}(z - \frac{1}{2}, \tau)}$$

and we again set the Lopez-Ros factor $\rho = 1$ for the appropriate normalizations.

The torus *is* invariant under $-id$ (which is here the hyperelliptic involution). We indicate the conformal structure of the branched cover and the relevant cycles in Figures 4.11, 4.12.

4.3.1. Flat structures. The 1-forms Gdh, $\frac{1}{G}dh$, and dh each place a flat structure on the torus which, after taking the quotient with $-id$, descends to the sphere. We study each flat structure independently:

4.3.1.1. *dh flat structure for the H surface.* Since the dh flat structure descends as dz, the flat structure for the torus is simply the rectangle.

4.3.1.2. *Gdh flat structure for the H surface.* As noted in Section 2.4.2, the order of the zeros and poles of the 1-form Gdh produce cone angles on the torus of $\frac{10\pi}{3}i$ at 0 and of $\frac{2\pi}{3}$ at $\frac{1}{2}$. The remaining fixed points, at $\frac{\tau}{2}$ and $\frac{1}{2} + \frac{\tau}{2}$, are regular points. The involution $-id$ halves the cone angles in the quotient, so that on the sphere the cone angles are:

- A cone point of angle $\frac{10\pi}{6}$ at 0.
- A cone point of angle $\frac{\pi}{3}$ at $\frac{1}{2}$.
- A cone point of angle π at each of $\frac{\tau}{2}$ and $\frac{1}{2} + \frac{\tau}{2}$.

The flat structure is a hexagon:

LEMMA 4.3. *By cutting along the shortest geodesics on the sphere from $\frac{\tau}{2}$ to 0, 0 to $\frac{1}{2}$, and from $\frac{1}{2}$ to $\frac{1}{2} + \frac{\tau}{2}$, we obtain a hexagon shown in black in Figure 4.13. The hexagon has the following properties:*

i) the length of l_i is equal to the length of l_i^* for $i = 1, 2, 3$

ii) the angle between l_1 and l_2 and the angle between l_1^* and l_2^* are both $\frac{5\pi}{6}$.
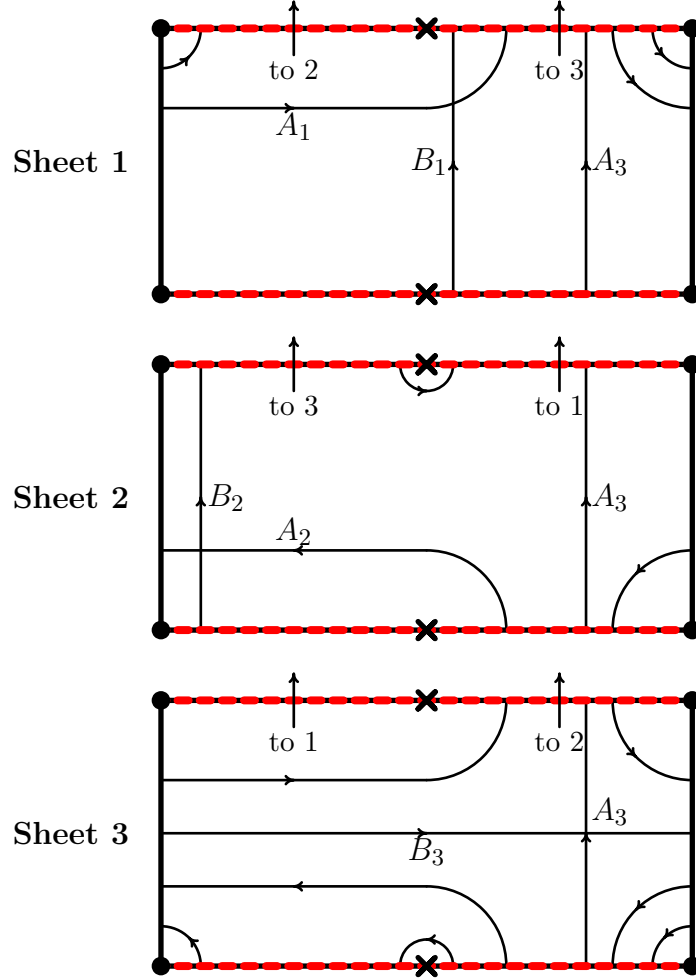
FIGURE 4.11. The conformal structure of the H surface branched cover of a torus. Cuts are shown in red.

iii) the angle between l_1 and l_1^* is $\frac{\pi}{2}$ and the angle between l_3 and l_3^* is π.

The proof is precisely analogous to Lemma 4.1. We find this flat structure somewhat inconvenient to work with when the flat structure on the entire torus (without the $-id$ identification) is so simple. The flat structure on the entire torus is obtained by rotating by π about the vertex between l_3 and l_3^* (the $-id$ map descends on the developed image to the $-id$ map since $\frac{1}{2} + \frac{\tau}{2}$ is a regular point). Doing so, we obtain the flat structure shown in Figure 4.13 (compare to the P surface flat structure).
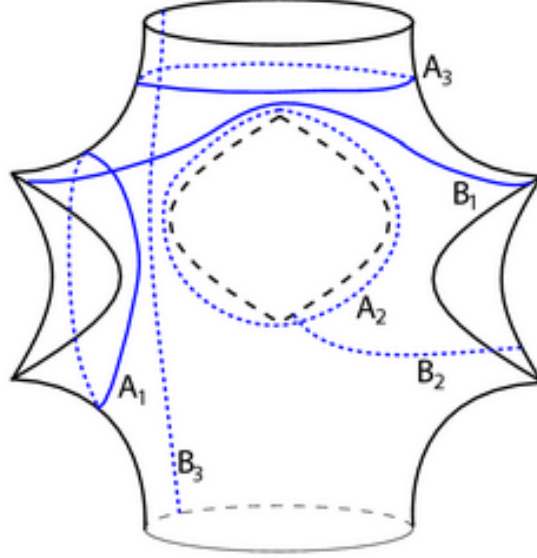
FIGURE 4.12. A canonical set of generators of $H_1(H, \mathbb{Z})$

Again we have not chosen the imaginary part of τ as we expect to recover a family of surfaces.

4.3.1.3. $\frac{1}{G}dh$ *flat structure for the H surface.* By precisely the same argument as in Section 4.1.1.3, the $\frac{1}{G}$ flat structure is simply a translate of the Gdh flat structure (with the Lopez-Ros factor $\rho = 1$). The blue outline in Figure 4.13 shows this translation.

4.3.2. The period problem for the H surface. We illustrate in Figure 4.11 the conformal structure of the H surface with the six cycles that generate the homology $H_1(H/\Lambda, \mathbb{Z})$ (since there are more than two sheets, note the indicators on the cuts showing the proper identifications). These cycles are shown on the surface in Figure 4.12. Again, we compute using the flat structures:

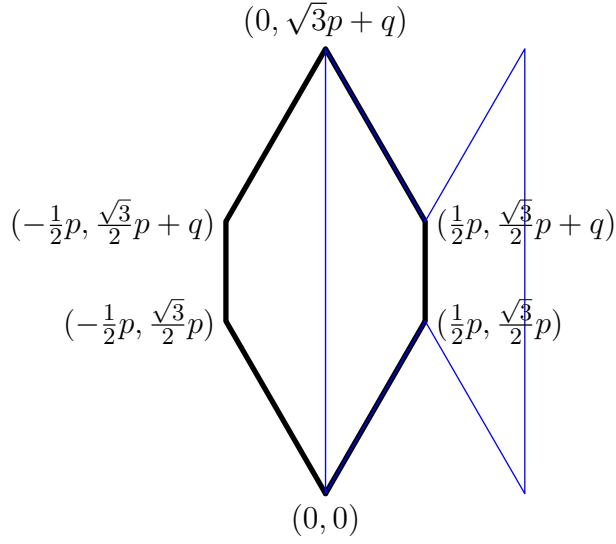$$(4.38) \qquad \int_{A_1} Gdh = -\frac{1}{2}p + i\frac{\sqrt{3}}{2}p$$

$(0, \sqrt{3}p + q)$

$(-\frac{1}{2}p, \frac{\sqrt{3}}{2}p + q)$ $(\frac{1}{2}p, \frac{\sqrt{3}}{2}p + q)$

$(-\frac{1}{2}p, \frac{\sqrt{3}}{2}p)$ $(\frac{1}{2}p, \frac{\sqrt{3}}{2}p)$

$(0, 0)$

FIGURE 4.13. The Gdh (in black) and $\frac{1}{G}dh$ (in blue) flat structures for the H surface. Labeled vertices are for the Gdh flat structure (the corresponding points on $\frac{1}{G}dh$ are obtained by translation by $(-\frac{1}{2}p, -\frac{\sqrt{3}}{2}p)$.

$$(4.39) \qquad \int_{A_1} \frac{1}{G}dh = -\frac{1}{2}p - i\frac{\sqrt{3}}{2}p$$

$$(4.40) \qquad \int_{B_1} Gdh = \sqrt{3}p \cdot i + qi$$

$$(4.41) \qquad \int_{B_1} \frac{1}{G}dh = qi$$

$$(4.42) \qquad \int_{A_2} Gdh = -e^{\frac{2\pi i}{3}}p$$

$$(4.43) \qquad \int_{A_2} \frac{1}{G}dh = -e^{-\frac{2\pi i}{3}}p$$

$$(4.44) \qquad \int_{B_2} Gdh = e^{\frac{2\pi i}{3}}qi$$

$$(4.45) \qquad \int_{B_2} \frac{1}{G}dh = e^{\frac{-2\pi i}{3}}(\sqrt{3}p + q)i$$

$$(4.46) \qquad \int_{A_3} Gdh = 0$$

$$(4.47) \qquad \int_{A_3} \frac{1}{G}dh = 0$$

$$(4.48) \qquad \int_{B_3} Gdh = e^{2 \cdot \frac{2\pi i}{3}}p$$

$$(4.49) \qquad \int_{B_3} \frac{1}{G} dh = e^{-2 \cdot \frac{2\pi i}{3}} p$$

The calculation of these periods is, for the first time, somewhat different because of the introduction of three sheets (instead of two). For example, to develop the cycle B_2, we need to study the developed segment connecting the points that correspond to 0 and to τ *on sheet 2*. We can use the developed image on sheet 1 (which is drawn in Figure 4.13, then multiply the difference in the endpoints by $e^{\frac{2\pi i}{3}}$ to find the difference in the endpoints on the second sheet. (This is because, under the order 3 rotation, the Gauß map (stereographic projection of the normal map), changes by $e^{\frac{2\pi i}{3}}$ for each rotation.)

The vertical periods are easily read off of the torus as simply the difference in the endpoints of the curves drawn on the torus in Figure 4.11. Again, since

$$(4.50) \qquad P(\gamma) = \begin{pmatrix} \mathrm{Re} \left(-\int_\gamma G dh + \overline{\int_\gamma \frac{1}{G} dh} \right) \\ \mathrm{Im} \left(-\int_\gamma G dh + \overline{\int_\gamma \frac{1}{G} dh} \right) \\ \mathrm{Re} \int_\gamma dh \end{pmatrix}$$

we write

$$(4.51) \qquad P(A_1) = (0,0,0)$$

$$(4.52) \qquad P(A_2) = (0,0,0)$$

$$(4.53) \qquad P(A_3) = (0,0,0)$$

$$(4.54) \qquad P(B_1) = (0, -\sqrt{3}p - 2q, 0)$$

$$(4.55) \qquad P(B_2) = R_{\frac{2\pi i}{3}}(0, -\sqrt{3}p - 2q, 0)$$

$$(4.56) \qquad P(B_3) = (0,0,1)$$

(Here the notation $R_{\frac{2\pi i}{3}}$ means a rotation by $\frac{2\pi i}{3}$ about the x_3 axis.)

It is again immediately clear that these periods generate a 3-dimensional lattice Λ *for all values of p and q.* In other words, the period problem is solved no matter what the actual lengths of the segments in the developed flat structure are. Thus *any value of a (and therefore, any quotient torus) solves the period problem.* Again, then, we have proven:

THEOREM 4.4. *There exists a (1 real parameter) continuous family of embedded triply periodic minimal surfaces of genus 3 that contains the H surface. Each member of the family admits an order 3 rotational symmetry.*

We will call this family of minimal surfaces the rH family (again, see [**FH99**] for the motivation for this notation). Notice that the limit $\tau \to 0$ looks like a pair of parallel planes joined with small catenoidal necks. The limit $\tau \to \infty$ looks like a three intersecting planes that are desingularized along the intersection by adding handles.
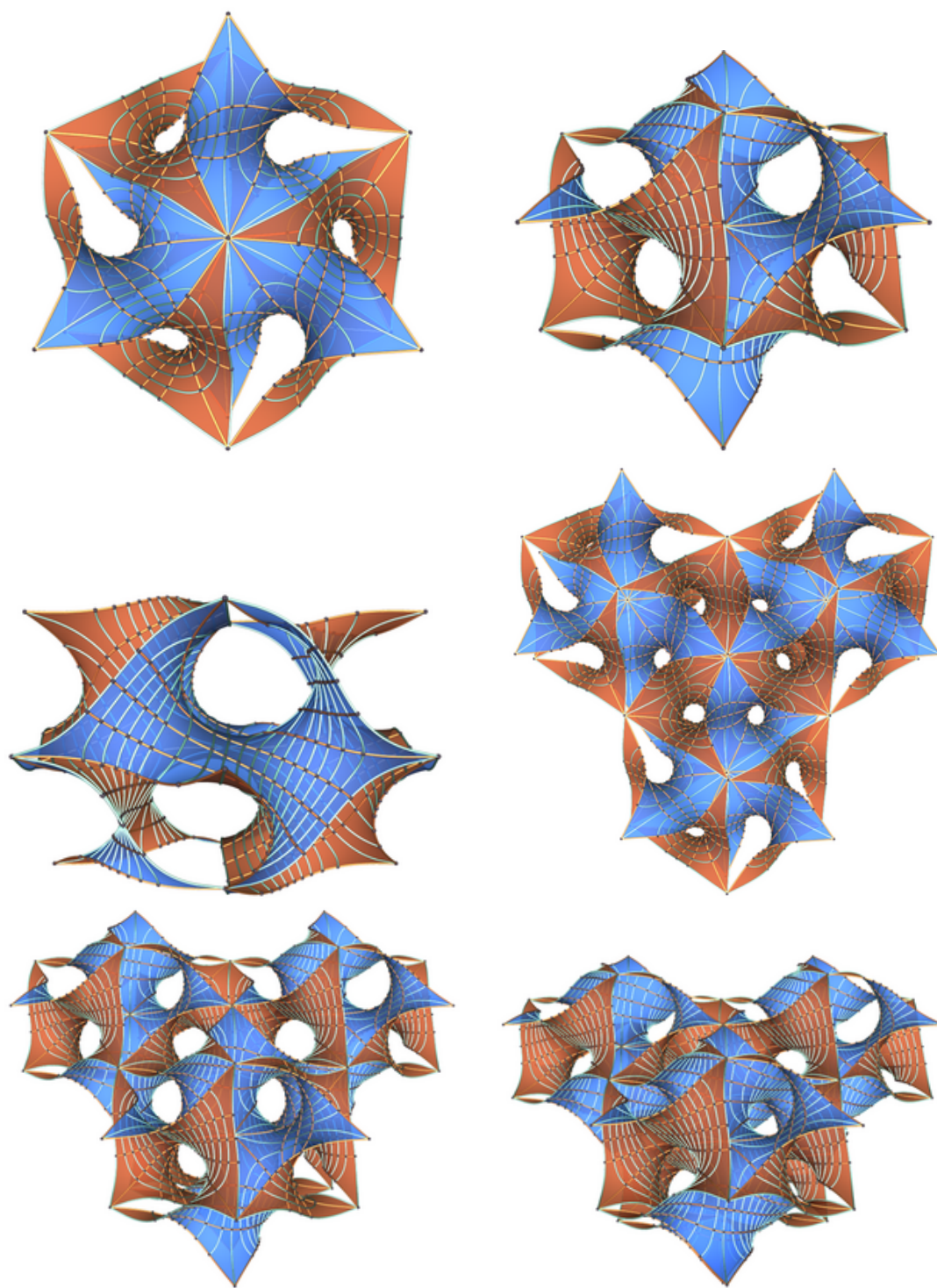
4.4. The Lidinoid

The Lidinoid is constructed analogously to the gyroid, except that it lies in the associate family of a member of the rH surface family (instead of in the associate family of the P surface). Recall that for each member of the tP family it is possible to compute the angle of association that is required to close the vertical periods. Similarly, for each member of the family it is possible to compute the angle of association that is required to close the horizontal periods. The first of these two curves is monotone decreasing, the second monotone increasing. (We prove this assertion rigorously for the gyroid in Lemma 5.5.) An analogous situation happens for the rH family. We will refer to this special member of the rH family as "the H surface". Unfortunately, we know of no geometric conditions (for instance, symmetries) which allow us to identify this surface, making this situation less pleasing than for the gyroid. Lidin first suggested the existence of the Lidinoid (what he humbly called the HG surface) in 1990 [**LL90**]. Große-Brauckman and Wohlgemuth showed its embeddedness at the end of [**GBW96**]. Like the gyroid, the Lidinoid contains neither straight lines nor planar symmetries. Curiously, while the author finds the P surface easier to visualize than the H surface, he finds the Lidinoid easier to visualize than the gyroid. See Figure 4.15 for several viewpoints.

As previously noted, both the P surface and the H surface come in a rather straightforward family of surfaces. For the tP family, there is clearly a most symmetric surface (what we call the standard P surface or just P surface). This is the (unique) surface in the family tP that admits both an order 2 and an order 3 symmetry (the order 3 symmetry permutes

FIGURE 4.14. The rH deformation of the H surface.

$\tau = 0.185$ $\tau = 0.250$

$\tau = 0.390$ $\tau = 0.500$

$\tau = 0.900$ $\tau = 2.500$
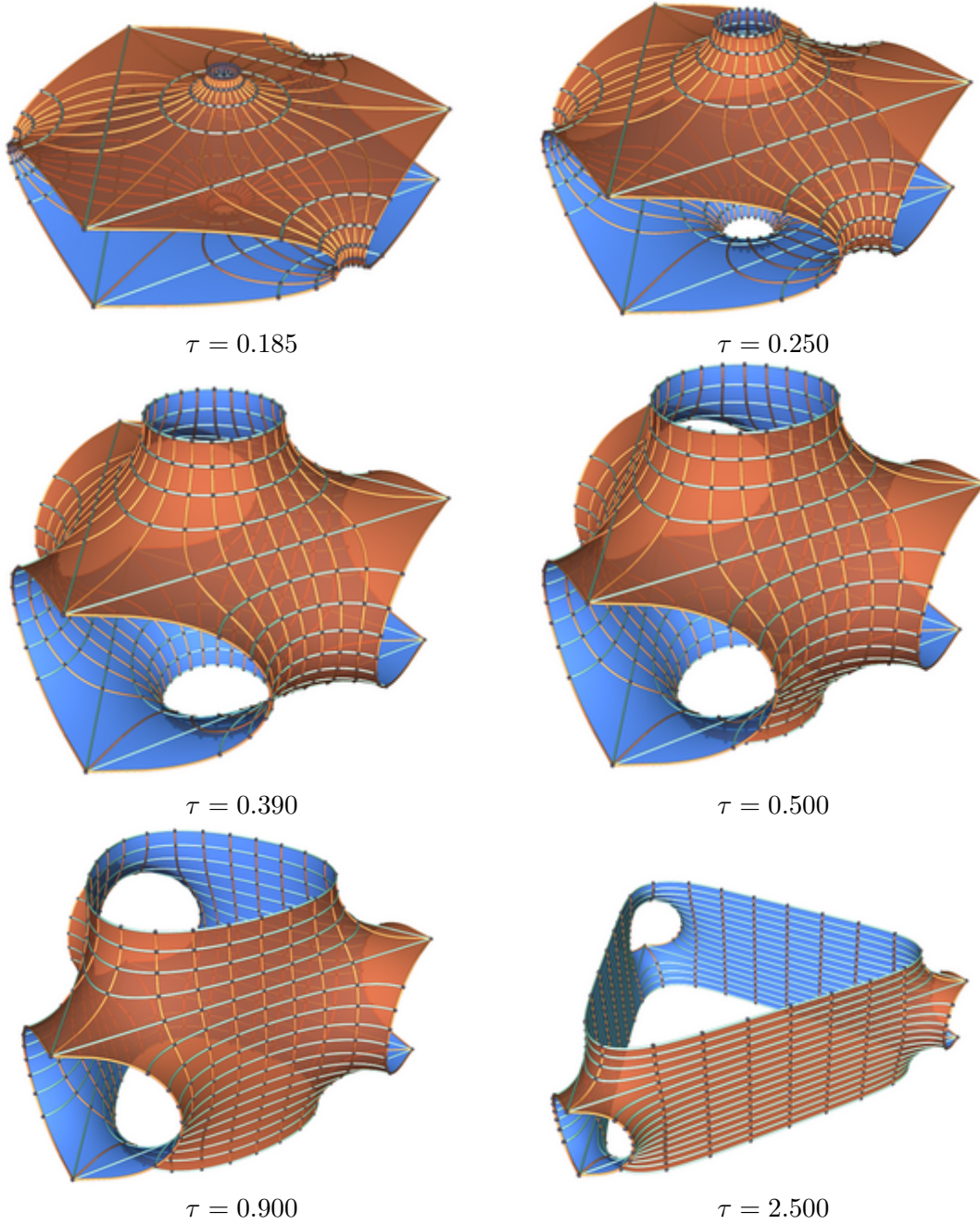
the handles). The situation for the H surface is somewhat murkier. Every member of the rH family admits both an order 2 and an order 3 symmetry. We are unaware of any reason to call a certain H surface more symmetric than others.

FIGURE 4.15. The Lidinoid

To construct the Lidinoid, let (X, G, dh) be the Weierstraß data describing a member of the rH family. Lidin [**FHL93, FH99**] gives that the angle of association is approximately

$$\theta \approx 64.2098°.$$

Furthermore, we expect, as with the gyroid, that the vertical period problem is solved by having the dh flat structure be "tipped" on end as in the case of the gyroid (see, e.g., 4.7). We can compute the conformal structure of the quotient torus, therefore, as the torus generated by 1 and ai, where

$$(4.57) \qquad\qquad a = \text{arccot}(64.2098°)$$

As in the case of the gyroid, we can easily calculate the periods for all members of the associate family by using the H surface flat structures. For instance, one can compute that for all $0 \leq \theta \leq 2\pi$, the associate surface has periods:

$$(4.58) \qquad\qquad P(A_1) = (\sqrt{3}p\sin(\theta), p\sin(\theta), --)$$

$$(4.59) \qquad\qquad P(B_3) = (-\sqrt{3}p\sin(\theta), p\sin(\theta), --)$$

These two periods clearly generate the horizontal part of the lattice, so we must ensure the others are compatible. For instance,

$$(4.60) \qquad\qquad P(B_1) = (\sqrt{3}p\sin(\theta), -(2q + \sqrt{3}p)\cos(\theta), --)$$

We see that, since $\sin(\theta) \neq 0$ for non-trivial members of the associate family, we must have

$$(4.61) \qquad\qquad \mp(2q + \sqrt{3}p)\cos(\theta) = \sin(\theta).$$

Examining the periods for B_2 shows that we must choose the "+" equation, so that

$$(4.62) \qquad\qquad \theta = \arctan\left(\frac{-\sqrt{3}p - 2q}{p}\right).$$

Similarly to the gyroid, Equation 4.62 puts a constraint on θ, and the vertical period condition places another condition; these two conditions are compatible for exactly one value of θ — the value that gives the Lidinoid.

We record here the full set of periods of the Lidinoid for our parameterization:

$$(4.63) \qquad\qquad P(A_1) = R_{\frac{2\pi i}{3}}(0, -1, 0)$$

$$(4.64) \qquad\qquad P(A_2) = -R_{\frac{2\pi i}{3}}(0, -1, 0)$$

$$(4.65) \qquad\qquad P(A_3) = (0, 0, 3s)$$

$$(4.66) \qquad\qquad P(B_1) = -R_{\frac{4\pi i}{3}}(0, -1, s)$$

$$(4.67) \qquad\qquad P(B_2) = -R_{\frac{4\pi i}{3}}(0, -1, s)$$

$$(4.68) \qquad\qquad P(B_3) = R_{\frac{4\pi i}{3}}(0, -1, s)$$

where $s \in \mathbb{R}^+$ is calculated with an elliptic integral.

4.5. The P Surface from the standpoint of an order 3 symmetry

In addition to the order 2 rotational symmetry, the *standard, most symmetric* P surface also admits an order 3 symmetry. This symmetry permutes the handles of the P surface and is obtained by rotating by $\frac{2\pi}{3}$ though the normal at one of the eight points where the Gaußian curvature $K = 0$. As discussed in the introduction, these are precisely the hyperelliptic points. The P surface can be viewed as being tiled by right-angled hexagons; the hyperelliptic points are the centers of these hexagons.

We repeat the procedure discussed above for the P surface (viewed as invariant under an order 2 rotation), and we obtain again a one-parameter family of P surfaces, this time invariant under an order 3 rotation.

The quotient torus is again rectangular (because the surface admits a plane of reflection that commutes with the rotation that has disconnected fixed point sets), the branch points cannot be situated at 0 and $\frac{1}{2}$ (since this describes the H surface, as we have already seen). By the discussion in Section 3.1.1, we are forced to place the zero of the Gauß map at 0 and the pole of the Gauß map at $\frac{1}{2} + \frac{\tau}{2}$. We illustrate in Figure 4.16 the rather complicated conformal model of the order-3 P surface, showing the branch cuts, the three sheets, and the cycles on the quotient torus. We illustrate in Figure 4.17 the cycles that generate $H_1(P, \mathbb{Z})$.
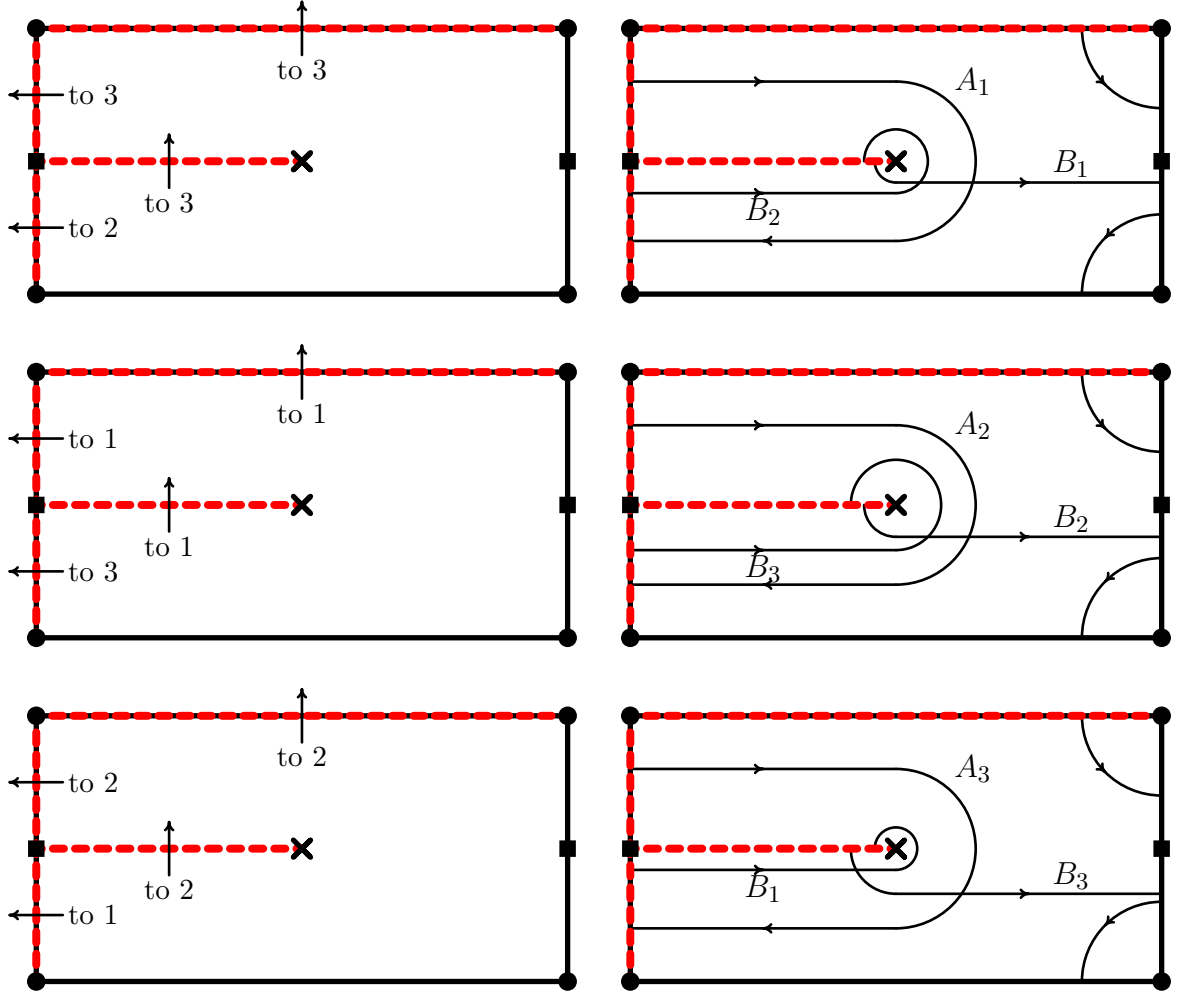
FIGURE 4.16. The conformal structure of the order 3 P surface

4.5.1. Flat structures. The 1-forms Gdh, $\frac{1}{G}dh$, and dh each place a flat structure on the torus which, after taking the quotient with $-id$, descends to the sphere. As before, we study each flat structure independently:

4.5.1.1. *dh flat structure for the rPD surface.* Since the dh flat structure descends as dz, the flat structure for the torus is simply the rectangle.

4.5.1.2. *Gdh flat structure for the rPD surface.* As noted in Section 2.4.2, the order of the zeros and poles of the 1-form Gdh produce cone angles on the torus of $\frac{10\pi}{3}i$ at 0 and of
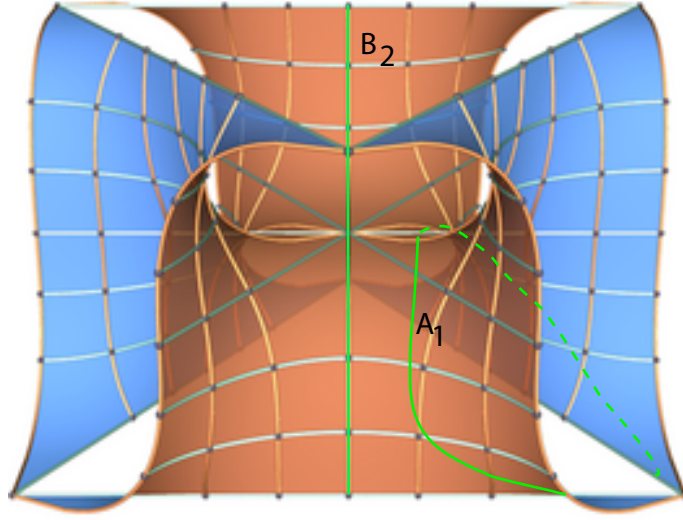
FIGURE 4.17. Generating cycles for the homology of the order 3 P surface. Notice that, for convenience we have not chosen a "standard" basis (i.e., $B_1 \cap B_2 \neq \emptyset$).

$\frac{2\pi}{3}$ at $\frac{1}{2} + \frac{\tau}{2}$. The remaining fixed points, at $\frac{1}{2}$ and $\frac{\tau}{2}$, are regular points. The involution $-id$ halves the cone angles in the quotient, so that on the sphere the cone angles are:

- A cone point of angle $\frac{10\pi}{6}$ at 0.

- A cone point of angle $\frac{\pi}{3}$ at $\frac{1}{2} + \frac{\tau}{2}$.

- A cone point of angle π at each of $\frac{\tau}{2}$ and $\frac{1}{2}$.

The flat structure is a hexagon:

LEMMA 4.5. *By cutting along the shortest geodesics on the sphere from $\frac{\tau}{2}$ to 0, 0 to $\frac{1}{2}$, and from $\frac{1}{2}$ to $\frac{1}{2} + \frac{\tau}{2}$, we obtain a hexagon shown in black in Figure 4.19 (the vertices of the hexagon have labeled coordinates). The hexagon has the following properties:*

i) *the length of l_i is equal to the length of l_i^* for $i = 1, 2, 3$*

ii) *the angle between l_1 and l_2 and the angle between l_1^* and l_2^* are both $\frac{5\pi}{6}$.*

iii) *the angle between l_1 and l_1^* is π and the angle between l_3 and l_3^* is $\frac{\pi}{6}$.*

iv) *the angle between l_2 and l_3 and the angle between l_2^* and l_3^* are both $\frac{\pi}{2}$.*

We again omit the proof, but it is precisely analogous to Lemma 4.1. Again we have not chosen the imaginary part of τ as we expect to recover a family of surfaces.

4.5.1.3. $\frac{1}{G}dh$ *flat structure for the rPD surface.* The symmetry between the Gdh and $\frac{1}{G}dh$ flat structures are now somewhat different, since $\frac{1}{G}(z)$ and $G(z + \frac{1}{2})$ *do not* have the same zeros and poles. Consider instead the maps $\frac{1}{G}(z)$ and $G(z + \frac{1}{2} + \frac{\tau}{2})$. These have the exactly the same zeros and poles. By Liouville's theorem, $G^2(z + \frac{w_1+w_2}{2})$ and $\frac{1}{G^2}(z)$ are equal up to a complex scalar multiple. Therefore we can understand $\frac{1}{G}$ in region R (a partial fundamental domain for our developing map) by understanding G in region S (see Figure 4.18). However, under $-id$, R and S are identified, so that, after a relabeling, the development of region R by the Gdh flat structure and the development of R by the $\frac{1}{G}dh$ flat structure differ by only a dilation and rigid motion. We adjust ρ to correct this deficiency, and obtain the flat structures shown in Figure 4.19.
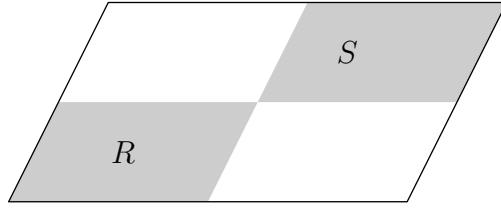

FIGURE 4.18. The shaded regions on the torus are identified under ι

4.5.2. The period problem for the rPD surface. Again, we develop the cycles shown in Figure 4.16 and obtain the following periods:

$$(4.69) \qquad \int_{A_1} Gdh = 2i(\sqrt{3}p + q)$$

$$(4.70) \qquad \int_{A_1} \frac{1}{G}dh = -2i(\sqrt{3}p + q)$$

$$(4.71) \qquad \int_{B_1} Gdh = e^{\frac{4\pi i}{3}}(-2p - \sqrt{3}q + i(2\sqrt{3}p + 3q))$$

$$(4.72) \qquad \int_{B_1} \frac{1}{G}dh = e^{\frac{-4\pi i}{3}}(-p - \sqrt{3}pi)$$

$$(4.73) \qquad \int_{A_2} Gdh = e^{\frac{2\pi i}{3}}2i(\sqrt{3}p + q)$$

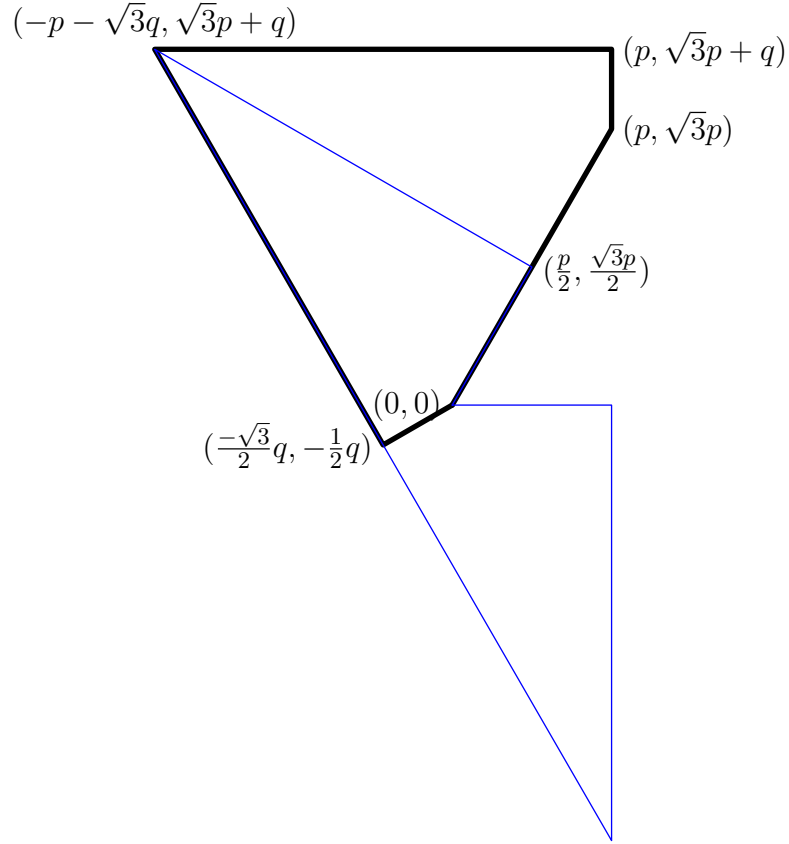$$(4.74) \qquad \int_{A_2} \frac{1}{G}dh = -e^{\frac{2\pi i}{3}}2i(\sqrt{3}p + q)$$

FIGURE 4.19. Gdh (in black) and $\frac{1}{G}dh$ (in blue) flat structures for the P surface viewed as invariant under an order 3 rotation.

$$\text{(4.75)} \qquad \int_{B_2} Gdh = -2p - \sqrt{3}q + i(2\sqrt{3}p + 3q)$$

$$\text{(4.76)} \qquad \int_{B_2} \frac{1}{G}dh = -p - \sqrt{3}pi$$

$$\text{(4.77)} \qquad \int_{A_3} Gdh = e^{\frac{4\pi i}{3}} 2i(\sqrt{3}p + q)$$

$$\text{(4.78)} \qquad \int_{A_3} \frac{1}{G}dh = -e^{\frac{4\pi i}{3}} 2i(\sqrt{3}p + q)$$

$$\text{(4.79)} \qquad \int_{B_3} Gdh = e^{\frac{2\pi i}{3}}(-2p - \sqrt{3}q + i(2\sqrt{3}p + 3q))$$

$$\text{(4.80)} \qquad \int_{B_3} \frac{1}{G}dh = e^{\frac{-2\pi i}{3}}(-p - \sqrt{3}pi)$$

$$(4.81) \qquad\qquad P(A_1) = (0,0,0)$$

$$(4.82) \qquad\qquad P(A_2) = (0,0,0)$$

$$(4.83) \qquad\qquad P(A_3) = (0,0,0)$$

$$(4.84) \qquad\qquad P(B_1) = R_{\frac{4\pi i}{3}}(p + \sqrt{3}q, -\sqrt{3}p - 3q, 1)$$

$$(4.85) \qquad\qquad P(B_2) = (p + \sqrt{3}q, -\sqrt{3}p - 3q, 1)$$

$$(4.86) \qquad\qquad P(B_3) = R_{\frac{2\pi i}{3}}(p + \sqrt{3}q, -\sqrt{3}p - 3q, 1)$$

(Again, the notation $R_{\frac{2\pi i}{3}}$ means a rotation by $\frac{2\pi i}{3}$ about the x_3 axis.)

The rPD family has one additional feature that we have not seen in the other families: it is *self-adjoint*. We consider the developed image of the dh flat structure. For the P surface, one of the branch points is at zero (the zero of the Gauß map) and the other is at $\frac{1}{2} + \frac{\tau}{2}$ (the pole of the Gauß map). To obtain the conjugate surface, we change dh to $e^{i\frac{\pi}{2}} dh$. This puts the developed image of the branch points at 0 and $-\frac{1}{2} + \frac{\tau}{2}$. By double periodicity, this is precisely the same developed image as for the P surface (with torus generators swapped). Thus, both the P and D surfaces are in the same family. The CLP surface (below) also shares this characteristic.

4.5.3. The order 3 gyroid. Since the standard P surface is a member of the rPD family, the gyroid can also be parameterized in terms of this family. We outline the construction of the gyroid in this way, so that in Chapter 5 we can construct (a second) family of gyroids — the order 3 gyroids rG.

To begin, we need to locate the conformal parameter τ that yields the standard, most symmetric P surface. From the end of Section 4.2, recall that the standard P surface can be described in terms of the 1-forms $\omega_1, \omega_2,$ and ω_3 (these forms are considered with the orientation of the P surface in space so that the lattice is the standard, cubical lattice). These are permuted by the rotation ρ_3. After a rotation of the surface in space so that the axis of rotation is vertical, $dh = \omega_1 + \omega_2 + \omega_3$. We understand the periods of these 1-forms

FIGURE 4.20. Members of the rPD family. The lower right image shows a close up of helicoids forming in the limit.

$\tau = 0.2$

$\tau = 0.45$

$\tau = 1.0$

$\tau = 1.5$

$\tau = 2.5$
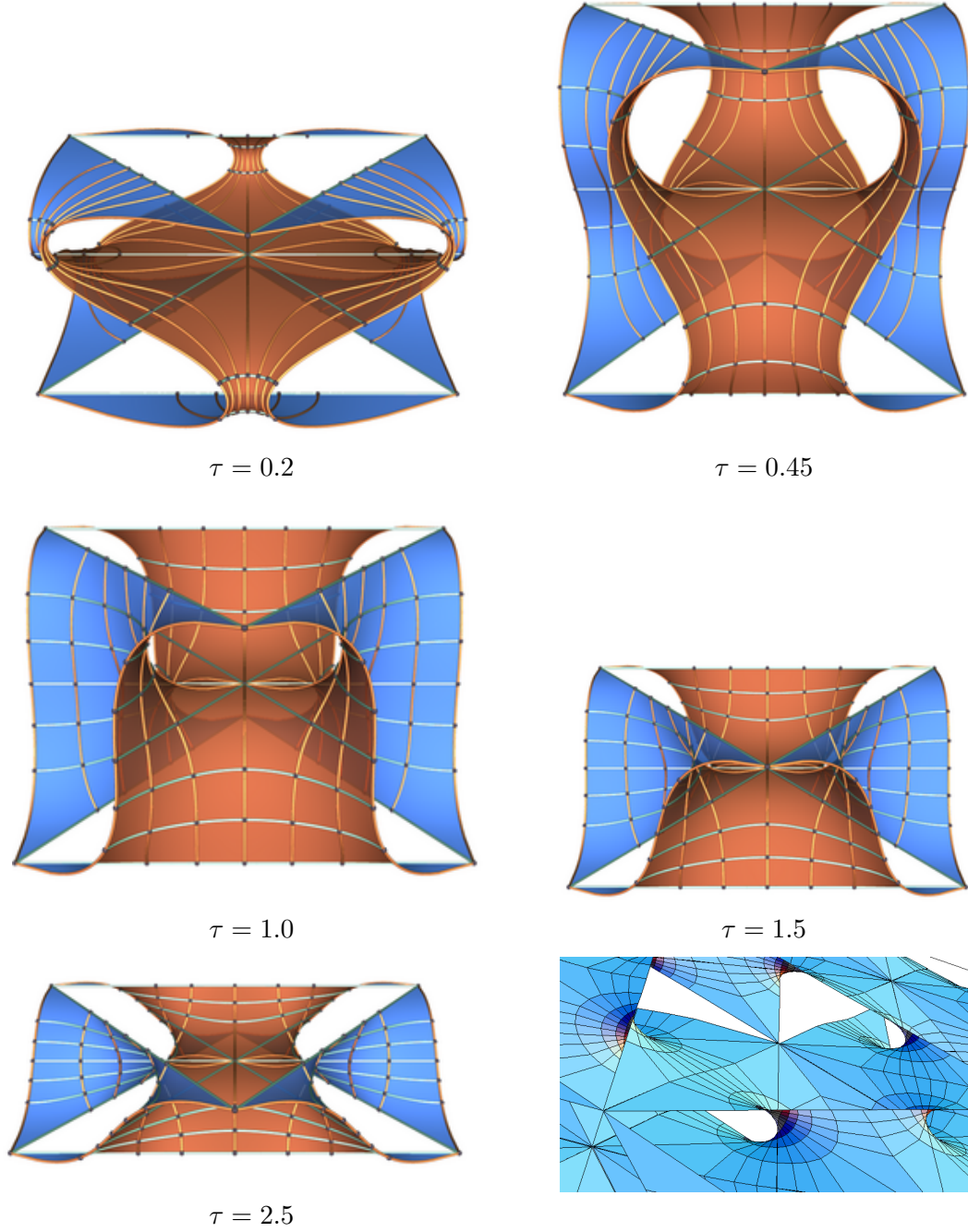
explicitly from our work with the P surface. Denote by γ_1 the cycle generated by the vector 1 on the order 2 P surface torus. Its period on each of the ω_i flat structures is 1, i.e.,

$$(4.87) \qquad \int_{\gamma_1} \omega_i = 1$$

so that

$$(4.88) \qquad \int_{\gamma_1} dh = \int_{\gamma_1} \omega_1 + \omega_2 + \omega_3 = 1$$

This implies that one generator of the quotient torus P/ρ_3 is 1, since the location of the branch cuts implies that this cycle γ_1 continues onto *all three sheets*.

Considering the other generator of the torus (rather, the cycle γ_2 coinciding with this generator), we note that

$$(4.89) \qquad \int_{\gamma_2} \omega_i = 2a$$

since the cycle continues onto both sheets of the torus P/ρ_2 (recall that $a = \operatorname{Im} \tau \approx 0.78$). On the other hand, if we denote the generators of the torus P/ρ_3 by 1 and σ, then

$$(4.90) \qquad \int_{\gamma_2} dh = \int_{\gamma_2} \omega_1 + \omega_2 + \omega_3 = 6a$$

but also

$$(4.91) \qquad \int_{\gamma_2} dh = 3 \operatorname{Im} \sigma$$

since the cycles continues onto both sheets. Thus, the standard P surface is obtained when $\sigma = 2\tau$. Since this is *the* standard P surface, the angle of association that yields the gyroid is the same

$$(4.92) \qquad \theta = \operatorname{arccot} \operatorname{Im} \tau$$

We remark that this is *precisely the same surface* as that obtain in Section 4.2, but viewed from a different perspective and using a different parameterization. Another view of the gyroid is in Figure 4.21.

FIGURE 4.21. Top: a translational fundamental domain of the gyroid, viewed as invariant under an order 3 rotation. Bottom: several copies of a fundamental domain. Notice the similarity to the Lidinoid.
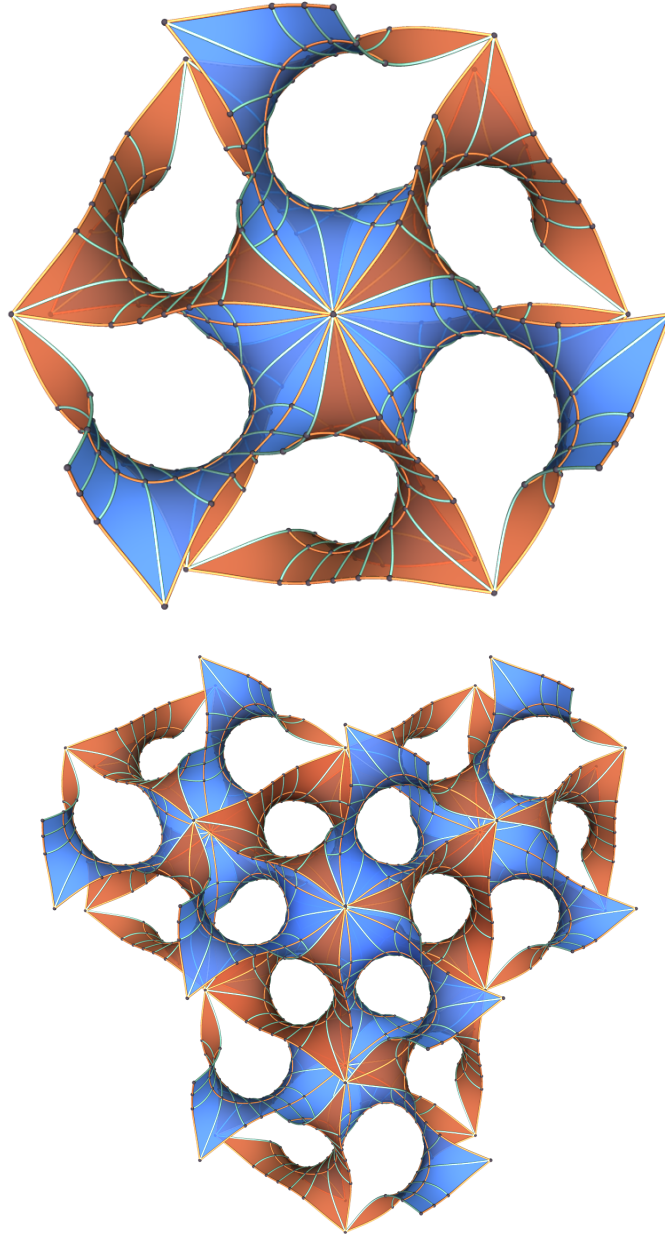
4.6. The CLP surface

Another classical surface, the CLP surface (for "crossed layers of parallels"), is shown in Figure 4.22. This genus 3 surface also admits an order 2 rotation with four fixed points.

FIGURE 4.22. A fundamental domain for the CLP surface
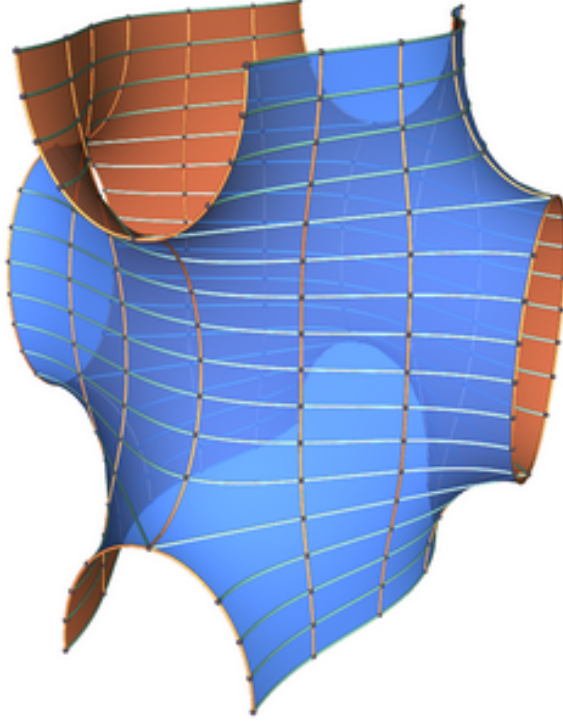
The quotient torus is rectangular (again, by symmetry considerations); Figure 4.25 shows the conformal model. Figure 4.24 shows a schematic view of the CLP surface with cycles illustrated.

4.6.1. Flat structures and periods for the CLP surface. As in the case of the P and H surfaces, $G^2\left(z + \frac{1}{2}\right)$ and $\left(\frac{1}{G}\right)^2(z)$ have precisely the same zeros and poles to the same order. Again, by Liouville's theorem, the quotient is constant (since it is holomorphic *(no poles)* and doubly periodic):

$$(4.93) \qquad G^2\left(z + \frac{1}{2}\right) + \left(\frac{1}{G}\right)^2(z) = r_1 e^{i\phi_1}$$

By adjusting the Lopez-Ros parameter, we can ensure that this factor is 1, and we do that for the CLP surface. Therefore, the $\frac{1}{G}dh$ flat structure is simply a translation of the (infinite, periodic) Gdh flat structure. This is reflected in the blue outline of the $\frac{1}{G}dh$ flat structure in Figure 4.26.
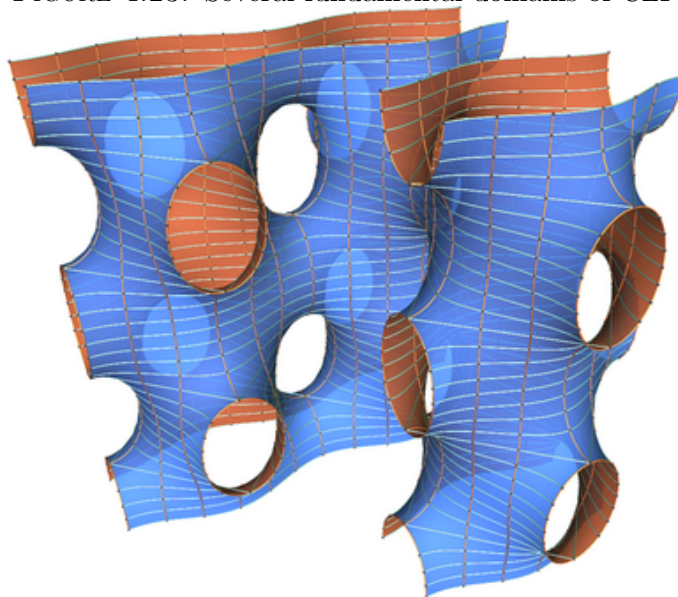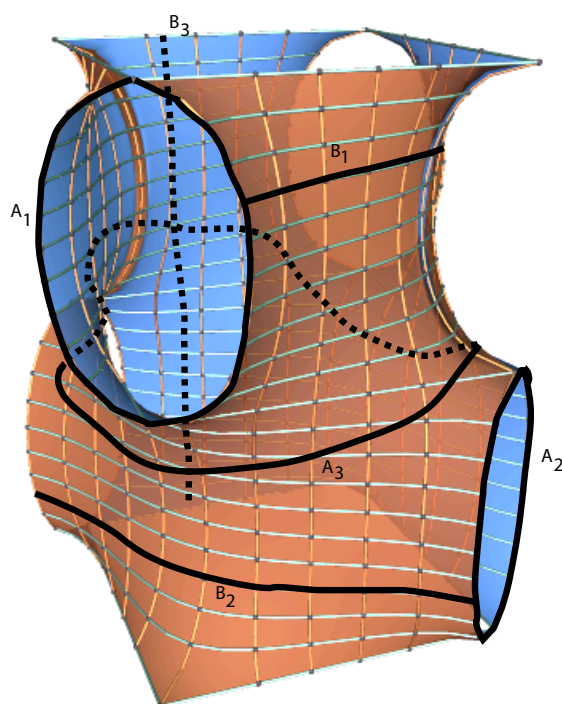
FIGURE 4.23. Several fundamental domains of CLP

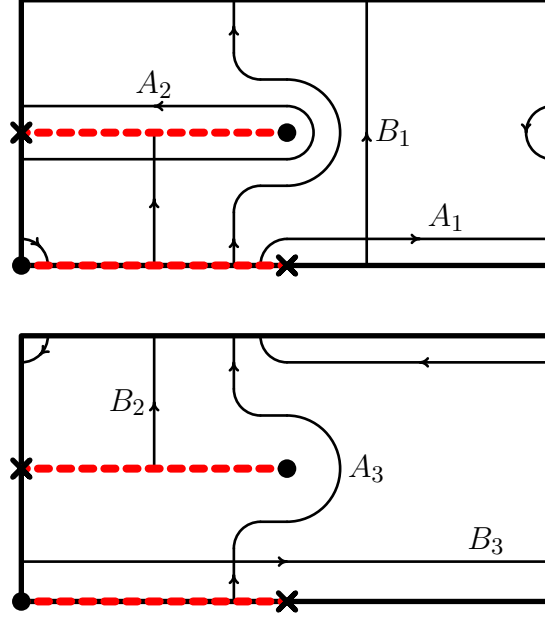FIGURE 4.24. Alternate view of the CLP surface, showing the cycles.

FIGURE 4.25. The quotient torus M/ρ for the surface $M = CLP$, showing the location of the branch points and the six generators of the homology. A conformal model for the full surface is obtained by gluing along the indicated branch cuts (in red).
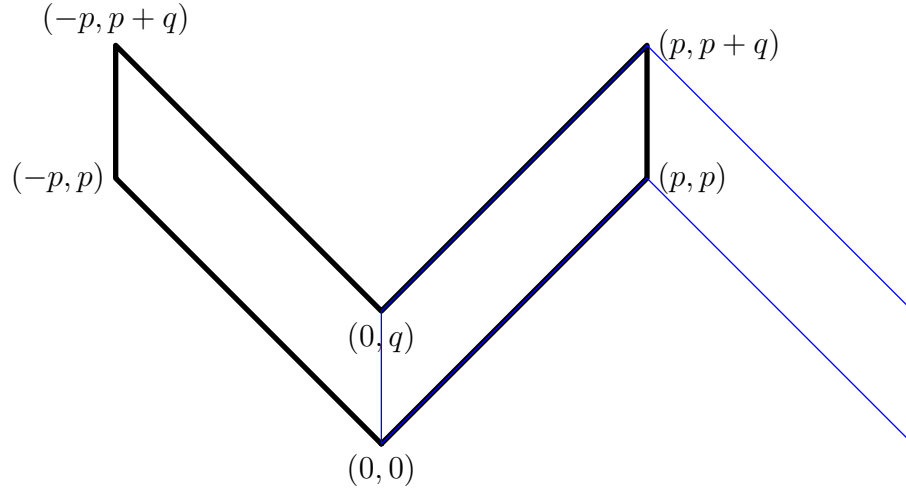

FIGURE 4.26. The Gdh (in black) and $\frac{1}{G}dh$ (in blue) flat structures for the CLP surface. Labeled vertices are for the Gdh flat structure (the corresponding points on $\frac{1}{G}dh$ are obtained by translation by $(-p, p)$).

We now calculate the periods for the CLP surface; we have omitted the calculation for A_3 since the period is always 0 under the order 2 assumption.

$$(4.94) \qquad \int_{A_1} G dh = (1 - i)(p + p \cdot i)$$

$$(4.95) \qquad \int_{A_1} \frac{1}{G} dh = (1 + i)(p - p \cdot i)$$

$$(4.96) \qquad \int_{B_1} G dh = (1 - i)qi$$

$$(4.97) \qquad \int_{B_1} \frac{1}{G} dh = (1 + i)qi$$

$$(4.98) \qquad \int_{A_2} G dh = (1 - i)(p - p \cdot i)$$

$$(4.99) \qquad \int_{A_2} \frac{1}{G} dh = (1 + i)(p + p \cdot i)$$

$$(4.100) \qquad \int_{B_2} G dh = (1 + i)qi$$

$$(4.101) \qquad \int_{B_2} \frac{1}{G} dh = (1 - i)qi$$

$$(4.102) \qquad \int_{B_3} G dh = 2p$$

$$(4.103) \qquad \int_{B_3} \frac{1}{G} dh = 2p$$

$$(4.104) \qquad P(A_1) = (0, 0, 0)$$

$$(4.105) \qquad P(A_2) = (0, 0, 0)$$

$$(4.106) \qquad P(A_3) = (0, 0, 0)$$
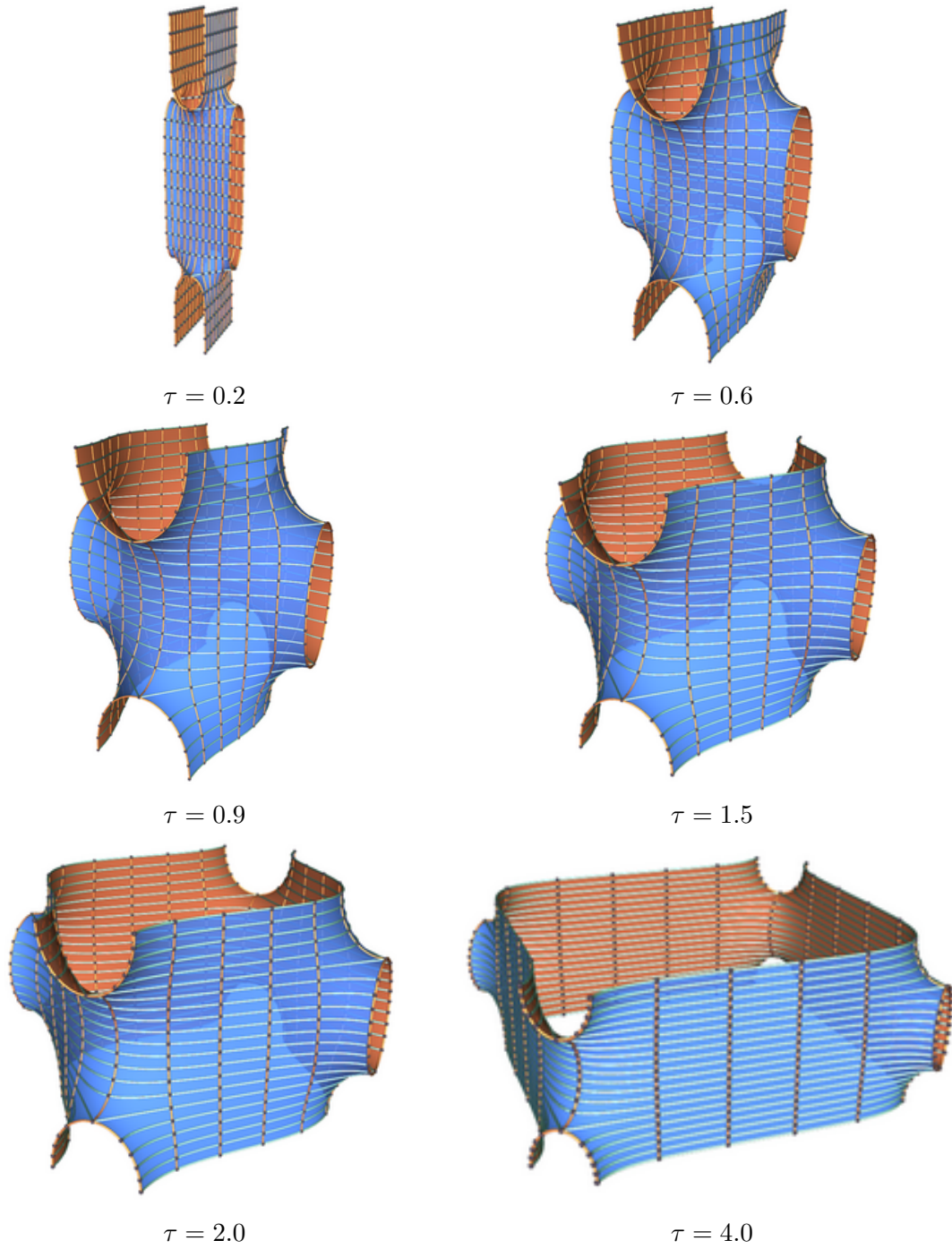
$$(4.107) \qquad P(B_1) = (-2q, -2q, 0)$$

$$(4.108) \qquad P(B_2) = (2q, -2q, 0)$$

$$(4.109) \qquad P(B_3) = (0, 0, 1)$$

There are no known embedded members of the associate family of any surface in the tCLP family.

FIGURE 4.27. The tCLP deformation of the CLP surface.

$\tau = 0.2$ $\tau = 0.6$

$\tau = 0.9$ $\tau = 1.5$

$\tau = 2.0$ $\tau = 4.0$

CHAPTER 5

Proof of the Existence of the Gyroid and Lidinoid Families

In this chapter, we prove Theorem 1.2: the existence of a family of gyroids all preserving an order 2 rotational symmetry. We now outline the proof.

First, define a moduli space of polygons $\mathcal{H}(G)$ that solve the horizontal period problem. That is, suppose there that X is a Riemann surface constructed as the branched (double) cover of a torus T, a Gauß map G, and a height differential dh so that the developed image of the torus T with cone metric induced by Gdh is in $\mathcal{H}(G)$. Then the horizontal periods will be closed (will lie in a lattice). Furthermore, the generators of the lattice will be the same cycles that generate the lattice for the gyroid. (In fact, our tori will have the property that they are invariant under $-id$, so we only develop $T/-id$.) Notice that the lattice *will not* be constant throughout the deformation. Since the horizontal period problem requires knowledge about not only Gdh but also $\frac{1}{G}dh$, we impose a normalization so that the $\frac{1}{G}dh$ flat structure is a translate of the Gdh developed flat structure.

Second, define a moduli space of polygons $\mathcal{V}(G)$ that solve the vertical period problem. Since the conformal model of a Riemann surface is, in our case, always the (two or three)-fold cover of a torus, the vertical moduli space will always consist of parallelograms. The critical issue here will be the orientation of the developed image of the parallelograms. (In fact, orientation of the developed flat structure is also the critical issue for $\mathcal{H}(G)$. Philosophically, the reason is that once the proper moduli space is established, the only parameter that remains uncontrolled is the associate family parameter θ.)

Then, we show that there exists a set of Weierstraß data $\{X_\eta, G_\eta, dh_\eta\}$, $\eta \in \mathbb{R}$ so that the developed image of the torus T_η under the flat structure induced by Gdh is in $\mathcal{H}(G)$ *and* under dh is in $\mathcal{V}(G)$. This shows that both the horizontal and the vertical period problems can be solved simultaneously by a family of Weierstraß data. To accomplish this, define a

continuous function $h : \mathbb{C} \to \mathbb{R}$ with the property that $h(\tau) = 0$ implies that there exists $\theta(\tau)$ such that the Gdh flat structure (respectively, the dh flat structure) will be in $\mathcal{H}(G)$ (resp. $\mathcal{V}(G)$) provided that $dh = e^{i\theta}$). The Gauß map will be determined by the conformal structure of the torus and the normalization we impose that the Gdh and $\frac{1}{G}dh$ flat structures are translates. We then show that $h^{-1}(0)$ contains a continuous curve and that this curve contains the value τ what determines the standard gyroid. This guarantees the existence of a continuous family of immersed triply periodic minimal surfaces that contains the gyroid. To study the zero set of h, we use the fact that we can compute h more or less explicitly for rectangular tori. Furthermore, we can compute h for $\tau = n + yi$, $n \in \mathbb{Z}$, by studying the effect of Dehn twists on the torus and the flat structures. This allows us to compute sufficiently many values to use an intermediate value type argument.

Finally, we show that the surfaces obtained in this way are embedded (and not just immersed). This last fact is a consequence of the *maximum principal for minimal surfaces* (see, for example, the thorough survey [**LM99**]). We separate the embeddedness portion of the proof into a more general proposition (Proposition 5.6).

In Section 5.1 we set up the moduli spaces $\mathcal{H}(G)$ and $\mathcal{V}(G)$. In Section 5.2 we prove the remaining statements. We do this in detail for the tG family. For the remaining families rG and rL, we construct the moduli spaces in Sections 5.4, 5.3. The other statements of the proof for these families are clear (once the moduli spaces are properly constructed).

5.1. Horizontal and vertical moduli spaces for the tG family

In the most general setting, it is not possible to split the period problem into vertical and horizontal components. In our case however, we are considering surfaces that are invariant under rotation. Therefore, since the height is invariant under this rotation the height differential dh establishes a consistent x_3 direction that is invariant throughout the family. Therefore, the lattice Λ is a product $\mathbb{Z} \times \Lambda_1$, so we can split the period problem into two parts. We need to show that there is a single vertical period, and we need to show that the horizontal periods lie in a two-dimensional $\mathbb{Z}$−lattice.

5.1.1. Definition of $\mathcal{V}(G)$ and calculation of the vertical periods. In this sub-section we describe the conformal models of the surfaces we wish to construct. Recall that the underlying Riemann surface structure for the gyroid was a 2-fold branched cover of a rectangular torus (with modulus calculated in Appendix A).

Denote by $\widetilde{\mathcal{V}(G)}$ be the space of marked parallelograms in $\mathbb{C}$ up to equivalence by *translations* (we consider marked parallelograms to distinguish the cone point 0). Notice that if $\Gamma = \langle 1, \tau \rangle$ is a $\mathbb{Z}$-lattice in $\mathbb{C}$, the torus $\mathbb{C}/\Gamma$, once equipped with the flat structure induced by $e^{i\theta}dz$, develops to an element of $T \in \widetilde{\mathcal{V}(G)}$. If M is a triply periodic minimal surface with symmetry ρ_2 so that $M/\Lambda/\rho_2 = \mathbb{C}/\Gamma$, and if we develop generators of the homology $H_1(M, \mathbb{Z})$ onto T, then M is immersed only if both the horizontal and the vertical period problems are solved. Notice that the period problem is in general *not* solved if $\mathbb{C}/\Gamma$ develops into $\widetilde{\mathcal{V}(G)}$.

We will now define a subset of $\widetilde{\mathcal{V}(G)}$ that *does* solve the vertical period problem. There are generally many such subsets, but we seek a deformation of the gyroid. Recall (Figure 4.7) that the gyroid's dh flat structure for the torus satisfies $\operatorname{Re} e^{i\theta} = -\operatorname{Re} e^{i\theta}\tau$. With this motivation, we define

$$(5.1) \qquad \mathcal{V}(G) = \{(\omega_1, \omega_2) \in \mathbb{C} \times \mathbb{C} \mid |\omega_1| = 1 \text{ and } \operatorname{Re} \omega_1 = -\operatorname{Re} \omega_2\}$$

Developing the cycles shown in Figure 4.3 onto this flat structure, one easily sees that the vertical period problem is solved. Using the notation of the cycles from Figure 4.4, the vertical periods are:

$$(5.2) \qquad\qquad\qquad P(A_1) = (--, --, 0)$$

$$(5.3) \qquad\qquad\qquad P(A_2) = (--, --, 0)$$

$$(5.4) \qquad\qquad\qquad P(A_3) = (--, --, \operatorname{Re} \omega_1)$$

$$(5.5) \qquad\qquad\qquad P(B_1) = (--, --, -\operatorname{Re} \omega_1)$$

$$(5.6) \qquad\qquad\qquad P(B_2) = (--, --, -\operatorname{Re} \omega_1)$$

$$(5.7) \qquad\qquad\qquad P(B_3) = (--, --, 2\operatorname{Re} \omega_1).$$

5.1.2. Definition of $\mathcal{H}(G)$ and calculation of the horizontal periods. Suppose that M is any immersed, genus 3, triply periodic minimal surface that has as a conformal model a two-fold branched cover of a generic torus $\mathbb{C}/\Gamma$ (without loss of generality we write $\Gamma = \langle 1, \tau \rangle$). Suppose further that the square of the Gauss map descends to $\mathbb{C}/\Gamma$ and has simple poles at $\frac{1}{2}$ and $\frac{1}{2} + \frac{\tau}{2}$ and simple zeros at 0 and $\frac{\tau}{2}$. (This is the case for the gyroid, except that the torus is rectangular.) The quotient $S = \mathbb{C}/\Gamma/(-id)$ is a sphere, and Gdh again induces a cone metric on S. Under this cone metric, the sphere is a tetrahedron, with two vertex angles $\frac{3\pi}{2}$ and two vertex angles $\frac{\pi}{2}$. The developed image of this sphere has a particularly nice parameterization:

LEMMA 5.1. *For any torus $\mathbb{C}/\Gamma$ ($\Gamma = \langle 1, \tau \rangle$), the cone metric Gdh descends to S. By cutting along shortest geodesics on S from $\frac{1}{2}$ to 0, 0 to $\frac{\tau}{2}$, and from $\frac{\tau}{2}$ to $\frac{1}{2} + \frac{\tau}{2}$, we obtain a hexagon shown in Figure 5.1. The hexagon has the property that*

  i) the length of l_i is equal to the length of l_i^* for $i = 1, 2, 3$
  ii) l_2 is parallel to l_2^*
 iii) the angle between l_1 and l_1^* and the angle between l_3 and l_3^* are both $\frac{\pi}{2}$.

  We can parameterize the space of possible hexagons by $\xi_1, \xi_2 \in \mathbb{C}$ as shown in Figure 5.1.

We call the space of all hexagons satisfying the conditions of Lemma 5.1 $\widetilde{\mathcal{H}(G)}$.

PROOF. Since $\mathbb{C}/\Gamma/(-id)$ is a sphere and since $-id$ fixes the branch points of $\mathbb{C}/\Gamma$, the flat structure induced by Gdh makes S a tetrahedron with cone angle $\frac{3\pi}{2}$ at 0 and $\frac{\tau}{2}$ and with cone angle $\frac{\pi}{2}$ at $\frac{1}{2}$ and $\frac{1+\tau}{2}$. By making the indicated cuts (shown in Figure 5.4 in thick black lines), we obtain a hexagon with sides $l_1, l_2, l_3, l_1^*, l_2^*$, and l_3^*. We denote the points in the developed image corresponding to $\frac{1}{2}, 0, \frac{\tau}{2}$, and $\frac{1+\tau}{2} \in \mathbb{C}/\Gamma$ by p_1, p_2, p_3, and p_4 respectively. By making a translation, we arrange so that $p_2 = 0 \in \mathbb{C}$. Each l_i was identified with l_i^* before the cutting, therefore, the length of l_i is equal to l_I^*. Also, since there is a $\frac{\pi}{2}$ cone angle at $\frac{1}{2}$, the angle between lines l_1 and l_1^* must be $\frac{\pi}{2}$ (similarly for l_3).
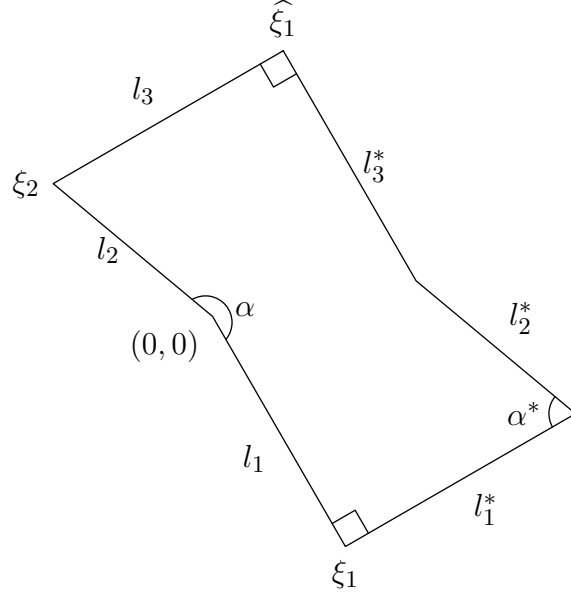
FIGURE 5.1. A generic member of the $\widetilde{\mathcal{H}(G)}$ moduli space.

Let α denote the angle between l_1 and l_2 and let α^* denote the angle between l_1^* and l_2^*. The cone angle at 0 is $\frac{3\pi}{2}$, therefore, since both p_2 and p_2^* correspond to $0 \in T$, the sum $\alpha + \alpha^* = \frac{3\pi}{2}$. (One can see this by developing a small circle about 0 and noting that in the developed image we must obtain an arc that subtends an angle of $\frac{3\pi}{2}$.) $\qquad\square$

To understand the horizontal periods, we again adjust ρ, if necessary, to normalize the $\frac{1}{G}dh$ flat structure as in Section 4.1.1.3 so that the developed flat structure for $\frac{1}{G}dh$ is simply a translate of that for Gdh (ρ is uniquely determined by this normalization). Then in terms of these flat structures, we compute the periods of the six generators of $H_1(M, Z)$ to be:

$$(5.8) \qquad \int_{A_1} Gdh = (1+i)(\widehat{\xi_1} - \xi_2)$$

$$(5.9) \qquad \int_{A_1} \frac{1}{G}dh = (1-i)(\xi_2 + iw - \widehat{\xi_1} + \xi_1)$$

$$(5.10) \qquad \int_{B_1} Gdh = (1+i)(\widehat{\xi_1} - \xi_1)$$

$$(5.11) \qquad \int_{B_1} \frac{1}{G}dh = (1-i)\xi_2$$

$$(5.12) \qquad \int_{A_2} G dh = (i-1)\xi_1$$

$$(5.13) \qquad \int_{A_2} \frac{1}{G} dh = (1-i)\xi_1$$

$$(5.14) \qquad \int_{B_2} G dh = (1-i)\xi_2$$

$$(5.15) \qquad \int_{B_2} \frac{1}{G} dh = (1+i)(\widehat{\xi_1} - \xi_1)$$

$$(5.16) \qquad \int_{A_3} G dh = (-1-i)\xi_1$$

$$(5.17) \qquad \int_{A_3} \frac{1}{G} dh = (-1-i)\xi_1$$

$$(5.18) \qquad \int_{B_3} G dh = 2(\widehat{\xi_1} - \xi_1)$$

$$(5.19) \qquad \int_{B_3} \frac{1}{G} dh = 2\xi_2$$

The notation $\widehat{\xi_1}$ is the complex number corresponding to p_4 (see Lemma 5.1), i.e.,

$$\widehat{\xi_1} = -\xi_1 + \xi_2 + \frac{(2+2i)\xi_1^2 \bar{\xi_1}}{2|\xi_1|^2}.$$

To simplify the calculations, we make the change of variables

$$(5.20) \qquad a = 2(\mathrm{Re}\ \xi_1 + \mathrm{Im}\ \xi_2)$$

$$(5.21) \qquad b = 2(\mathrm{Im}\ \xi_1 - \mathrm{Im}\ \xi_2).$$

One can then compute the horizontal periods to be

$$(5.22) \qquad P_{A_1} = (a+b, 0, --)$$

$$(5.23) \qquad P_{A_2} = (a+b, 0, --)$$

$$(5.24) \qquad P_{A_3} = (0, a+b, --)$$

$$(5.25) \qquad P_{B_1} = (a, b, --)$$

$$(5.26) \qquad P_{B_2} = (-a, b, --)$$

$$(5.27) \qquad P_{B_3} = (0, 0, --)$$

Notice that when $b = 0$, the period problem is solved. In particular, when $b = 0$ the periods coincide with those of the gyroid (Equations 4.31-4.36). Recall that $b = 2(\text{Im } \xi_1 - \text{Im } \xi_2)$; define

(5.28) $$\mathcal{H}(G) = \{(\xi_1, \xi_2) \in \mathcal{H}(G) | \text{Im } \xi_1 = \text{Im } \xi_2\}.$$

Then every flat structure in $\mathcal{H}(G)$ solves the horizontal period condition (and does so with the same relations among the generating curves as for the gyroid). Figure 5.2 shows a typical member of $\mathcal{H}(G)$.
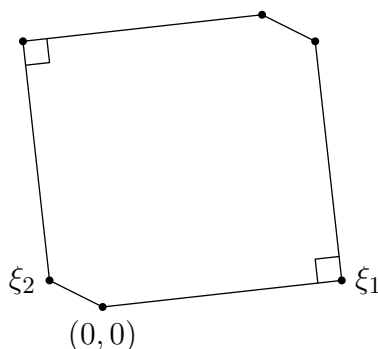

FIGURE 5.2. A generic member of the $\mathcal{H}(G)$ moduli space.

Of course, there are other choices for a, b that also solve the horizontal period problem. We make this choice because we want the family to contain the gyroid, and it is this relationship among the horizontal periods that is necessary to obtain the gyroid. Setting, for example, $a = -b$ would yield the tP family of Section 4.1. In principle, we have computed the horizontal periods of *all* triply periodic minimal surface that admit an order 2 rotation and whose branch points on the torus are in the same configuration as these. In practice, however, that is not enough for a classification, because without the use of a "base surface" that we know is embedded, it is quite difficult to say if any of these surfaces are embedded.

We have shown, thus far, that if (X, G, dh) has as flat structures members of $\mathcal{H}(G)$ and $\mathcal{V}(G)$, then the period problem is solved. Certainly the Weierstraß data for the gyroid do solve the period problem. It remains to find a 1-parameter family of such data. We will then show that the surfaces are all embedded.

5.2. Proof of the tG family

To prove the existence of the tG family, our first task is to show that there exists a family of Weierstraß data (X, G, dh) (that varies continuously) with X the double branched cover of a torus so that the developed image of $\mathbb{C}/\Gamma/(-id)$ under Gdh is in $\mathcal{H}(G)$ and so that the developed image of $\mathbb{C}/\Gamma/(-id)$ under dh is in $\mathcal{V}(G)$. This will show that the period problem is solved.

Let $\Gamma = \langle 1, \tau \rangle$. Define $dh = dz$ on $\mathbb{C}/\Gamma$. Define X_τ to be the Riemann surface obtained from the double cover of $\mathbb{C}/\Gamma$, with branch points at $0, \frac{1}{2}, \frac{\tau}{2},$ and, $\frac{1}{2} + \frac{\tau}{2}$ and with branch cuts as shown in Figure 4.4. The square of the Gauss map will be well-defined on $\mathbb{C}/\Gamma$ as the unique meromorphic function with zeros at 0 and $\frac{\tau}{2}$ and poles at $\frac{1}{2}$ and $\frac{1}{2} + \frac{\tau}{2}$ (up to a complex multiple ρ). Define ρ so that the Gdh and $\frac{1}{G}dh$ flat structures are normalized as in Section 4.1.1.3, i.e., so that they are translates.

For each choice $\tau \in \mathbb{C}$, this data describes a minimal surface. Define

DEFINITION 5.2. *The* vertical relative turning angle $\theta_\mathcal{V}(\tau)$ *is*

$$(5.29) \qquad\qquad \theta_\mathcal{V}(\tau) := \frac{\pi}{2} - \arg(1 + \tau)$$

(This is precisely the angle by which the dh flat structure fails to be in $\mathcal{V}(G)$.)

The horizontal relative turning angle $\theta_\mathcal{H}(\tau)$ *is the angle by which the Gdh flat structure must be rotated so that it satisfies* $\operatorname{Im} \xi_1 = \operatorname{Im} \xi_2$.

If $\theta_\mathcal{V}(\tau) = \theta_\mathcal{H}(\tau)$, then we could define $dh = e^{i\theta_\mathcal{V}(\tau)}dz = e^{i\theta_\mathcal{H}(\tau)}dz$. The definition of horizontal and vertical turning angle ensures that (X, G, dh) solves the horizontal and vertical period problem. Define

$$(5.30) \qquad\qquad b(\tau) := \theta_\mathcal{H}(\tau) - \theta_\mathcal{V}(\tau).$$

The period problem is solved exactly on the zero set of b. Let τ_G denote the value of τ which yields the gyroid (from the Appendix, $\tau \approx 0.781i$).

Our goal is to understand the zero set of b. Note that when $\tau \in i\mathbb{R}$, the resulting torus is rectangular. On rectangular tori, it is possible to explicitly develop the cone metric Gdh
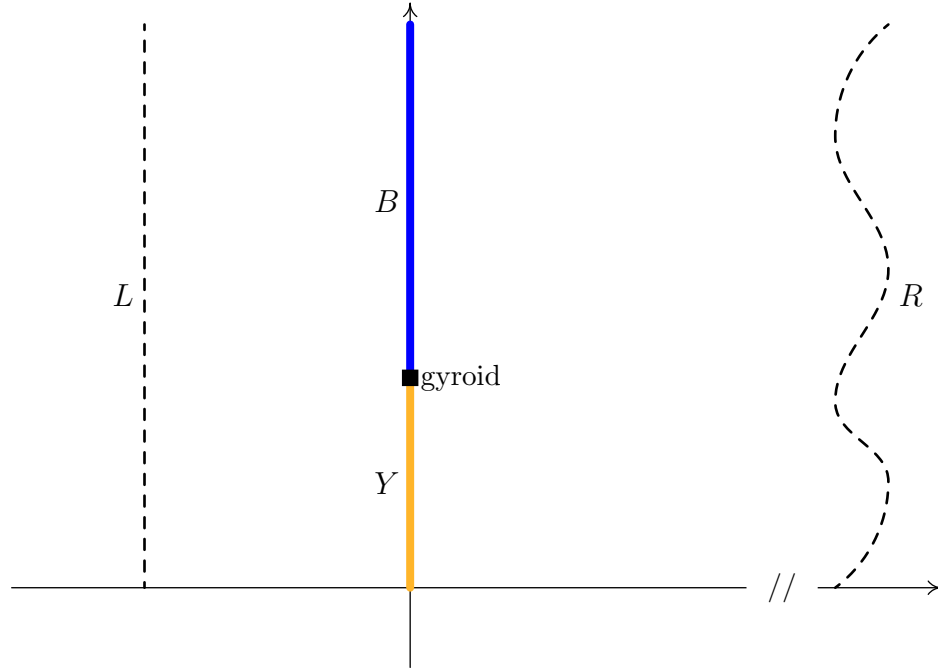
FIGURE 5.3. $b < 0$ on Y and $b > 0$ on B, so the zero set contains a curve separating B and Y (it must pass through the value that yields the gyroid)

.

into $\mathbb{C}$ by integrating the Gauß map (recall that the Gauß map can be explicitly given in terms of theta functions), and, therefore, to understand b. (On a generic, non-rectangular torus explicit computation is not possible, since the edges of a fundamental domain are no longer fixed point sets of an isometry and thus are not totally geodesic. It is no longer the case that these edges of a fundamental domain develop, under integration, to the shortest geodesic between cone points of the tetrahedron.)

Next, as in Figure 5.3, consider the half plane, with the $y-$axis divided into two segments B and Y. ($Y = \{(0, y) \mid \text{Im } (y) < \text{Im } \tau_G\}$). The line L is defined by $x = -1$; R is a curve with all x values sufficiently large.

LEMMA 5.3. $b > 0$ on L and $b > 0$ on R, where L is a vertical line $x = -1$, R is a vertical line $x = n$ for $n \in \mathbb{Z}$ sufficiently large.

PROOF. The quotient sphere of the torus generated by $(1, 1 + \tau)$ is related to the sphere obtained from the torus generated by $(1, \tau)$ by performing a Dehn twist on the cycle A_1.

The effect of this twist on the Gdh flat structure is clear in Figure 5.4 – where γ was the shortest geodesic between p_2 and p_3 is now changed to $\gamma + A_1$.
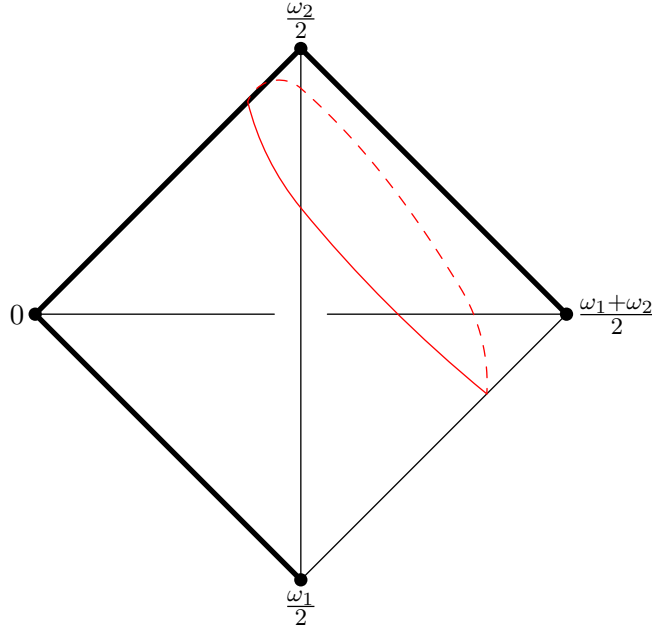

FIGURE 5.4. Tetrahedron with cycle of Dehn twist. The bold lines show cuts made for developing the tetrahedron into the plane.

We can compute the Gdh flat structure explicitly in the case of normalized rectangular tori and flat structures: for all rectangular tori, the angle between l_1 and l_2 is $\frac{3\pi}{4}$ and when normalized (recall that the normalization requires that the Gdh and $\frac{1}{G}$ flat structures are aligned) the segment l_2 is vertical with Im $\xi_2 > 0$ (this is a consequence of the symmetries of rectangular tori, see Section 4.1).

After a large number of positively oriented Dehn twists, we see a Gdh flat structure as in Figure 5.5; therefore for large $n \in \mathbb{Z}$, $\theta_{\mathcal{H}}(n + \tau) \approx \pi$ – a value larger than $\theta_{\mathcal{V}}(n + \tau) \approx \frac{\pi}{2}$. Thus $b \approx \frac{\pi}{2} > 0$ on R.
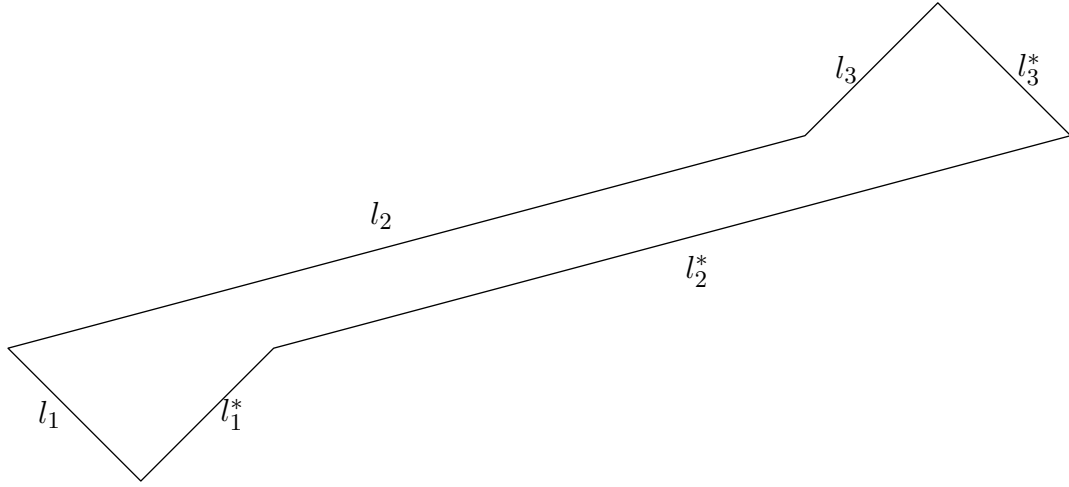
FIGURE 5.5. The *Gdh* flat structure after many positive Dehn twists

Showing that $b > 0$ on L is quite similar to the case above. After the application of a single negatively oriented Dehn twists, $\theta_{\mathcal{H}}$ remains positive ($\theta_{\mathcal{H}}$ is always positive), but $\theta_{\mathcal{V}}(-1 + ci) = 0$ for all $c \in i\mathbb{R}$. Therefore $b > 0$ on L, since a negatively oriented Dehn twist shifts the "top cone" of the the *Gdh* flat structure (see Figure 5.6).
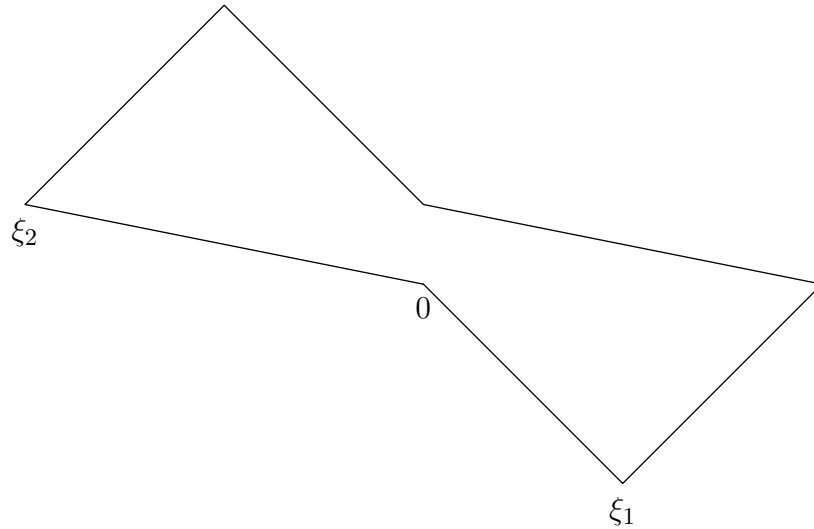
FIGURE 5.6. A "rectangular torus" *Gdh* flat structure after the application of a single negative Dehn twist.

$\square$

LEMMA 5.4. $b > 0$ on B and $b < 0$ on Y.

PROOF. We will show that both $\theta_{\mathcal{V}}$ and $\theta_{\mathcal{H}}$ are monotone – the first decreasing, the second increasing – as Im τ increases. This implies that the b has at most 1 zero (of course, we know that a zero occurs at τ_G yielding the gyroid).

Fortunately, we are able to explicitly calculate $\theta_{\mathcal{V}}$, namely

(5.31)
$$\theta_{\mathcal{V}}(\tau) = \operatorname{arccot}(\operatorname{Im} \tau).$$

It is a trivial matter to see that this function is monotone decreasing in Im τ.

The situation for the horizontal turning angle is not as simple. First, we note that the for all $\tau \in i\mathbb{R}$, the Gdh flat structure is normalized in the same orientation as it is for the gyroid, i.e., the straight line segment λ from the developed image of 0 to the developed image of 1 is horizontal. To see this, observe that in the rectangular case, there is a *vertical* symmetry curve in space that translates, on the torus, to a horizontal curve (straight line) connecting 0 and 1. The endpoints have no horizontal displacement, and so must be conjugate in the Gdh and $\frac{1}{G}dh$ flat structures. Since all surfaces in the tP family share this symmetry, the line λ must be horizontal.

Since for all $\tau \in i\mathbb{R}$ the *normalized* Gdh flat structure is aligned so that λ is horizontal (when the angle of association is 0), the relative turning angle (in the rectangular case) is computed in terms of the ratio of $|l_1|$ to $|l_2|$; precisely,

(5.32)
$$\theta_{\mathcal{H}}(\tau) = \pi - \arg\left(\frac{|l_2|}{|l_1|}i - e^{-i\pi/4}\right)$$

We see, therefore, that $\theta_{\mathcal{H}}(\tau)$ increases as the ratio $\frac{|l_2|}{|l_1|}$ increases. We now show that $\frac{|l_2|}{|l_1|}$ is monotone in Im τ.

Suppose that there exist $\tau_1, \tau_2 \in i\mathbb{R}$ such that $\frac{|l_2^{\tau_1}|}{|l_1^{\tau_1}|} = \frac{|l_2^{\tau_2}|}{|l_1^{\tau_2}|}$. Because of the restrictions on the flat structures imposed by the rectangular torus (see Lemma 4.1), this implies that the Gdh flat structures are dilations of each other. Call the developing map from the torus $\mathbb{C}/\langle 1, \tau_i \rangle$ to the plane (yielding a hexagon) g_i. The Schwarz-Christoffel maps f_i map the upper half plane to the tori $\mathbb{C}/\langle 1, \tau_i \rangle$. Composing gives two maps from the upper half plane to similar hexagons (see Figure 5.7).
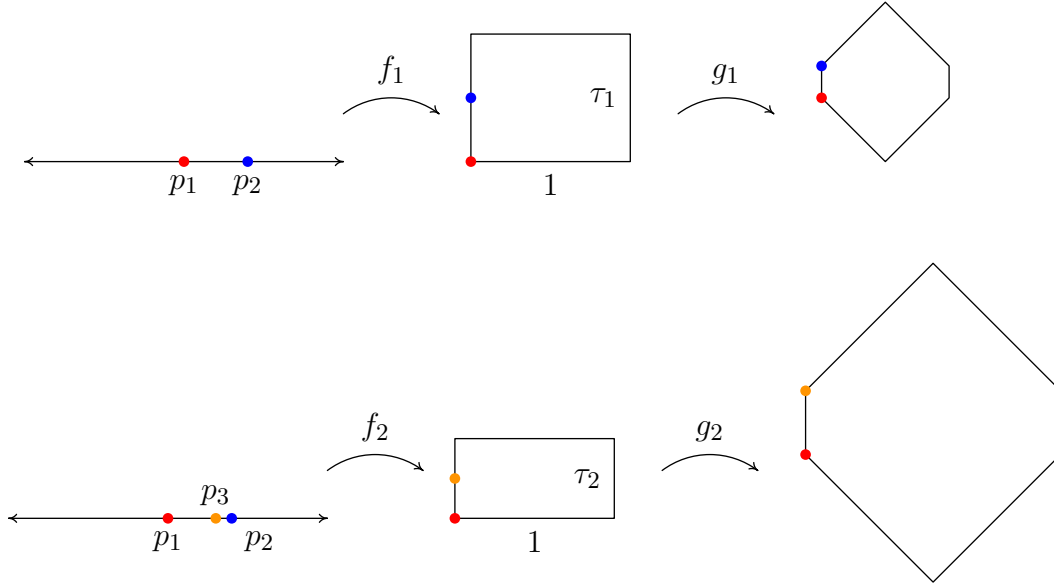
FIGURE 5.7. Two maps from the upper half plane to a hexagon.

Thus $g_1 \circ f_1$ and $\frac{1}{2} \cdot g_2 \circ f_2$ are two maps from the upper half plane to the *same* hexagon. By the Riemann mapping theorem, there is a unique such map up to Möbius transformation. Both maps send p_1 to the same point (fixing the Möbius transformation). Since $g_1 \circ f_1(p_2) = \frac{1}{2} \cdot g_2 \circ f_2(p_3)$ these maps are *distinct* (a contradiction with the Riemann mapping theorem) unless $p_2 = p_3$. But these points are determined by the conformal structure of the torus, so $\tau_1 = \tau_2$. This shows that the ratio $\frac{|l_2|}{|l_1|}$ is monotone. By computing the ratio for two different values, one can easily see that it is, in fact, increasing in Im τ. $\square$

LEMMA 5.5. *There exists a continuous curve* $c : \mathbb{R} \to \mathbb{C}$ *such that* $\tau_G \in c(\mathbb{R})$ *and* $c(\mathbb{R}) \subset b^{-1}(0)$.

PROOF. Since b is continuous, $b < 0$ on Y and $b > 0$ on B, the zero set of b must separate (topologically!) B and Y, in particular, it contains a curve c such that $\tau_G \in c$. Note that this curve does not intersect L or R (there are no zeros on either). Thus, as $t \to \pm\infty$, Im $(c(t)) \to 0$ or Im $(c(t)) \to \infty$ $\square$

Finally, the following proposition proves embeddedness.

PROPOSITION 5.6. *Let M_η, $0 \leq \eta \leq 1$ be a continuous family of immersed triply periodic minimal surfaces. If some member M_{η_0} of the family is embedded, then M_η is embedded for all $0 \leq \eta \leq 1$.*

PROOF. Let t_0 be the first time that a surface is not embedded, that is,

$$t_0 := \inf\{\eta > \eta_0 \mid M_\eta \text{is not embedded}\}$$

We assume that t_0 exists and arrive at a contradiction. Since it is not embedded, M_{t_0} has a point p of self-intersection. Suppose that at p, the tangent planes to the surface are transverse. Since transversality is an open condition, by the continuity of the family there exists $\epsilon > 0$ such that the tangent planes for $G_{t_0 - \epsilon}$ will also be transverse at p. Therefore, $G_{t_0 - \epsilon}$ has a self-intersection at p, a contradiction, with the minimality of t_0. Therefore, if t_0 exists the tangent planes must be coincident.

Let $F : X \to \mathbb{R}^3$ be the immersion, with $F(x_1) = F(x_2) = P$. For sufficiently small $r > 0$, $B_r(x_i)$ is an immersed minimal disk M_i. Each is a minimal graph over their common tangent plane. Define a height function h_i on M_i as the height of graph M_i. By the maximum principle for minimal surface, we cannot have $h_1 - h_2 > 0$ on $B_r(p) - \{p\}$. Thus $h_1 - h_2$ assumes some negative values. This, however, is an open condition, so there is $\epsilon > 0$ such that $h_1 - h_2$ is also negative on a neighborhood of $G_{t_0 - \epsilon}$. If $h_1 - h_2$ is both negative and positive, the surface $G_{t_0 - \epsilon}$ can not be embedded since the two graphs M_1 and M_2 intersect, a contradiction with the minimality of t_0. Therefore, the family must be embedded for all $\eta > \eta_0$. A similar argument holds for $0 < \eta < \eta_0$, and so the family is embedded.   □

We now have all the tools required to prove the existence and embeddedness of the tG family:

THEOREM 1.2. *There is a one parameter family of minimal embeddings $tG_\eta \subset \mathbb{R}^3/\Lambda_\eta$, $\eta \in \mathbb{R}^+$, such that tG_η is an embedded minimal surface of genus 3. The gyroid is a member of this family. Furthermore, each tG_η admits a rotational symmetry of order 2.*

PROOF. By Lemma 5.5, there exists a family of tori so that the developed (and normalized) flat structures have the same vertical and horizontal turning angle θ. We use

the Gauß map used to develop these flat structures, and set $dh = e^{i\theta}dz$. This choice of height differential ensures that the flat structures are in the moduli spaces $\mathcal{V}(G)$ and $\mathcal{H}(G)$. Therefore, the period problem is solved for this Weierstraß data. The branched torus cover provides the conformal model of the triply periodic minimal surface, and the Gauß map G and dh that we have defined lift (via the rotation ρ_2) to a well-defined Gauß map and height differential for the triply periodic surface. This one-parameter family does contain the gyroid (because of the description of the gyroid in Section 4.2). The entire family is embedded because of Proposition 5.6. □

5.3. Moduli spaces for the rL family of Lidinoids

**5.3.1. Vertical moduli space $\mathcal{V}(L)$.** The vertical moduli space is defined in precisely the same way as for the gyroid, i.e.,

$$(5.33) \qquad\qquad\qquad \mathcal{V}(L) = \mathcal{V}(G)$$

5.3.2. Horizontal moduli space $\mathcal{H}(L)$. Suppose that M is any immersed, genus 3, triply periodic minimal surface that has as a conformal model a three-fold branched cover of a generic torus $\mathbb{C}/\Gamma$ (without loss of generality we write $\Gamma = \langle 1, \tau \rangle$. Suppose further that the square of the Gauss map descends to $\mathbb{C}/\Gamma$ and has a double order pole at $\frac{1}{2}$ and a double order zero at 0. (This is the case for the Lidinoid, except that the torus is rectangular.) The quotient $S = \mathbb{C}/\Gamma/-id$ is a sphere, and Gdh again induces a cone metric on S. Under this cone metric, the sphere is a tetrahedron, with vertex angle of $\frac{5\pi}{3}$ (corresponding to the zero), a vertex angle of $\frac{\pi}{3}$ (corresponding to the pole), and two vertex angles of π (corresponding to the remaining fixed points of $-id$: $\frac{\tau}{2}$ and $\frac{1}{2} + \frac{\tau}{2}$). The developed image of this sphere is parameterized by:

LEMMA 5.7. *For any torus $\mathbb{C}/\Gamma$ ($\Gamma = \langle 1, \tau \rangle$), the cone metric Gdh descends to S. By cutting along shortest geodesics on S from $\frac{1}{2}$ to 0, 0 to $\frac{\tau}{2}$, and from $\frac{\tau}{2}$ to $\frac{1}{2} + \frac{\tau}{2}$, we obtain a hexagon shown in Figure 5.8. The hexagon has the property that*

  i) the length of l_i is equal to the length of l_i^* for $i = 1, 2, 3$
  ii) l_2 is parallel to l_2^*
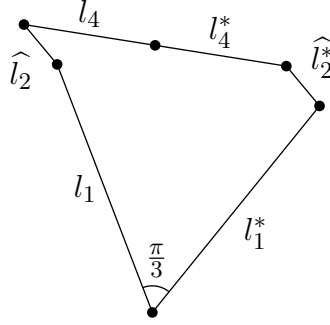
FIGURE 5.8. A developed flat structure for the Lidinoid *before* rotation by π.
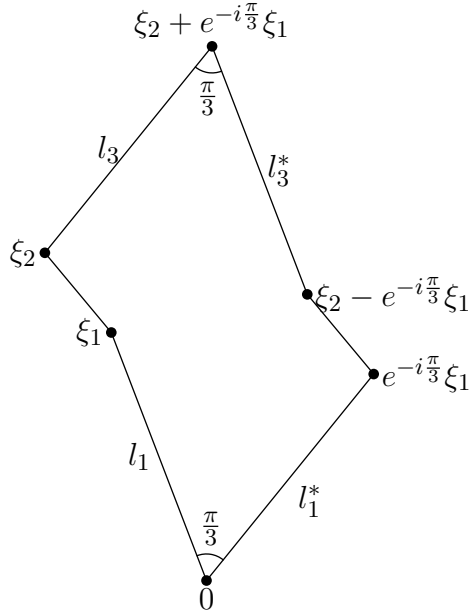
FIGURE 5.9. A generic member of the $\widetilde{\mathcal{H}(L)}$ moduli space.

iii) the angle between l_1 and l_1^* and the angle between l_3 and l_3^* are both $\frac{\pi}{2}$.

Since the fixed point $\frac{1}{2} + \frac{\tau}{2}$ is regular before the application of $-id$, we can extend this to a developing map on the whole torus by rotation by π about the intersection of l_4 and l_4^*. Doing this, we obtain the hexagon flat structure shown in Figure 5.9. We can parameterize this final space of possible hexagons by $\xi_1, \xi_2 \in \mathbb{C}$ as shown in Figure 5.9.

We call the space of all hexagons satisfying the conditions of Lemma 5.7 $\widetilde{\mathcal{H}(G)}$.

The proof is *precisely* analogous to the proof of Lemma 5.1, and we omit the details here.

To understand the horizontal periods, we again adjust ρ, if necessary, to normalize the $\frac{1}{G}dh$ flat structure as in Section 4.1.1.3. Then in terms of these flat structures, we compute the periods of the six generators of $H_1(M, Z)$ to be:

$$(5.34) \qquad \int_{A_1} Gdh = (1 + e^{2\pi i/3})e^{i\pi/3}\xi_1$$

$$(5.35) \qquad \int_{A_1} \frac{1}{G}dh = (1 + e^{-2\pi i/3})\xi_1$$

$$(5.36) \qquad \int_{B_1} Gdh = \xi_2 + e^{-\pi i/3}\xi_1$$

$$(5.37) \qquad \int_{B_1} \frac{1}{G}dh = \xi_2 - \xi_1$$

$$(5.38) \qquad \int_{A_2} Gdh = e^{2\pi i/3}(1 + e^{2\pi i/3})\xi_1$$

$$(5.39) \qquad \int_{A_2} \frac{1}{G}dh = \xi_1(1 + e^{-2\pi i/3})$$

$$(5.40) \qquad \int_{B_2} Gdh = e^{2\pi i/3}(\xi_2 - \xi_1)$$

$$(5.41) \qquad \int_{B_2} \frac{1}{G}dh = e^{-2\pi i/3}(\xi_2 + e^{-i\pi/3}\xi_1)$$

$$(5.42) \qquad \int_{B_3} Gdh = (-1 - e^{4\pi i/3})\xi_1$$

$$(5.43) \qquad \int_{B_3} \frac{1}{G}dh = e^{-4\pi i/3}(e^{-\pi i/3} - 1)\xi_1$$

(As before, we omit A_3 since the period is zero (recall that A_3 continuous on all three sheets.)

We make the substitution

$$(5.44) \qquad c = -\frac{1}{2}(\text{Im } \xi_1 + \sqrt{3}\text{Re } \xi_1)$$

$$(5.45) \qquad d = \frac{1}{2}(\text{Im } \xi_1 - 4\text{Im } \xi_2 + \sqrt{3}\text{Re } \xi_1)$$

The periods can then be expressed as

$$(5.46) \qquad\qquad P(A_1) = (\sqrt{3}c, ci, 0)$$

$$(5.47) \qquad\qquad P(A_2) = (-\sqrt{3}c, -ci, 0)$$

$$(5.48) \qquad\qquad P(A_3) = (0, 0, 3s)$$

$$(5.49) \qquad\qquad P(B_1) = (\sqrt{3}c, d, s)$$

$$(5.50) \qquad\qquad P(B_2) = (-\frac{\sqrt{3}}{2}(d-c), -\frac{1}{2}(d-c), s)$$

$$(5.51) \qquad\qquad P(B_3) = (-\sqrt{3}c, c, s)$$

Again, s is a factor determined by the torus. Since, for the Lidinoid, $P(B_1) = P(B_2)$, we are forced to set $c = -d$ to solve the period problem. Therefore, the period problem is solved if

$$(5.52) \qquad\qquad\qquad\qquad \text{Im } \xi_2 = 0.$$

(Notice that, apart from parameterizing the flat structure differently (0 corresponds to a different cone angle on the P surface) this is precisely the same condition as for the gyroid flat structures.)

The consequence of Equation 5.52 is that any member of $\widetilde{\mathcal{H}(L)}$ solves the period problem after a rotation (and so we can again define the relative turning angles). We define

$$(5.53) \qquad\qquad \mathcal{H}(L) = \{(\xi_1, \xi_2) \in \widetilde{\mathcal{H}(L)} \mid \text{Im } (\xi_2) = 0\}.$$

The remainder of the proof of the existence of a family of Lidinoids proceeds analogously to that of the tG family. Dehn twists have a similar affect, making it possible to again use an intermediate value type argument. We again rely on a single numerical calculation on rectangular tori to verify the existence of a "horizontal separating curve". This proves the following theorem:

THEOREM 1.3. *There is a one parameter family of minimal embeddings $rL_\eta \subset \mathbb{R}^3/\Lambda_\eta$, $\eta \in \mathbb{R}^+$, such that rL_η is an embedded minimal surface of genus 3. The Lidinoid is a member*

of this family. Furthermore, each embedded surface admits a rotational symmetry of order 3.

5.4. Moduli spaces for the rG family of gyroids

5.4.1. Vertical moduli space $\mathcal{V}(rG)$. As indicated in Section 4.5.3, to obtain the standard gyroid from the order 3 perspective, we take as the torus parameter $\tau = 2 \cdot ai$, where a is the conformal parameter for the standard P surface obtained in Appendix A. We then use the same angle of association as in the order 2 parameterization, obtaining:

$$\text{(5.54)} \qquad\qquad \text{Re } e^{i\theta} = -2\text{Re } e^{i\theta}\tau.$$

We therefore define

$$\text{(5.55)} \qquad \mathcal{V}(rG) = \{(\omega_1, \omega_2) \in \mathbb{C} \times \mathbb{C} \mid |\omega_1| = 1 \text{ and Re } \omega_1 = -2\text{Re } \omega_2\}$$

so that the vertical period problem is solved.

5.4.2. Horizontal moduli space $\mathcal{H}(rG)$. Let M be any immersed, genus 3, triply periodic minimal surface that has as a conformal model a three-fold branched cover of a generic torus $\mathbb{C}/\Gamma$ (without loss of generality we write $\Gamma = \langle 1, \tau \rangle$. Suppose further that the square of the Gauss map descends to $\mathbb{C}/\Gamma$ and has a double order pole at $\frac{1}{2} + \frac{\tau}{2}$ and a double order zero at 0. (This is the case for the order 3 gyroid, except that the torus is rectangular.) The quotient $S = \mathbb{C}/\Gamma/-id$ is a sphere, and Gdh again induces a cone metric on S. Under this cone metric, the sphere is a tetrahedron, with vertex angle of $\frac{5\pi}{3}$ (corresponding to the zero), a vertex angle of $\frac{\pi}{3}$ (corresponding to the pole), and two vertex angles of π (corresponding to the remaining fixed points of $-id$: $\frac{\tau}{2}$ and $\frac{1}{2}$). The developed image of this sphere is described by:

LEMMA 5.8. *For any torus $\mathbb{C}/\Gamma$ ($\Gamma = \langle 1, \tau \rangle$), the cone metric Gdh descends to S. By cutting along shortest geodesics on S from $\frac{1}{2}$ to 0, 0 to $\frac{\tau}{2}$, and from $\frac{\tau}{2}$ to $\frac{1}{2} + \frac{\tau}{2}$, we obtain a hexagon shown in Figure 5.10. The hexagon has the property that*

i) the length of l_i is equal to the length of l_i^* for $i = 1, 2, 3$
ii) $l_2 = e^{i2\pi/3}l_2^*$

iii) the angle between l_1 and l_1^* if π and the angle between l_3 and l_3^* is $\frac{\pi}{3}$.

We can parameterize this final space of possible hexagons by $\xi_1, \xi_2 \in \mathbb{C}$ as shown in Figure 5.10. For convenience, we use the notation $\widehat{\xi_1} = e^{-i\pi/3}(\xi_2 - \xi_1) + \xi_1 - e^{-2\pi i/3}\xi_1$.

We call the space of all hexagons satisfying the conditions of Lemma 5.8 $\widetilde{\mathcal{H}(rG)}$.
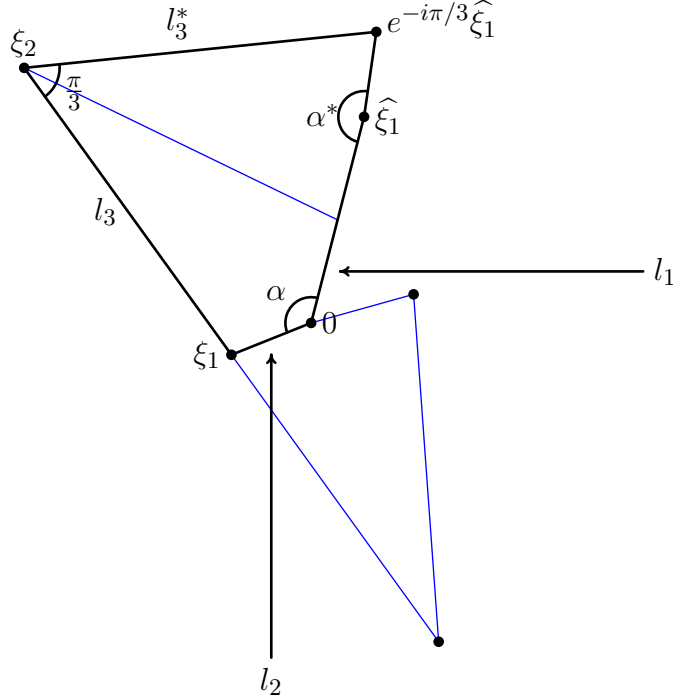

FIGURE 5.10. A generic member of the $\mathcal{H}(rG)$ moduli space.

The proof is *precisely* analogous to the proof of Lemma 5.1, and we omit the details here.

To understand the horizontal periods, we again adjust ρ, if necessary, to normalize the $\frac{1}{G}dh$ flat structure as in Section 4.1.1.3. Then in terms of these flat structures, we compute the periods of the six generators of $H_1(M, Z)$ to be:

$$\text{(5.56)} \qquad \int_{A_1} G\,dh = \xi_2 + e^{i\pi/3}(\widehat{\xi_1} - \xi_2)$$

$$\text{(5.57)} \qquad \int_{A_1} \frac{1}{G}dh = -\xi_2 + e^{-i\pi/3}(2\xi_1 - \xi_2)$$

$$(5.58) \qquad \int_{B_1} G dh = e^{4\pi i/3}(2(\xi_2 - \xi_1))$$

$$(5.59) \qquad \int_{B_1} \frac{1}{G} dh = e^{-4\pi i/3}(-\widehat{\xi_1})$$

$$(5.60) \qquad \int_{A_2} G dh = e^{2\pi i/3}(\xi_2 + e^{i\pi/3}(\widehat{\xi_1} - \xi_2))$$

$$(5.61) \qquad \int_{A_2} \frac{1}{G} dh = e^{-2\pi i/3}(-\xi_2 + e^{-i\pi/3}(2\xi_1 - \xi_2))$$

$$(5.62) \qquad \int_{B_2} G dh = 2(\xi_2 - \xi_1)$$

$$(5.63) \qquad \int_{B_2} \frac{1}{G} dh = -\widehat{\xi_1}$$

$$(5.64) \qquad \int_{A_3} G dh = e^{4\pi i/3}(\xi_2 + e^{i\pi/3}(\widehat{\xi_1} - \xi_2))$$

$$(5.65) \qquad \int_{A_3} \frac{1}{G} dh = e^{-4\pi i/3}(-\xi_2 + e^{-i\pi/3}(2\xi_1 - \xi_2))$$

$$(5.66) \qquad \int_{B_3} G dh = e^{2\pi i/3}(2(\xi_2 - \xi_1))$$

$$(5.67) \qquad \int_{B_3} \frac{1}{G} dh = e^{-2\pi i/3}(-\widehat{\xi_1})$$

$$(5.68)$$

We make the substitution

$$(5.69) \qquad a = 2\sqrt{3}\mathrm{Im}\ \xi_1 - \sqrt{3}\mathrm{Im}\ \xi_2 + 2\mathrm{Re}\ \xi_1 - 3\mathrm{Re}\ \xi_2$$

$$(5.70) \qquad b = \sqrt{3}\mathrm{Im}\ \xi_1 - \frac{\sqrt{3}}{2}\mathrm{Im}\ \xi_2 + \mathrm{Re}\ \xi_1 - \frac{5}{2}\mathrm{Re}\ \xi_2$$

The periods can then be expressed as

$$(5.71) \qquad P(A_1) = (a, 0, -s)$$

$$(5.72) \qquad P(A_2) = (a, 0, -s)$$

$$(5.73) \qquad P(A_3) = (a, 0, -s)$$

$$(5.74) \qquad P(B_1) = (b, \sqrt{3}(a - b), 2s)$$

$$(5.75) \qquad P(B_2) = (b, \sqrt{3}(a - b), 2s)$$

$$(5.76) \qquad P(B_3) = (b, \sqrt{3}(a - b), 2s)$$

Again, s is a factor determined by the torus. Since, for the gyroid, one computes that $P(A_1) = P(B_2)$, we are forced to set $a = b$ to solve the period problem. Therefore, the period problem is solved if

$$(5.77) \qquad \sqrt{3}\text{Im } \xi_1 - \frac{\sqrt{3}}{2}\text{Im } \xi_2 + \text{Re } \xi_1 - \frac{1}{2}\text{Re } \xi_2 = 0$$

We remark that this seemingly complicated expression is actually very reasonable: Equation 5.77 holds if and only if

$$(5.78) \qquad \arg\left(\widehat{\xi_1} - \xi_2\right) = \frac{\pi}{3}.$$

(This is a simple computation, which we omit.)

The consequence of Equation 5.78 is that for any member of $\widetilde{\mathcal{H}(rG)}$ solves the period problem after a rotation (and so we can again define the relative turning angles). We define

$$(5.79) \qquad \mathcal{H}(rG) = \left\{(\xi_1, \xi_2) \in \widetilde{\mathcal{H}(L)} \mid \sqrt{3}\text{Im } \xi_1 - \frac{\sqrt{3}}{2}\text{Im } \xi_2 + \text{Re } \xi_1 - \frac{1}{2}\text{Re } \xi_2 = 0\right\}.$$

The remainder of the proof of the existence of a family of order 3 gyroids is analogous to the other two families discussed above, yielding:

THEOREM 1.4. *There is a one parameter family of minimal embeddings $rG_\eta \subset \mathbb{R}^3/\Lambda_\eta$, $\eta \in \mathbb{R}^+$, such that rG_η is an embedded minimal surface of genus 3. The gyroid is a member of this family. Furthermore, each embedded surface admits a rotational symmetry of order 3.*

CHAPTER 6

Questions, Conjectures, and Future Work

Throughout this work, a number of questions have arisen that should provide plenty of interesting future work. We record some of these questions here.

6.0.3. Rigidity of surfaces in a fixed lattice. Throughout this work, all deformations of a surface *changed the surface's lattice in space*; the deformed surface is embedded in a different 3-torus. We certainly expect the following to be true:

CONJECTURE 6.1. *Let $f_t : X_t \to \mathbb{R}^3/\Lambda_t$ be a continuous family of minimal embeddings from a family of genus 3 Riemann surfaces X_t. If Λ_t is constant in t, then so is X_t and f_t.*

Assuming the conjecture is true, one can easily prove the following:

PROPOSITION 6.2. *Assume that Conjecture 6.1 holds. Let M be an embedded triply periodic minimal surface of genus 3. Then the dimension of the space of all embedded deformations of M is at most 5.*

PROOF. By Conjecture 6.1, the lattice must vary for nearby deformations of M. Therefore, the dimension of the space of deformations is the same as the dimension of the space of "different" lattices. The dimension of all possible lattices is 9. Since scaling doesn't produce a "deformation" in our sense, we normalize so that $e_1 \in \Lambda$ has length 1; this normalization reduces the dimension to 8. Since rigid motions also don't produce a "deformed" surface, we subtract 3 more dimensions for the dimension of $SO(3)$. □

Resolving Conjecture 6.1 (either positively or negatively) would have interesting consequences. If answered positively, then we know that the maximal dimension can be achieved (by Meeks' family). If answered negatively, it seems that the hunt would be on for an example of a deformation that leaves the lattice invariant.

6.0.4. Dimension of a family of gyroids. Since the gyroid is *not* in Meeks' family, we are not automatically given a 5-parameter deformation of the gyroid. This dissertation proves the existence of two, 1-parameter families of minimal surfaces which contains the gyroid. What size of a gyroid family can we expect? More precisely,

QUESTION 6.3. *Let $\mathcal{F}$ be a maximal continuous family of embedded, triply periodic minimal surfaces of genus 3 that contains the (standard) gyroid. What is the real dimension of $\mathcal{F}$?*

It is not entirely clear what the dimension should be. On the one hand, the gyroid is very much like the P surface. More precisely, the P surface is a volume-preserving stable (v.p. stable) minimal surface [**Ros92**]. (Loosely, a triply periodic minimal surface $M \subset \mathbb{R}^3$ with lattice Λ is *v.p. stable* if the second derivative of the area functional is nonnegative over all compactly supported variations of M that preserve the volume enclosed by $M/\Lambda \subset \mathbb{R}^3/\Lambda$.) Furthermore, Ross mentions that all sufficiently close deformations of the P surface in the Meeks family are v.p. stable. The gyroid is also v.p. stable [**Ros92, GBW96**]. Since notions are stability are often connected to a certain amount of non-degeneracy, it's tempting to propose that the full dimension of gyroids is equal to that for the P surface. (By the discussion of the previous subsection, we expect that dimension to be 5.)

It bears mentioning here that the Meeks family relies on an underlying symmetry of all the surfaces in the family: their Gauß maps are branched over antipodal points of the sphere. This "hidden symmetry" is an essential ingredient in his proof. He further requires that the *angle of association* is either 0 or $\frac{\pi}{2}$ — a condition that does not hold for the gyroid. One approach to producing a 5-parameter family of gyroid surfaces is to find a different "hidden symmetry" — some relation or condition or property that all surfaces share that is not induced by a symmetry of the surfaces; one could not require the angle of association assumption here. The 1-parameter continua of examples that contain the gyroid permit a detailed study of their properties, which may point to other methods for enlarging the dimension of the family. Likewise, we do not know the answer to the following question:

QUESTION 6.4. *Do there exist genus three triply periodic minimal surfaces whose Weierstraß points on the sphere are not pairwise antipodal?*

It could be that members of our tG family do not have pairwise antipodal Weierstraß points; further investigation is warranted.

On the other hand, this author finds the gyroid to be, qualitatively, quite different that other surfaces. The additional requirements enforced by the non-trivial angle of association are often quite miraculously compatible; nonetheless, the tori are not symmetric. The presence of the glide reflection when assembling these surfaces is an additional different ingredient. Any knowledge of the dimension of the space would be beneficial.

6.0.5. Quotients which are rhombic tori. In the examples in Chapter 4, we took the quotient of the P and H surfaces by a rotational symmetry and obtained a *rectangular* torus. (Recall that the presence of reflectional symmetries with *disconnected* fixed point set implies that the torus is rectangular.) The following two examples indicate that certain highly symmetric surfaces can admit quotients which are instead *rhombic* tori.

6.0.5.1. *The P surface from an alternate order 2 rotation.* We previously considered the P surface from the point of view of being invariant by an order 2 symmetry where the symmetry was rotation about a line through opposite handles (as point sets in space, the axis of rotation was disjoint from the surface). The P surface, and in fact every member of the tP family, admit an additional order 2 symmetry. Consider the adjacent handles of the same size on a surface $M \in tP$. The handles are joined by a planar symmetry curve, as are the opposite two handles. The line connecting the midpoints of these two curves is the axis of rotation for the new symmetry we consider. (Alternatively, one can view the P surface as being generated by "square catenoids". This symmetry axis is perpendicular to the axis of the catenoid and intersects the "waist". We denote this symmetry by ρ_2^*.

The fixed points of this map are again those points with vertical normal; there are four fixed points (which are distinct from the previous fixed points for the order 2 rotation). Interestingly, none of the points are at the same height — thus, on the quotient torus no two branch points lie on a vertical line segment. Most importantly, when we consider the fixed

point set obtained by reflection in a vertical plane, we see that it has *only one component.* Therefore, the quotient surface $P/\Lambda/\rho_2^*$ is a *rhombic* torus. The *dh* flat structure is oriented so that the diagonals of the rhombus are vertical and horizontal.

To our knowledge, minimal surfaces whose quotients are rhombic tori have not been studied in the literature. The flat structure method employed to construct the families in this dissertation should apply immediately to the study of these rhombic tori. (The branch points lie on the real line in the *dh* flat structure, so the developed images of the flat structures should be reasonable to understand.)

Furthermore, we can find the gyroid in this parameterization (since the standard P surface can be parameterized this way, the gyroid can be parameterized by using the associate family parameter).

QUESTION 6.5. *Can one construct a family of gyroids using this alternate order 2 rotation? If so, is the family a previously discovered one? Does one obtain a P surface family in this way? If so, is the family distinct from previously discovered P surface families? Is it in Meeks' family?*

We know of no investigation of such surfaces, even in the physical chemistry / crystallography literature.

6.0.5.2. *The order 2 H surface.* While we have already studied the H surface as a surface invariant under an order 3 rotation (and have thus obtained the rH family), the H surface also admits an order 2 rotation (in fact, every member of the rH family admits this rotation). If we view the H surface as generated by "triangular catenoids", then this rotation interchanges the two triangles. The axis is the intersection of the vertical symmetry plane and the horizontal symmetry plane that does not intersect the small "nearly circular" handles.

There are again four fixed points[1], and again none lie at the same height as another.[2] The quotient is again a rhombic torus. Deformations under this parameterization (if they

_____

[1] recall that any order 2 automorphism of a Riemann surface has exactly four fixed points
[2] This statement is true for all but a single member of the rH family. For this surface, two of the branch points are at the same height.

exist) would destroy the 3-fold symmetry of the H surface. We would expect the triangular catenoids to no longer be equilateral, but rather "isosceles catenoids".

We would be surprised if this deformation did not yield a family of Lidinoids that preserve the two-fold symmetry. One can ask all of Question 6.5 in this context. Furthermore, it seems that the conformal structure of these surfaces may be rather closely related to that for the alternate order 2 P surface. If so, it could be worthwhile to investigate the presence of deformations between the P and H surfaces.

6.0.6. Limits of the tG and other families. At present, our proof only guarantees the existence of an analytic family of possibly small parameter space. A thorough understanding of the moduli space for the tG family is a clear next step for investigation. Optimistically, one expects that there exists a member of the tG family whose quotient torus has generators 1 and τ with Im $\tau = a$ for all $a \in \mathbb{R}$. Certainly, we expect the curve (in the moduli space of quotient tori) that describes the tG family to be continuous and complete.

QUESTION 6.6. *What properties does the moduli space of the tG family have? Is it connected? Smooth? Monotone (in the upper half plane)?*

We would find even numerical investigations interesting on this subject. Once the moduli space is more clearly understood, we need to understand the limits of each family.

In the case of the tP, rPD, and rH families, we can see from the pictures presented that, in at least one of the limits, we should expect to obtain parallel planes joined by small catenoidal necks. We would expect to be able to construct these families using Martin Traizet's beautiful "opening nodes" technique for minimal surfaces, see, e.g., [**Tra02, Tra06**]. Note also that helicoids are forming in the "upper" limit of the rPD family. One could optimistically hope for a more general existence theory by combining the techniques of Traizet with those of Traizet and Weber by gluing in helicoids at sufficiently "balanced" points, see, e.g., [**TW05, Tra06**].

More precisely, a program for obtaining a larger family of gyroids might be as follows. First, understand clearly the limits of the tG family, in particular, understand where, in

the limit, certain singularities (like catenoidal necks) form. Then, using this configuration as a starting point, find a more general (hopefully, 1 or 2 parameter) family of balanced configurations (see [**Tra02**]). Using Traizet's technique, glue in catenoids using these configurations, and finally solve the period problem using the implicit function theorem, to obtain a larger family of gyroids. (We should mention that the use of the implicit function theorem permits only the existence of a small family near these degenerate surfaces.)

6.0.7. Extension of the classification and size of families by removing hypothesis. The overarching goal of any minimal surface program is to classify the surfaces in some reasonable sense. Meeks' family goes a long way towards understanding the theory of genus three triply periodic minimal surfaces.

GOAL 6.7. *Make an exhaustive list of all genus three embedded triply periodic minimal surfaces.*

This is almost certainly too ambitious for the foreseeable future. An example of what we would expect to see here is that every genus three embedded triply periodic minimal surface is a member of either the Meeks family, or a list of other families.

More reasonable would be an approach like that of Chapter 3:

GOAL 6.8. *To classify all embedded, genus 3, triply periodic minimal surfaces that admit a given symmetry.*

Here, finally, we can have hopes of making forward progress. For instance, our classification theorems (Theorem 3.11, 3.14, 3.15) classify all surfaces that satisfy restrictive symmetry properties. (This theorem, recall, requires the presence of a rotational symmetry so that the quotient is a torus, and the presence of at least two planes of symmetry.) Removal of some of these symmetry conditions is likely possible. For instance, if we remove the requirement on the planes of symmetry and instead require that the quotient torus is rectangular, we obtain more freedom to vary the location of the branch points. Some deformations are already known to exist in this setting.

More generally, we would like to remove the requirement that the torus is rectangular. This is certainly an artificial assumption, as the gyroid family tG generally has non-rectangular, non-rhombic tori as quotients. At the moment, we do not know how to deal with generic tori unless the branch points are sufficiently symmetric (such as invariant under $-id$). The current obstruction is that we need a canonical way to transfer the flat structure induced on the torus to polygons in the plane. Under the $-id$ identification, we can obtain the polygon by cutting apart along the well-defined edges (shortest geodesics between cone points) of the tetrahedron obtained by taking the quotient of the torus by $-id$.

Of course, it bears mentioning that we have no reason to think minimal surfaces must have symmetries. (For the non-triply periodic case, see [**Tra02**]).

QUESTION 6.9. *Does there exist an embedded triply periodic minimal surface of genus 3 with no symmetries?*

6.0.8. Higher genus minimal surfaces. Finally, we must not fail to mention that throughout this work, we have considered only genus 3 surfaces: the topologically most simple case. There is a wealth of genus 4 and higher examples about which very little is known. For example:

QUESTION 6.10. *What genus 4 embedded triply periodic minimal surfaces admit continuous deformations? What can we say about a classification of genus 4 surfaces?*

Frequently, one uses the hyperellipticity of genus 3 surfaces as a tool in proving theorems. However, a result of Meeks' shows that a genus 4 triply periodic minimal surface is *never* periodic:

THEOREM 6.11 ([**Mee90**], Theorem 3.3). *A hyperelliptic surface of even genus is never periodic.*

This is at least one reason why these higher genus surfaces have been poorly studied. The flat structure methods used in this work do not rely on the hyperelliptic structure. We expect them to generalize to genus four surfaces.

Calculation of ρ and τ for the Schwarz P surface

A.1. Calculation of ρ

In Section 4.1, we showed that ρ could be calculated two different ways. Firstly, we want to normalize the flat structures, that is, we need $\rho = 1/(r_1 e^{i\phi_1})$. It is possible in our case to explicitly calculate r_1, ϕ_1.

$$(A.1) \qquad r_1 e^{i\phi_i} = G^2(z + \frac{1}{2}) \Big/ \frac{1}{G^2}(z)$$

$$(A.2) \qquad = \frac{\theta_{11}(z + \frac{1}{2}, \tau)\, \theta_{11}(z + \frac{1}{2} - \frac{\tau}{2}, \tau)}{\theta_{11}(z + \frac{1}{2} - \frac{1}{2}, \tau)\, \theta_{11}(z + \frac{1}{2} - \frac{1+\tau}{2}, \tau)} \cdot \frac{\theta_{11}(z, \tau)\, \theta_{11}(z - \frac{\tau}{2}, \tau)}{\theta_{11}(z - \frac{1}{2}, \tau)\, \theta_{11}(z - \frac{1+\tau}{2}, \tau)}$$

$$(A.3) \qquad = \frac{\theta_{11}(z + \frac{1}{2}, \tau)\, \theta_{11}(z + \frac{1}{2} - \frac{\tau}{2}, \tau)}{\cancel{\theta_{11}(z, \tau)\, \theta_{11}(z - \frac{\tau}{2}, \tau)}} \cdot \frac{\cancel{\theta_{11}(z, \tau)\, \theta_{11}(z - \frac{\tau}{2}, \tau)}}{\theta_{11}(z - \frac{1}{2}, \tau)\, \theta_{11}(z - \frac{1+\tau}{2}, \tau)}$$

$$(A.4) \qquad = \frac{\theta_{11}(z + \frac{1}{2}, \tau)\, \theta_{11}(z + \frac{1}{2} - \frac{\tau}{2}, \tau)}{1} \cdot \frac{1}{\theta_{11}(z + \frac{1}{2}, \tau)\, \theta_{11}(z + \frac{1-\tau}{2}, \tau)}$$

$$(A.5) \qquad = 1$$

(The second to last line is a consequence of the periodicity in the real direction.)

The second way in which we can calculate ρ is using the horizontal symmetry. Since the vertical line on the torus $L = \{z \in \mathbb{C} \mid \mathrm{Re}\,(z) = \frac{1}{4}\}$ corresponds to a *horizontal* planar symmetry curve on P, the Gauß map satisfies

$$(A.6) \qquad |G(z)| = 1 \quad \forall z \in L.$$

Recall that we have defined the Gauß map as

$$(4.1) \qquad G^2(z) := \rho \frac{\theta_{11}(z, ai)\, \theta_{11}(z - ai, ai)}{\theta_{11}(z - \frac{1}{2}, ai)\, \theta_{11}(z - \frac{1+ai}{2}, ai)}$$

LEMMA A.1. *Equation A.6 is satisfied when $\rho = 1$.*

PROOF. Let $0 \leq s \leq \mathrm{Im}\,(\tau) = a$. Since

$$(A.7) \qquad G^2\left(\frac{1}{4}+si\right) = \rho\frac{\theta_{11}\left(\frac{1}{4}+si,\tau\right)\,\theta_{11}(\frac{1}{4}-\frac{\tau}{2},\tau)}{\theta_{11}(-\frac{1}{4}+si,\tau)\,\theta_{11}(-\frac{1}{4}+si-\frac{\tau}{2},\tau)},$$

it suffices to show that

$$(A.8) \qquad \left|\theta\left(\frac{1}{4}+si,\tau\right)\right| = \left|\theta\left(-\frac{1}{4}+si,\tau\right)\right|$$

(we will roll $\frac{\tau}{2}$, when present, into s since $\tau \in i\mathbb{R}$). Notice that this relationship holds only for rectangular tori.

We first calculate $\theta(\frac{1}{4}+si,\tau)$ from the definition.

$$(A.9) \qquad \theta\left(\frac{1}{4}+si,\tau\right) = e^{\pi i \frac{\tau}{4}+\pi\left(\frac{1}{4}+si+\frac{1}{2}\right)}\theta_{0,0}\left(\frac{1}{4}+si+\frac{1}{2}+\frac{\tau}{2}\right)$$

$$(A.10) \qquad = e^{\pi i \frac{\tau}{4}+\pi i\left(\frac{1}{4}+si+\frac{1}{2}\right)}\sum_{j\in\mathbb{Z}} e^{\pi i j^2 \tau}e^{2\pi i j\left(si+\frac{1}{2}+\frac{\tau}{2}\right)}e^{2\pi i j\frac{1}{4}}$$

$$(A.11) \qquad = c_1\sum_{j\in\mathbb{Z}} e^{\pi i j^2 \tau}e^{2\pi i j\left(si+\frac{1}{2}+\frac{\tau}{2}\right)}e^{2\pi i j\frac{1}{4}}$$

On the other hand,

$$(A.12) \qquad \theta\left(-\frac{1}{4}+si,\tau\right) = e^{\pi i \frac{\tau}{4}+\pi\left(-\frac{1}{4}+si+\frac{1}{2}\right)}\theta_{0,0}\left(-\frac{1}{4}+si+\frac{1}{2}+\frac{\tau}{2}\right)$$

$$(A.13) \qquad = e^{\pi i \frac{\tau}{4}+\pi i\left(-\frac{1}{4}+si+\frac{1}{2}\right)}\sum_{j\in\mathbb{Z}} e^{\pi i j^2 \tau}e^{2\pi i j\left(si+\frac{1}{2}+\frac{\tau}{2}\right)}e^{-2\pi i j\frac{1}{4}}$$

$$(A.14) \qquad = c_2\sum_{j\in\mathbb{Z}} e^{\pi i j^2 \tau}e^{2\pi i j\left(si+\frac{1}{2}+\frac{\tau}{2}\right)}e^{-2\pi i j\frac{1}{4}}.$$

Now, notice that the final sums in each of A.11 and A.14 *are conjugate*; since $\tau \in i\mathbb{R}$ the only imaginary term in the sum of Equation A.14 is

$$e^{-2\pi i j\frac{1}{4}}.$$

It remains only to show that the constant terms have the same norms:

$$(A.15) \qquad c_1 = e^{\pi i \frac{\tau}{4}+\pi i\left(\frac{1}{4}+si+\frac{1}{2}\right)}$$

$$(A.16) \qquad = e^{i\frac{\pi}{2}}e^{\pi i \frac{\tau}{4}+\pi i\left(-\frac{1}{4}+si+\frac{1}{2}\right)}$$

$$(A.17) \qquad = e^{i\frac{\pi}{2}}c_2.$$

Thus $\left|\theta\left(\frac{1}{4} + si, \tau\right)\right| = \left|\theta\left(-\frac{1}{4} + si, \tau\right)\right|$ and so $|G(z)| = 1$ on L. $\qquad\square$

A.2. Calculation of τ

Here we explicitly calculate the value a (recall $\tau = ai$) that yields the standard P surface. The P surface is tiled by 8 regular right angled hexagons, as seen in Figure 1.2. We will give an expression expression for the map 1-form dh using Schwarz-Christoffel maps.

By the Riemann Mapping Theorem, we can map the regular hexagon conformally to the upper half plane with the vertices of the hexagon mapping to the real axis. Without loss of generality, we map one vertex to 0, another to 1, and another to ∞. The other points will be mapped to some $a, b, c \in \mathbb{R}$. Since the hexagon is regular, there is a order 6 conformal automorphism of the hexagon that cyclically permutes the vertices. The action descends to the upper half plane, so that the vertices must be arranged so that there exists a Möbious transformation that cyclically permutes the vertices. To construct such a Möbious transformation, we will require it maps $0 \mapsto 1$, $a \mapsto \infty$, and $\infty \mapsto b$. The transformation is:

$$b\frac{z+1}{z-a}.$$

Notice that this automatically sends $-1 \mapsto 0$, so that $c = -1$. To determine values of a and b, note that we must have $b \mapsto -1$ and $1 \mapsto a$ giving us the pair of equations

(A.18) $$b\frac{b+1}{b-a} = -1$$

(A.19) $$\frac{2b}{1-a} = a,$$

the unique solution of which is $a = 3$, $b = -3$.

Using the Schwarz-Christoffel formula, we can parameterize a map from the upper half plane with these marked vertices to the "hexagon" $\int dh$ in the following way. The mapping will be conformal up to the boundary where the normal on the surface is not vertical. Where the normal is vertical, the mapping will be regular. The mapping then is:

(A.20) $$p \mapsto \int_{.}^{p} (u^2 - 3^2)^{(-1/2)} (u^2 - 1)^{(-1/2)} du$$

This parameterizes one-quarter of (the developed $\int dh$ image of) the torus. Since this is sufficiently much to calculate the ratio of height to width, can compute that

(A.21)
$$a \cdot i = \frac{\int_1^3 (u^2 - 3^2)^{(-1/2)}(u^2 - 1)^{(-1/2)} du}{\int_0^1 (u^2 - 3^2)^{(-1/2)}(u^2 - 1)^{(-1/2)} du}.$$

Mathematica is happy to generate good approximations to a:

$$a \approx 0.7817009599368214.$$

Bibliography

[Bon53]   O. Bonnet. Deuxième note sur les surfaces à lignes de courbure sphériques. *C.R. Acad. Sci. Paris*, 36:389–91, 585–7, 1853.

[DHKW92] Ulrich Dierkes, Stefan Hildebrandt, Albrecht Küster, and Ortwin Wohlrab. *Minimal surfaces. I*, volume 295 of *Grundlehren der Mathematischen Wissenschaften [Fundamental Principles of Mathematical Sciences]*. Springer-Verlag, Berlin, 1992. Boundary value problems.

[DM98]   Yuru Deng and Mark Mieczkowski. Three-dimensional periodic cubic membrane structure in the mitochondria of amoebae Chaos carolinensis. *Protoplasma*, 203(1-2):16–25, 1998.

[FH99]   Andrew Fogden and Stephan T. Hyde. Continuous transformations of cubic minimal surfaces. *Eur. Phys. J. B*, 7(1):91–104, 1999.

[FHL93]   Andrew Fogden, M. Haeberlein, and Sven Lidin. Generalizations of the gyroid surface. *J. Physique I*, 3(12):2371–2385, 1993.

[FK92]   H. M. Farkas and I. Kra. *Riemann surfaces*, volume 71 of *Graduate Texts in Mathematics*. Springer-Verlag, New York, second edition, 1992.

[GBW96]   Karsten Große-Brauckmann and Meinhard Wohlgemuth. The gyroid is embedded and has constant mean curvature companions. *Calc. Var. Partial Differential Equations*, 4(6):499–523, 1996.

[GH78]   Phillip Griffiths and Joseph Harris. *Principles of algebraic geometry*. Wiley-Interscience [John Wiley & Sons], New York, 1978. Pure and Applied Mathematics.

[Kar89]   Hermann Karcher. The triply periodic minimal surfaces of Alan Schoen and their constant mean curvature companions. *Manuscripta Math.*, 64(3):291–357, 1989.

[Kar05]   Hermann Karcher. Introduction to conjugate plateau constructions. In *Global theory of minimal surfaces*, volume 2 of *Clay Math. Proc.*, pages 137–161. Amer. Math. Soc., Providence, RI, 2005.

[KK79]   Akikazu Kuribayashi and Kaname Komiya. On Weierstrass points and automorphisms of curves of genus three. In *Algebraic geometry (Proc. Summer Meeting, Univ. Copenhagen, Copenhagen, 1978)*, volume 732 of *Lecture Notes in Math.*, pages 253–299. Springer, Berlin, 1979.

[LL90]   Sven Lidin and Stefan Larsson. Bonnet transformation of infinite periodic minimal surfaces with hexagonal symmetry. *J. Chem. Soc. Faraday Trans.*, 86(5):769–775, 1990.

[LM99]   Francisco J. López and Francisco Martín. Complete minimal surfaces in $\mathbf{R}^3$. *Publ. Mat.*, 43(2):341–449, 1999.

[LR91]   Francisco J. López and Antonio Ros. On embedded complete minimal surfaces of genus zero. *J. Differential Geom.*, 33(1):293–300, 1991.

[Mee75]   William H. Meeks, III. *The Geometry and the Conformal Structure of Triply Periodic Minimal Surfaces in $\mathbb{R}^3$*. PhD thesis, University of California, Berkeley, 1975.

[Mee90]   William H. Meeks, III. The theory of triply periodic minimal surfaces. *Indiana Univ. Math. J.*, 39(3):877–936, 1990.

[Mum83]   David Mumford. *Tata lectures on theta. I*, volume 28 of *Progress in Mathematics*. Birkhäuser Boston Inc., Boston, MA, 1983. With the assistance of C. Musili, M. Nori, E. Previato and M. Stillman.

[Nit75]   Johannes C. C. Nitsche. *Vorlesungen über Minimalflächen*. Springer-Verlag, Berlin, 1975. Die Grundlehren der mathematischen Wissenschaften, Band 199.

[Oss69]   Robert Osserman. *A survey of minimal surfaces*. Van Nostrand Reinhold Co., New York, 1969.

[Ros92]   Marty Ross. Schwarz' P and D surfaces are stable. *Differential Geom. Appl.*, 2(2):179–195, 1992.

[Sch90]   H.A. Schwarz. *Gesammelte Mathematische Abhandlungen, 2 Bände*. Springer, Berlin, 1890.

[Sch70]   Alan H. Schoen. Infinite periodic minimal surfaces without self-intersections. *NASA Technical Note TN D-5541*, 1970.

[TAHH88]   Edwin L. Thomas, David M. Anderson, Chris S. Henkee, and David Hoffman. Periodic area-minimizing surfaces in block copolymers. *Nature*, 334(6183):598–601, 1988.

[Tra02]   Martin Traizet. An embedded minimal surface with no symmetries. *J. Differential Geom.*, 60(1):103–153, 2002.

[Tra06]   Martin Traizet. On the genus of triply periodic minimal surfaces. Preprint, 2006.

[TW05]   Martin Traizet and Matthias Weber. Hermite polynominals and helicoidal minimal surfaces. *Invent. Math.*, 161:113–149, 2005.

[Web98]   Matthias Weber. On the Horgan minimal non-surface. *Calc. Var. Partial Differential Equations*, 7(4):373–379, 1998.

[Web04]   Matthias Weber. Notes on minimal surfaces. Lecture notes for a course at Indiana University, April 2004.

[Web05]   Matthias Weber. Classical minimal surfaces in Euclidean space by examples: geometric and computational aspects of the Weierstrass representation. In *Global theory of minimal surfaces*, volume 2 of *Clay Math. Proc.*, pages 19–63. Amer. Math. Soc., Providence, RI, 2005.

[WW98]   M. Weber and M. Wolf. Minimal surfaces of least total curvature and moduli spaces of plane polygonal arcs. *Geom. Funct. Anal.*, 8(6):1129–1170, 1998.

[WW02]   Matthias Weber and Michael Wolf. Teichmüller theory and handle addition for minimal surfaces. *Ann. of Math. (2)*, 156(3):713–795, 2002.

Adam G. Weyhaupt

Place of Birth: Alton, Illinois

Birthdate: October 14, 1979

Education:

- Bachelor of Arts (Mathematics) *Summa Cum Laude*, 2001, Eastern Illinois University, Charleston, Illinois
- Bachelor of Science (Mathematics and Computer Science) *Summa Cum Laude*, 2001, Eastern Illinois University, Charleston, Illinois
- Master of Arts (Mathematics), 2002, Indiana University, Bloomington, Indiana